molecules

MDPI

Review

Recent Advances in the Chemistry of Metal Carbamates

Giulio Bresciani, Lorenzo Biancalana, Guido Pampaloni * and Fabio Marchetti *

Department of Chemistry and Industrial Chemistry, University of Pisa, Via G. Moruzzi 13, I-56124 Pisa, Italy; giulio.bresciani@dcci.unipi.it (G.B.); lorenzo.biancalana@unipi.it (L.B.)

* Correspondence: guido.pampaloni@unipi.it (G.P.); fabio.marchetti1974@unipi.it (F.M.)

Academic Editor: Barbara Modec

Received: 14 July 2020; Accepted: 3 August 2020; Published: 7 August 2020

check for updates

Abstract: Following a related review dating back to 2003, the present review discusses in detail the various synthetic, structural and reactivity aspects of metal species containing one or more carbamato ligands, representing a large family of compounds across all the periodic table. A preliminary overview is provided on the reactivity of carbon dioxide with amines, and emphasis is given to recent findings concerning applications in various fields.

Keywords: carbon dioxide activation; amines; carbamate; metal complexes; catalysis; material chemistry

Index:

1. Introduction

Carbon dioxide is a an easily available and non-toxic chemical, and at the same time, it is implicated in environmental, energy and sustainability issues [1–4]. Thus, the last two decades have witnessed an unprecedentedly intense effort of academic and industrial research in two main directions, i.e., to exploit CO_2 as a C_1 synthon for organic synthesis [5–11] and to develop more and more efficient systems able to capture and store CO_2 [12,13]. The former goal is challenging for a variety of reactions, and a wide number of metal catalysts have been proposed to access valuable organic compounds and materials via CO_2 fixation strategies, which, however, require harsh conditions (high temperature and CO_2 pressure) in several cases [14,15]. It is worthy to note that, differently to other small molecules such as its relative carbon monoxide, carbon dioxide is a "bad" ligand for transition metals; therefore, examples of simple coordination compounds are relatively rare [16–21] and, accordingly, metal catalysts working in CO_2 activation routes usually exert their action without the intermediacy of metal-CO_2 adducts. The "weak point" in the apparently unscratchable robustness of carbon dioxide is the susceptibility to nucleophilic attacks at the carbon atom [22–24]. Thus, a range of nucleophilic reagents, including neutral *N*-heterocyclic carbenes [25,26], are known to react with CO_2 even under mild conditions, and some chemistry at transition metal centers is provided by the possibility of CO_2 insertion into the bond between a metal atom and a suitable anionic ligand, e.g., alkyl, allyl, alkoxide and hydride [27–32]. In this context, amines are key reactants towards carbon dioxide, and indeed carbon dioxide/amine systems have been intensively investigated in the field of capture/storage [33–35] and exploited for the incorporation of the CO_2 moiety within organic structures [36–39]. Furthermore, CO_2 is also prone to insertion reactions into a variety of metal-amide bonds, generating a carbamato ligand; however, metal complexes containing carbamato ligands are easily available through diverse synthetic routes not requiring the use of pressurized CO_2. It is remarkable that the preliminary formation of a magnesium-carbamato adduct generated from a lysine residue is widely exploited by the universal Rubisco enzyme to incorporate CO_2 in biomolecules [40,41]. Notably, metal carbamates (either homoleptic or not) have been reported for a wide number of elements throughout the periodic table and, due to this systematicity and their intriguing properties that will be described below, the chemistry of metal carbamates has seen a significant advance in the recent times. This review follows up a previous review on the same topic published in 2003 by Calderazzo, Pampaloni and coworkers [42]; herein, we will summarize fundamental concepts regarding the reactivity of CO_2 with amines, then we will discuss synthetic, structural and reactivity aspects of metal carbamates and their potential in various applications, with a particular focus on the findings appeared in the literature after 2003.

2. The Reactivity of Carbon Dioxide with Amines and other *N*-Donors

An overview of the reactivity of CO_2 with amines is depicted in Scheme 1. When the lone pair on the nitrogen atom attacks the carbon atom of CO_2, a zwitterionic Lewis acid/base adduct can be formed. At this step, a hydrogen atom can migrate from nitrogen to oxygen, affording the elusive carbamic acid. The detection of this species is extremely difficult [43–46] and its isolation rare [47]. The fate of the carbamic acid depends on the nature of the amine and the reaction environment. Most frequently, a second equivalent of *N*-donor can act as a Brønsted base affording an ammonium carbamate salt. In some cases, deprotonation of a carbamic acid may be operated by a second basic group present in the structure of the employed amine (e.g., diamine), affording a zwitterionic carbamate. Furthermore, the deprotonation can be forced when an external base, B, is added to the system, producing a "B-inium" carbamate.

In principle, ammonia and primary amines hold the potential to undergo respectively three and two carbonations per molecule; this kind of reactivity was proposed for ethylamine and cyclohexylamine in acetonitrile in the presence of penta-alkylguananidines, based on a ^{15}N-NMR study [48], but no other data have been reported as of today.

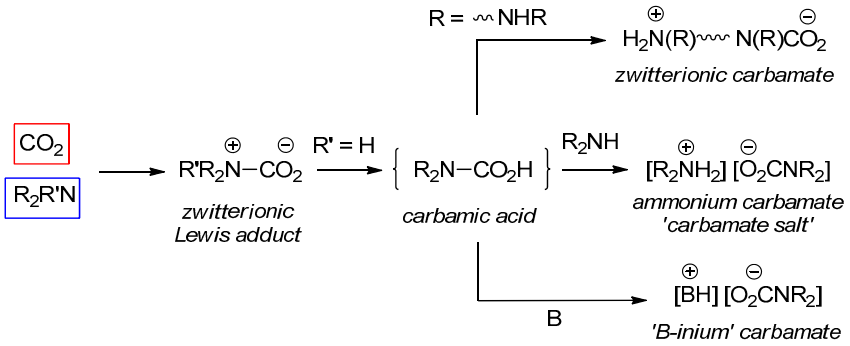

Scheme 1. Overall reactivity of CO_2/amine systems.

In agreement with the aim of this review, this section intends to summarize concepts reported in the previous review [42] and to provide information about recent developments in the study of CO_2/amine systems. The first part describes the carbonation of amines in aqueous solution and the most recent progress in this field achieved by using natural α-amino acids (Section 2.1). Next, the isolation and characterization of pure carbamate salts will be discussed (Section 2.2). Finally, recent advances in the stabilization of CO_2 adducts by using amidine/guanidine 'superbases' [49] and the CO_2/amine/superbase system is presented (Section 2.3).

2.1. CO_2/Amine Equilibria in Aqueous Solution

The CO_2/amine system is finely governed by parameters such as the nature of the solvent, temperature and solution pH. Thus, the concentration of carbamate in solution strictly depends on the experimental conditions. Many reactions involving amines and CO_2 have been performed in water, where the competition between the formation of the carbamato species and that of carbonate/bicarbonate anions must be taken into account (Scheme 2). Despite this complication, kinetic and thermodynamic aspects have been widely investigated [35,50,51], also in view of the search for optimal substrates and conditions for industrial CO_2 capture.

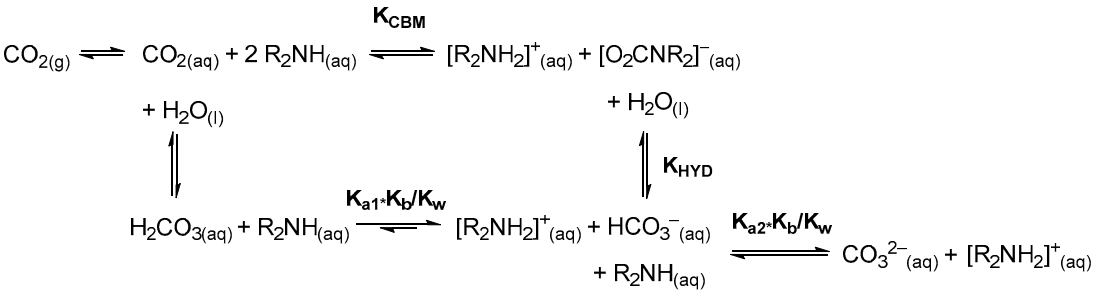

Scheme 2. Equilibria involving carbon dioxide and amines in aqueous solution.

A collection of thermodynamic parameters concerning the carbonation of amines in water is compiled in Table 1, including data from the most recent studies [42,52–58] and relevant to amino acids [59–63]. Additional data, including kinetic constants, are provided in Table S1 (Supplementary Information).

In most of the cases, either using ammonia, primary or secondary amines, the equilibrium constants regulating the hydrolysis of carbamate to bicarbonate ($\mathbf{K_{HYD}}$ in Scheme 2) are lower than 1, while equilibrium constants for the formation of carbamate ($\mathbf{K_{CBM}}$ in Scheme 2) are $>10^3$. The only exception to this trend ($\mathbf{K_{HYD}} >> \mathbf{K_{CBM}}$) was observed for aniline [64], while the formation of carbamato salts derived from diisopropylamine [65], di-*sec*-butylamine [66] and 2-amino-2-methyl-1-propanol (AMP) [52] was not assessed. Piperazine may form a bis-carbamate, but the generation of the second carbamato unit is unfavorable ($\mathbf{K_{HYD}} > \mathbf{K_{CBM}}$) [53].

Overall, $\mathbf{K_{CBM}}$ and $\mathbf{K_{HYD}}$ values outline the absence of a clear correlation with the Brønsted basicity (pK_b) of the amine function [42]. Among other factors, the Lewis basicity of the corresponding amide, R_2N^-, appears to play a significant role in the stabilization of the ammonium carbamate.

In the last decades, the capture of CO_2 has attracted the interest of the scientific community, and the possibility of storing and releasing carbon dioxide using non-toxic or even natural products represents an intriguing prospect [12,67–70]. In this context, the use of amino acids as adsorbers for PCC (post-combustion capture) of CO_2 has been intensively investigated [51,71]; nevertheless, thermodynamic and kinetic studies on the carbonation of amino acids did not receive adequate attention. Equilibrium constants for the formation (K_{CBM}) and hydrolysis (K_{HYD}) of amino acid carbamates were extrapolated from experimental data collected on sodium or potassium aminocarboxylates in aqueous solution (Table 1). In particular, Jensen and Faurholt [61] reported that β-alanine reacts with CO_2 approximately 1.5 times faster than α-alanine, and its carbamate is more stable toward hydrolysis. The formation and hydrolysis constants of lysine carbamate were recently calculated [63]. The presence of a second amino group on the side chain of lysine allows the formation of two carbamato moieties, but the second carbonation occurs under high CO_2 loading, making the hydrolysis predominant.

Table 1. Carbamate formation rate (k) and equilibrium (K_{CBM}) constants at 18 °C in water (Reaction: 2NHRR′ + CO_2 ⇋ [NH_2RR′][O_2CNRR′]). Carbamate hydrolysis equilibrium constants (K_{HYD}) at 18 °C in water (Reaction: NRR′CO_2^- + H_2O ⇋ HCO_3^- + NHRR′). More data available in Table S1.

Amine	pK_b [a]	K_{CBM}	K_{HYD}	Ref.
NH_3	4.76	2.3×10^3	4.4×10^{-1}	[42]
NH_2Me	3.38	4.0×10^6	6.0×10^{-3}	[42]
$NHMe_2$	3.22	1.6×10^6	2.2×10^{-2}	[42]
NH_2Et	3.19	2.0×10^6	1.8×10^{-2}	[42]
$NHEt_2$	3.51	7.4×10^4	2.4×10^{-1}	[42]
$NH_2{}^iPr$	3.37	3.6×10^5	6.3×10^{-2}	[42]
NH^iPr_2	3.17	None	-	[42]
$NH_2{}^sBu$	3.44	3.8×10^5	4.9×10^{-2}	[42]
NH^sBu_2	-	None	-	[42]
NH_2Ph	9.30	8.1×10^{-3}	3.6	[42]
Piperidine	2.95	7.9×10^5	8.1×10^{-2}	[42]
3-MPD	3.12	6.9×10^6	6.2×10^{-3}	[58]
4-MPD	3.06	5.9×10^6	8.3×10^{-3}	[58]
Pyrrolidine	3.16	1.9×10^7	2.0×10^{-3}	[54,55]
MEA	4.42	6.0×10^4	1.9×10^{-2}	[42]
DEA	4.98	2.1×10^3	1.5×10^{-1}	[42]
1-AP [b]	4.75	9.6×10^3	1.1×10^{-1}	[54]
2-AP [b]	4.75	4.0×10^3	2.5×10^{-1}	[52]
MPA [b]	4.18	2.5×10^5	1.5×10^{-2}	[52]
AMP [b]	4.73	None	-	[52]
4-PIPDM [b]	3.71	2.7×10^5	4.1×10^{-2}	[54,55]
4-PIPDE [b]	3.65	3.0×10^5	4.2×10^{-2}	[55]
Morpholine [b]	5.78	1.4×10^3	6.8×10^{-2}	[54,55]
Thiomorpholine [b]	5.57	9.3×10^2	1.6×10^{-1}	[54,55]
Piperazine	4.50 8.67	5.5×10^4 2.6×10^{-1}	3.2×10^{-2} 4.6×10^{-1}	[53]
MPIPZ	4.96	5.1×10^3	1.2×10^{-1}	[54]
4-AMTHP [b]	4.37	1.9×10^5	1.3×10^{-2}	[56]
Taurine [b],[c]	5.19	7.1×10^3	5.1×10^{-2}	[57]
		Amino acids		
Glycine[d]	4.49	4.4×10^4	4.2×10^{-2}	[59]
Sarcosine [b],[d]	4.22	3.3×10^4	1.0×10^{-1}	[60]
α-Alanine [d]	4.40	1.8×10^4	1.1×10^{-1}	[61]

Table 1. *Cont.*

Amine	pK_b [a]	K_{CBM}	K_{HYD}	Ref.
β-Alanine [d]	3.86	1.9×10^5	3.1×10^{-2}	[61]
Proline [c]	3.57	5.4×10^5	2.8×10^{-2}	[62]
Lysine [b],[c]	4.44 [e]	1.7×10^4	1.2×10^{-1}	[63]
	3.24 [f]	6.3×10^4	5.1×10^{-1}	

More data on alkyl- and aryl-amines are reported in Table S1. [a] pK_b values are from ref. [42,52–59,62,63]. For a list of pK_b see ref. [72,73]. ($K_w = 10^{-14.27}$); [b] Measured at 25 °C; [c] Potassium salt; [d] Sodium salt; [e] Deprotonation of the α-amino group; [f] Deprotonation of the amino group on the lateral chain; 3-MPD = 3-methylpiperidine, 4-MPD = 4-methylpiperidine, MEA = monoethanolamine, DEA = diethanolamine, 1-AP = 2-amino-1-propanol, 2-AP = 1-amino-2-propanol, MPA = 3-amino-1-propanol, AMP = 2-amino-2-methyl-1-propanol, 4-PIPDM = 4-piperidinemethanol, 4-PIPDE = 4-piperidineethanol, MPIPZ = 1-methylpiperazine, 4-AMTHP = 4-aminomethyltetrahydropyran.

2.2. Amine/CO_2 Interaction: Isolation and Characterization of Carbamato Salts

The previous considerations are valid for aqueous solutions, and are not extensible to other solvents, including the use of the amine itself as solvent. In fact, bulky amines are not reactive to CO_2 in water, whereas the same amines may be able to generate the corresponding carbamate under anhydrous, non-competitive conditions [47]. The uptake of CO_2, measured under anhydrous conditions and at atmospheric pressure in neat amines NHR_2 (R = Bu, ^{i}Pr, Cy), corresponds to a CO_2/amine molar ratio of approximately 0.5, as expected for the formation of the ammonium carbamate $[NH_2R_2][O_2CNR_2]$. Under such conditions, pure alkylammonium alkylcarbamates of several primary and secondary amines were isolated as colorless solids [42].

Since 2003, many other alkylammonium alkylcarbamates of cyclic amines [74–77], substituted amines [78–82] and diamines [83–85] have been isolated and characterized by IR and NMR spectroscopy, and by X-Ray diffraction in a number of cases. Noteworthy, some of these carbamates were obtained upon air exposure, revealing the capability of the respective amines of trapping CO_2 from the environment [74–76,81–84]. All the compounds cited above show intense bands due to C=O vibrations in the IR spectral region between 1650 and 1400 cm^{-1}.

In the course of a study on the crystallization of amines assisted by 1,5-dichloro-trans-9,10-diethynyl-9,10-dihydroanthracene-9,10-diol (DDDA), Mondal and Bhunia [75] found that cyclohexylamine (Scheme 3a), cycloheptylamine and piperidine undergo aerial carbonation affording the corresponding ammonium carbamate. Interestingly, no carbonation was observed for cyclopentylamine, even in the presence of DDDA. This result was attributed to the envelope conformation of cyclopentylamine, which is more rigid respect to the chair conformations of other cycloamines.

The first examples of chiral ammonium carbamates derived from chiral primary amines were described by Neda et al. [80], as obtained by the treatment of amino derivatives of quincorine and quincoridine with carbon dioxide in diethyl ether (Scheme 3b). The isolated colorless solids are stable for several days in solution at ambient temperature and thermally stable until 120 °C in a solid state. Above this temperature, the compounds lose carbon dioxide re-converting into amines, and the overall procedure represents a convenient purification method of quincorine and quincoridine. As previously discussed, AMP carbamate (AMP = 2-amino-2-methyl-1-propanol) has a very low formation constant in water and its hydrolysis is rapid, thus, only traces of this compound were detected by NMR in aqueous solution (see Table 1 and related discussion). On the other hand, when neat AMP was exposed to air for five days, AMP carbamate was recovered as a white solid (Scheme 3c). It survives in air for a limited time (max. 10 days) [82]. The crystal structure reveals asymmetric units composed of $AMPH^+$ and AMP carbamate, both involved in intermolecular hydrogen bonds. Notably, aerial CO_2 capture was also observed for "amino bile acids" [81], probably enhanced by the presence of OH groups in the structure (Scheme 3d). In general, synthesis and crystallization of carbamates are usually facilitated for precursors containing hydrogen bonding groups [74–76,79,82].

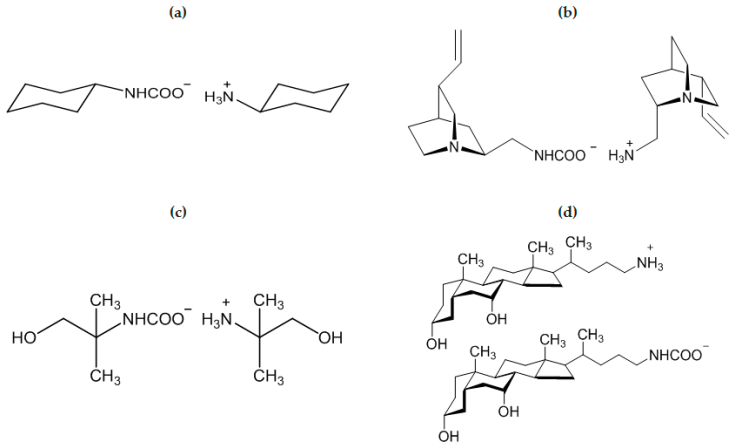

Scheme 3. Structures of alkylammonium alkylcarbamate derived from cyclohexylamine (**a**) [75], 2-amino-2-methyl-1-propanol, AMP (**b**) [82], quincoridine (**c**) [80], C24 amine derivative of chenodeoxycholic acid (**d**) [81].

In theory, a diamine/CO_2 system should lead to either a zwitterionic carbamate, a diammonium dicarbamate salt or a mixture of both species (Scheme 1) [86,87]. In addition to the two polymorph structures of the zwitterionic ethylenediamine carbamate [$^+NH_3(CH_2)_2NHCOO^-$] [86], only few crystallographic data are available for this class of compounds [79,83–85], in particular when compared to the number of structurally characterized ammonium carbamates (see [42] and references above). The diamine/CO_2 system described above has been recently investigated [85], and both the zwitterionic carbamate (Scheme 4a) and the ammonium dicarbamato species were isolated as crystalline materials from water and a 1:1 water/ethanol mixture (Scheme 4b); the "classical" ammonium carbamate was also obtained (Scheme 4c). In summary, the stability of ammonium carbamates benefits from the presence of sterically hindered or non-flexible substituents on the amine, and this feature may find application for the capture of carbon dioxide from the environment.

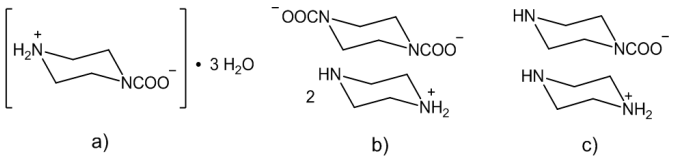

Scheme 4. Carbonation products of piperazine: zwitterionic carbamate (**a**), di-carbamate (**b**) and "ammonium" carbamate (**c**).

2.3. Stabilization of Carbamates by Superbases

The interaction of a tertiary alkylamine or pyridine with CO_2 is expected to lead to a zwitterionic Lewis acid-base adduct (Scheme **1**). However, this type of compounds has never been experimentally observed, even for *N*-donors bearing a significant nucleophilicity (e.g., DABCO, quinuclidine, 4-dimethylaminopyridine) [88]. In the light of the mechanistic implications for CO_2 activation, considerable efforts have been directed to the exploration of the topic in the last 15 years. These studies have outlined that zwitterionic CO_2 adducts may increase their stability when the *N*-donor is an amidine or guanidine (Scheme 5). Indeed, amidines and guanidines, the most famous representatives of each category being 1,5-diazabiciclo(5.4.0)undec-7-ene (DBU) and 1,1,3,3-tetramethylguanidine (TMG), are labeled as "superbases" (SB), in that they possess higher Brønsted basicity respect to common alkylamines [49]. Delocalization of the positive charge within the NC(N) system may compensate unfavorable energetics for charge separation in the zwitterion [24].

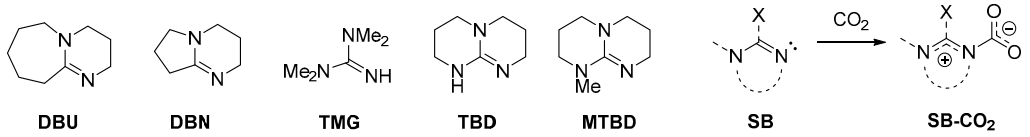

Scheme 5. Structures of commonly employed amidines/guanidines "superbases" (SB) and reaction with CO_2 affording a zwitterionic carbamate. **DBU** = 1,5-diazabiciclo(5.4.0)undec-7-ene; **DBN** = 1,5-diazabicyclo[4.3.0]non-5-ene; **TMG** = 1,1,3,3-tetramethylguanidine; **TBD** = 1,5,7-triazabicyclo[4.4.0]dec-5-ene; **MTBD** = 7-methyl-1,5,7-triazabicyclo(4.4.0)dec-5-ene; **SB** = superbase (general structure).

The first experimental evidences of SB-CO_2 adducts were collected analyzing the solid materials obtained from the reactions of 1,5,7-triazabicyclo[4.4.0]dec-5-ene (TBD), 1,5-diazabicyclo[4.3.0]non-5-ene (DBN) and related systems with carbon dioxide in acetonitrile [89,90]. A ^{13}C-NMR signal occurring at circa 150 ppm was attributed to the NCO_2 moiety, whereas a signal around 160 ppm is related to the co-presence of bicarbonate ions. Unambiguous identification of the zwitterionic carbamates TBD-CO_2 and DBN-CO_2 (Scheme 6) was later provided by single crystal X-ray diffraction [91,92].

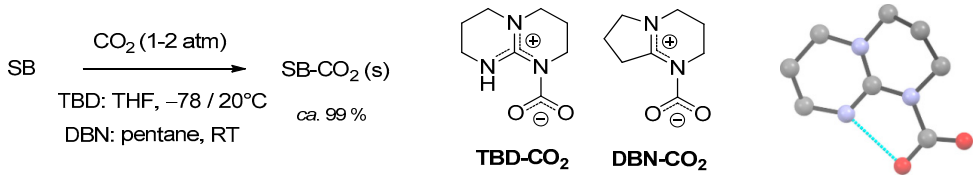

Scheme 6. Synthesis of TBD-CO_2 and DBN-CO_2, and view of the X-ray structure of TBD-CO_2 (H atoms omitted, hydrogen bond evidenced as cyano line) [91,92].

The TBD-CO_2 adduct is stable in the solid state up to 70 °C under CO_2 atmosphere and for over 1 month at ambient temperature under Ar. This remarkable stability is ascribable to a hydrogen bonding interaction in the solid state, involving a carbamato oxygen and the neighboring N-H unit. Accordingly, DBN-CO_2 is less stable and must be conserved under CO_2 atmosphere.

However, both TBD-CO_2 and DBN-CO_2 have to be prepared and subsequently manipulated under rigorously anhydrous conditions, being extremely sensitive to moisture. As a matter of fact, several attempts to isolate CO_2 adducts of amidines or guanidines were hampered by the presence of adventitious water in the reaction systems, leading to the crystallization of the corresponding bicarbonates (Scheme 7) [89,91,93–95]. This reactivity, common to ordinary alkylamines, is probably enhanced by the higher Brønsted basicity of the "superbases".

Scheme 7. Formation of bicarbonates by reaction of CO_2 with wet superbases (SB) or by hydrolysis of pre-formed SB-CO_2 adducts.

Some amidines and guanidines do not form zwitterionic carbamates, despite being effective in activating CO_2, most notably DBU [92,96,97]. A DBU-CO_2 adduct has been frequently proposed as an intermediate in CO_2-transfer reactions [93,98–100], but DBU does not form a carbamate even under a CO_2 pressure of 57 bar in anhydrous conditions [96]. Instead, DBU immediately reacts with traces of moisture under CO_2 atmosphere to afford the bicarbonate [DBUH][HCO_3].

Electronic and steric effects may play a crucial role in the stabilization of zwitterionic carbamates, as recently demonstrated by the preparation and X-ray characterization of a series of CO_2 adducts of *N*-heterocyclic imines (Scheme 8) [92]. Some of these derivatives display remarkable thermal stability

(up to 70 °C under Ar) and resistance towards hydrolysis. In these compounds, the carbamato group is perpendicular to the *N*-heterocyclic ring, at variance to other SB-CO_2 adducts (e.g., TBD-CO_2, DBN-CO_2) that are planar molecules. This conformation promotes π-delocalization in the NCO_2 fragment, as indicated by the shortening of the N-C bond, while the positive charge is stabilized by the aromaticity of the five-membered imidazolium ring. A collection of bond angles and distances is given in Table S2.

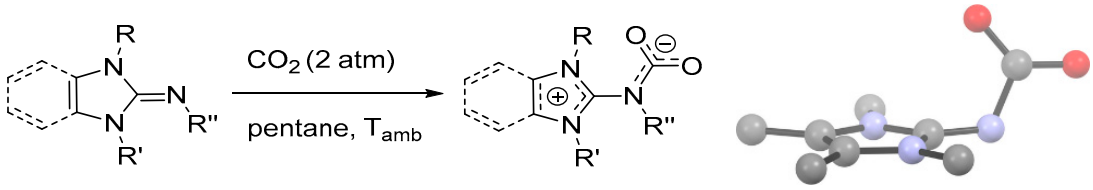

Scheme 8. Carbonation of 1,3-dihydro-2*H*-imidazol-2-imines and benzo[*d*]imidazole analogues, and view of the crystal structure of the CO_2 adduct of 1,3-di-tert-butyl-*N*-methyl-1,3-dihydro-2*H*-imidazol-2-imine (R = R′ = ^{t}Bu; R″ = Me) as a representative example. Drawing based on published structural data, H atoms omitted for clarity [92].

Amidines and guanidines are capable of activating CO_2 not only by direct interaction (i.e., formation of zwitterionic adducts) but also indirectly, e.g., in combination with alkylamines. In such reactions, the superbase behaves as a Brønsted base and the amide, generated upon deprotonation of the amine, acts as a Lewis base, resulting in the formation of amidinium/guanidinium carbamates (Scheme 9). Amidinium/guanidinium carbamates [SBH][R_2NCO_2] are considerably more stable with respect to related alkylammonium alkylcarbamates [R_2NH_2][R_2NCO_2], by virtue of the higher pK_a (lower acidity) of the associated cation (amidinium/guanidinium vs. alkylammonium) [101].

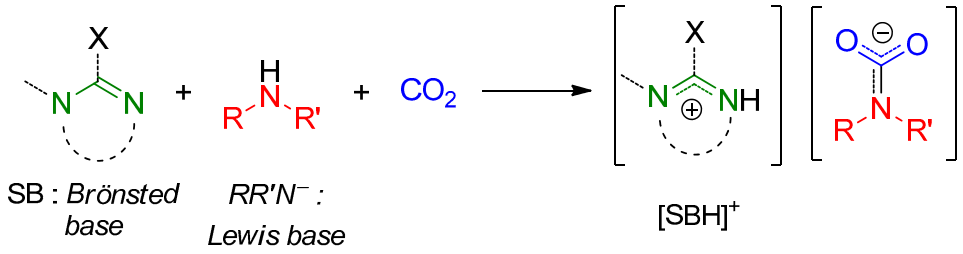

Scheme 9. Formation of amidinium/guanidinium carbamates in the amine/superbase/CO_2 system.

Spectroscopic evidences (^{15}N-NMR) that DBU, TMG and related systems favor the formation of carbamates of primary and secondary amines in organic solvents were presented almost 30 years ago [48,102,103]. The in situ formed carbamates were used for the synthesis of carbamato esters. However, more recently, such concept gained increasing attention for its broader implications. In a series of papers between 2005–2008, it was reported that equimolar mixtures of amidines and NH/OH donors, such as alcohols [104], primary alkylamines [105], α-aminoalcohols [106] or α-aminoesters [107], rapidly react with CO_2 at ambient pressure quantitatively yielding the respective amidinium alkylcarbonate or carbamate. Most of these amidinium salts are liquids at ambient temperature (or low-melting solids) and their formation can be reversed by heating or by bubbling an inert gas through the liquid phase. Hence, these systems have been classified as "switchable ionic liquids," with CO_2 as the element of reversibility. Later, the substrate scope has been extended to the use of guanidines (TMG, TBD) as superbases and secondary alkylamines or α-aminoacids as NH donors [108–115]. These reactions can be carried out by exposing a neat superbase/*N*-donor 1:1 mixture to CO_2 atmosphere or by using classical inert organic solvents. In principle, either two components of the superbase/amine/CO_2 system can be preliminarily mixed and then allowed to react with the third component, as exemplified by the case of morpholine (Scheme 10) [112,114].

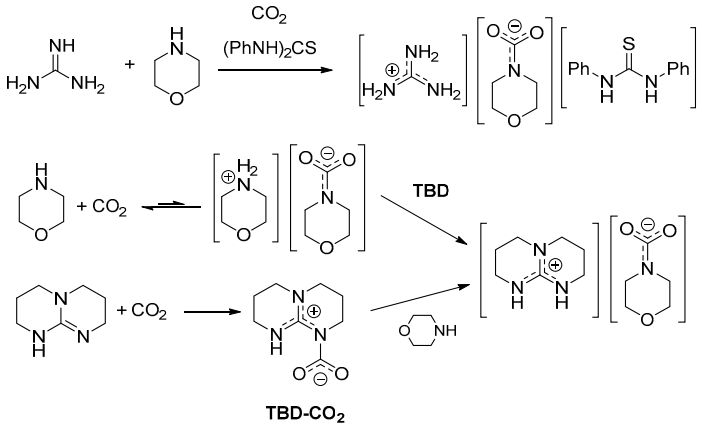

Scheme 10. Three different syntheses of a guanidinium carbamate of morpholine.

It appears that the sensitivity to hydrolysis as well as the overall stability (and associated "switchable" properties) of amidinium/guanidinium carbamates is very much dependent on the superbase/amine combination. In some cases, the "water tolerance" has been referred to the persistence of the (ionic) liquid phase after exposure of the system to air/moisture, even though the formation of bicarbonates was readily observed (Scheme 11a) [105,107].

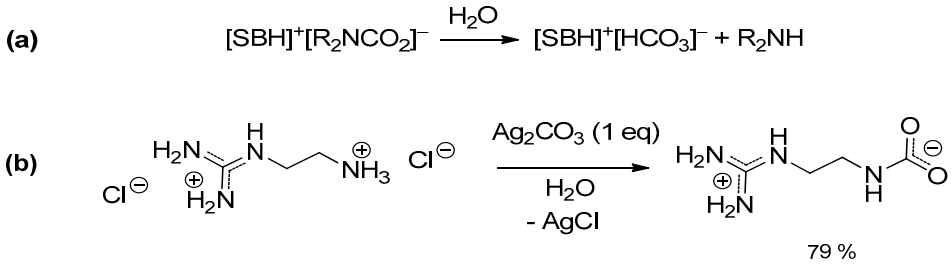

Scheme 11. Hydrolysis of amidinium/guanidinium carbamates (SB = superbase) (**a**); synthesis of (2-amminoethyl)guanidine carbamate (**b**).

It is noteworthy that (2-ammoniumethyl)guanidinium dichloride reacts with Ag_2CO_3 directly in water, affording the corresponding guanidinium carbamate in high yield (Scheme 11b) [116]. This is a rare example of indirect generation of a carbamate (i.e., not using CO_2) and where the superbase and the amine belong to the same molecule. An extensive network of H-bonding is present in the solid state structure, presumably contributing to the stabilization of the system (vs. bicarbonate formation).

The high proton affinity of superbases can stabilize carbamates formed by NH-donors more acidic (and thus less Lewis basic) than alkylamines. In this setting, 1:1 mixtures of amidines/guanidines and azoles or pyrrolidone react in a Brønsted acid/base fashion, forming "protic ionic liquids" (PILs) (Scheme 12). These systems are capable of absorbing significant amounts of CO_2 (generally ≤ 1 equivalent) and spectroscopic data (IR, ^{13}C-NMR) agree with the formation of carbamates [117–121].

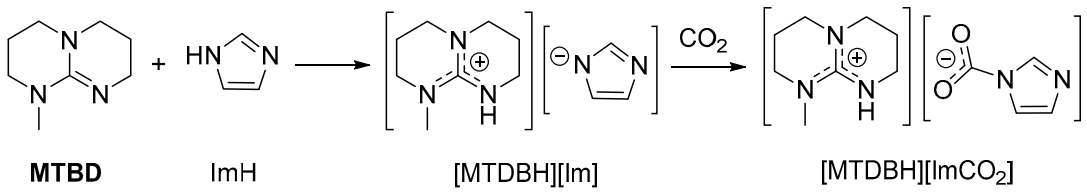

Scheme 12. Reaction of MTBD and imidazole, affording the "protic ionic liquid" [MTDBH][Im], and the subsequent CO_2 uptake in the form of a carbamate.

In conclusion, the study of the interaction of superbases with CO_2 has led to the isolation of unique zwitterionic carbamato adducts and has highlighted new pathways for CO_2 activation. Importantly, the synergistic role of amidines/guanidines in combination with ordinary alkylamines (or other NH-donors) allows the stabilization of a wide range of carbamates and enables their use for stoichiometric and catalytic CO_2 transfer reactions.

3. Synthesis, Structure and Reactivity of Metal Carbamates

Carbamato ligands, as previously defined [42], are monoanionic species with general formula $R_2NCO_2^{(-)}$ (R = H, alkyl or aryl group), resulting from the combination of carbon dioxide with ammonia or most frequently primary/secondary amines. Such anions usually behave as *O*-donors towards metal centers, giving rise to metal carbamato complexes (Scheme 13a). In the present review, we will adopt a general definition of carbamato ligands, which includes those derived from other *N*-donors (e.g., pyridines and related systems) and also dianionic carbamyldiide species, $RN^{(-)}CO_2^{(-)}$ (Scheme 13b).

Carbamates are versatile ligands, offering a wide variety of coordination modes to metal centers, as recognized in solid state structures. The most frequent coordination modes are those wherein the carbamato ligand is bonded to a metal center in monodentate (***M/1***) or chelating (***C/1***) fashion or is bridged between two metal centers (***B/2***). Other possibilities (***C/3***, ***C/5***, ***B/3***, ***B/4*** and ***B/5***) arise from binding additional metal(s) per oxygen atom. Special coordination modes are available to dianionic carbamyldiide ligands, involving the nitrogen atom in the coordination (***D/1*** and ***D/2***).

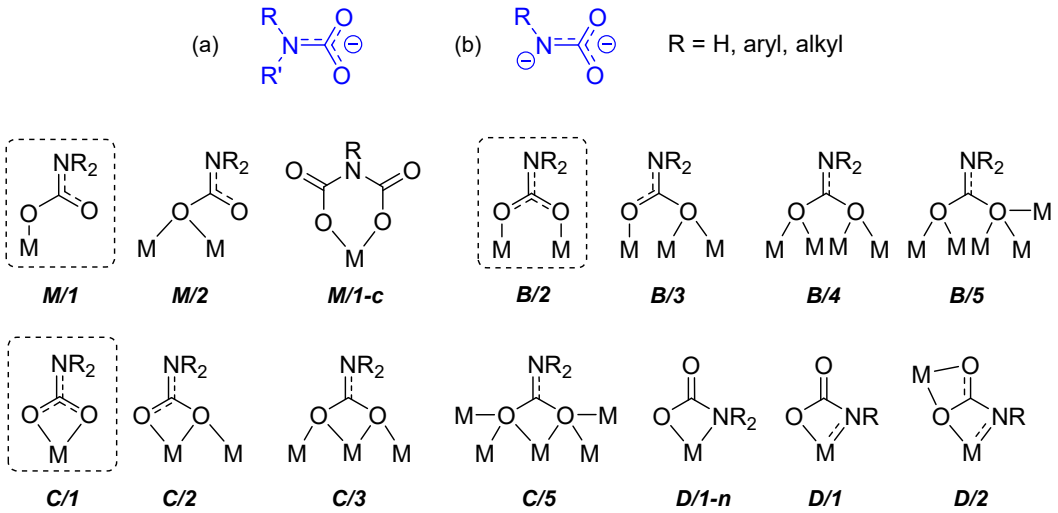

Scheme 13. General structure of a carbamato (**a**) and a carbamyldiide (**b**) ligand and coordination motifs observed in solid-state structures (the most common ones are circled).

Over 380 publications describing the preparation and/or application of circa 1000 metal carbamato complexes have appeared in the literature hitherto, some of them described in 2003 [42]. Herein, we will present a concise but comprehensive description of the preparative methods, structures and reactivity of metal carbamato complexes, with specific reference to the most recent results and novelties.

The first Section 3.1 gives an overall description of the preparative routes and structural aspects of homoleptic metal carbamato complexes, i.e., coordination compounds possessing only carbamato ligands within their coordination sphere. The second Section 3.2 describes the synthetic methodologies employed to introduce (a) carbamato ligand(s) on a generic metal scaffold, thus covering 'heteroleptic' metal complexes. The third Section 3.3 is dedicated to the dynamics and reactivity of carbamato complexes, taking homoleptic complexes as prototypical examples. The final Section 3.4 focuses on spectroscopic and crystallographic data related to carbamato ligands and their coordination modes.

3.1. Homoleptic Carbamato Complexes

Homoleptic carbamato complexes have been reported for a great number of metallic (or semimetallic) elements in the periodic table (Scheme 14). The vast majority of such derivatives are neutral species, complemented by few anionic complexes, and can be represented with the general formula $[M(O_2CNR_2)_n]_m^{0/-}$, where m represents the nuclearity of the system. Homoleptic carbamato complexes are generally associated to the most common oxidation state for M; moreover, they have also been reported for the same metal in different oxidation states (e.g., Ce, Ti, Nb, Ta, Sn). Their distribution in the periodic table reflects a preference for 'hard' oxophilic metal centers, being carbamates effective *O*-donor ligands. However, it has to be considered that a more extended coverage of metals and oxidation states is achieved including a suitable ligand in the coordination sphere, e.g., as for mixed chlorido-carbamato or amino-carbamato complexes (see Section 3.2) [42].

	1	2	3	4	5	6	7	8	9	10	11	12	13	14	15
2	$[LiX]_n$	BeX_2											$[BX_3]_2$		
3	$[NaX]_n$	$[MgX_2]_m$ m = 1,3,6											$[AlX_3]_2$ $[AlX_3]_n$	$[SiX_4]_n$ $[SiX_4]_3$	
4	$[KX]_n$	Ca	Sc	$[TiX_4]$ $[TiX_3]_2$ $[Ti_2X_7]^-$	$[VX_3]_2$ $[VX_3]_n$ $[V_2X_7]^-$	$[CrX_3]_n$	$[MnX_2]_6$ $[MnX_2]_n$	$[FeX_2]_m$ m = 6,n $[FeX_3]_n$	$[CoX_2]_6$	$[NiX_2]_n$	$[CuX]_n$ $[CuX_2]_n$	$[ZnX_2]_n$ $[Zn_2X_5]^-$	Ga	Ge	As
5	Rb	Sr	$[YX_3]$	$[ZrX_4]$	$[NbX_5]$ $[NbX_4]$ $[NbX_3]_2$	$[MoX_2]_2$	Tc	Ru	Rh	Pd	$[AgX]_m$ m = 2,n	Cd	$[InX_3]_n$	$[SnX_2]_2$ $[SnX_4]$	$[SbX_3]_2$ $[SbX_3]$
6	Cs	Ba	*	$[HfX_4]$	$[TaX_5]$ $[TaX_3]_2$	$[WX_3]_2$	Re	Os	Ir	Pt	Au	Hg	Tl	Pb	$[BiX_3]_n$ $[BiX_3]_4$
7	Fr	Ra	*												
6	$[LaX_3]_n$	$[CeX_3]_4$ $[CeX_4]^-$ $[CeX_4]$	$[PrX_3]_4$	$[NdX_3]_4$ $[NdX_3]_n$	$[PmX_3]_4$	$[SmX_3]_4$ $[SmX_3]_n$	$[EuX_3]_4$ $[EuX_3]_n$	$[GdX_3]_4$ $[GdX_3]_n$	$[TbX_3]_4$ $[TbX_3]_n$	$[DyX_3]_4$	$[HoX_3]_4$	$[ErX_3]_4$	$[TmX_3]_4$ $[TmX_3]_n$	$[YbX_3]_4$ $[YbX_3]_n$	$[LuX_3]_4$
7	Ac	$[ThX_4]$	Pa	$[UX_4]$	Np	Pu	Am	Cm	Bk	Cf	Es	Fm	Md	No	Lr

Scheme 14. Periodic table of homoleptic carbamato complexes $[MX_n]_m^{0/-}$ (X = O_2CNR_2; R = H or alky/aryl group); only isolated and characterized compounds are included. Examples not covered in the previous review are highlighted in red (new compounds of already-known types) or in blue (first metal carbamate ever reported). n = unknown nuclearity or polymeric.

Preparative methods. The main synthetic routes to homoleptic metal carbamato complexes are outlined in Scheme 15. They encompass different reactivities, often relying on the in situ generation of the carbamato ligand from the amine/CO_2 system. The possibility and convenience to use one method or another depend on the availability and reactivity of the required metal precursor as well as solubility issues. The various methods are described below, with selected examples taken from the recent literature.

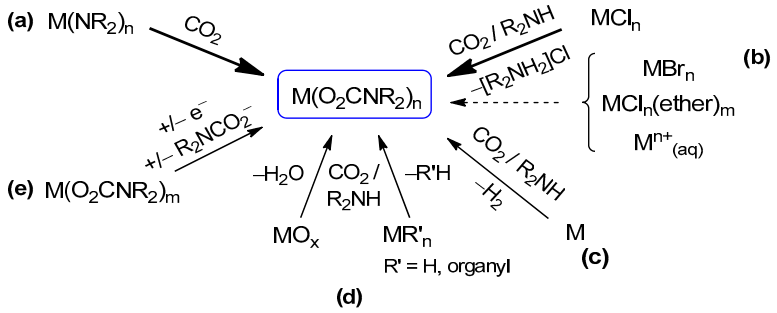

Scheme 15. Synthetic routes to homoleptic metal carbamato complexes: (**a**) carbonation of a metal amide, (**b**) ligand substitution reaction from a metal chloride or related species, (**c**) reaction of CO_2/R_2NH with oxidation of elemental metal, (**d**) reaction of CO_2/R_2NH with a metal oxide or a metal hydride/organyl, (**e**) redox reaction and/or ligand transfer.

The first method entails the carbonation of a metal amide (Scheme 15a). Indeed, $[Ti(O_2CNMe_2)_4]$, the first carbamato complex to be reported, was obtained by exhaustive carbonation of the *N*,*N*-dimethylamido complex of titanium(IV), $Ti(NMe_2)_4$ [122]. Since then, the $M(NR_2)_n/CO_2$ route has been successfully employed in the preparation of homoleptic complexes of the main group metals [42,123], early transition elements [124–131], uranium(IV) and thorium(IV) [132]. In 2010, Kennedy et al. applied this methodology to obtain Li^+, Na^+ and K^+ 2,2,6,6-tetramethylpiperidine (TMP) carbamates [133]. A few years ago, the same method was applied to synthesize homoleptic cerium carbamates $[Ce_3(O_2CMe_2pz)_3]_4$ and $[Ce(O_2CMe_2pz)_4]$ (Me_2pz = 3,5-dimethylpyrazole) from the respective amides $[Ce(Me_2pz)_3]_4$ and $[Ce(Me_2pz)_4]_2$ (Scheme 16a) [134]. These compounds are peculiar in that they contain only ligands of the same type (hence they are 'homoleptic') but one nitrogen atom of the pyrazole ring is also involved in coordination (vide infra).

Concerning p-block metals, carbonation of metal amides was recently used to obtain $[Bi(O_2CN^iPr_2)_3]_4$ from $Bi(N^iPr_2)_3$ [135] and $[Sn(O_2CNMe_2)_2]_2$ from $Sn(NMe_2)_2$ [136] (Scheme 16b,c). Most notably, these complexes represent the first examples of structurally characterized bismuth carbamate and homoleptic Sn(II) carbamate, respectively.

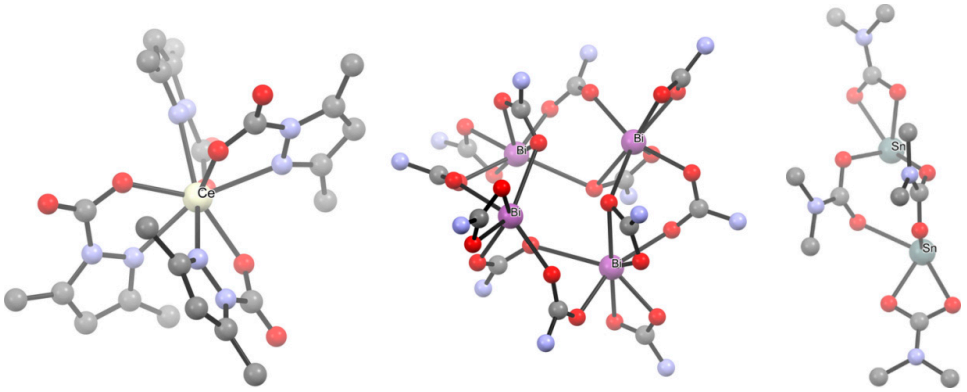

(**a**) (**b**) (**c**)

Scheme 16. View of the X-ray crystal structure of (**a**) $[Ce(O_2CMe_2pz)_4]$, (**b**) $[Bi(O_2CN^iPr_2)_3]_4$ (^{i}Pr groups omitted for clarity), (**c**) $[Sn(O_2CNMe_2)_2]_2$. Drawings based on published data [134–136], H atoms omitted for clarity.

The instability of some metal *N*,*N*-dialkylamides and the difficulties in their preparation, particularly with aryl or complex alkyl groups, prompted the development of alternative synthetic methods. Thus, in 1978, Calderazzo et al. reported the synthesis of uranium(IV) *N*,*N*-dialkylcarbamates, $[U(O_2CNR_2)_4]$, starting from the corresponding anhydrous metal chloride as precursor and NHR_2 saturated with CO_2 as the carbamato source [137]. Since then, the R_2NCO^-/Cl^- metathetical reaction (Scheme 15b) has been employed for the synthesis of a vast number of metal carbamates, including heteroleptic derivatives (see Section 3.2), and can be regarded as the most general synthetic method [42,138]. In the case of secondary amines, the reaction is conveniently carried out in toluene or aliphatic hydrocarbons, wherein the insoluble dialkylammonium chloride byproduct can be easily filtered off, leaving a solution of the metal carbamato product.

Recent examples of homoleptic carbamates obtained by ligand substitution from the respective metal chlorides include $[Ti(O_2CNPyr)_4]$, being the first pyrrolidine-based metal carbamate (Scheme 17a) [139], $[Cu(O_2CN(allyl)_2)_2]$ [140], $[NH_2{}^iPr_2][B(O_2CN^iPr_2)_4]$ and $[B_2(O_2CN^iPr_2)_6]$ [141] and $[In(O_2CNEt_2)_3]$ [142].

Drawbacks along the $MCl_n/R_2NH/CO_2$ route may occur in the case of poorly soluble, unreactive metal chlorides, and can be overcome by employing metal bromide or metal chloride adducts with labile ligands, such as $MCl_n(DME)_m$ or $MCl_n(THF)_m$, as precursors. For instance, $MnCl_2(THF)_{1.6}$ and $FeCl_2(THF)_{1.5}$ were used in the syntheses of $[M(O_2CNEt_2)_2]_6$ and $[M(O_2CN^iPr_2)_2]_n$ (M = Fe,

Mn) [143]. In the case of lanthanides, the use of $LnCl_3(ether)_x$ allowed straightforward preparation of $[Ln(O_2CN^iPr_2)_3]_4$ (Scheme 17b) and $[Ln(O_2CNBu_2)_3]$ (Ln = La, Ce, Pr, Nd, Sm, Eu, Gd, Dy, Ho, Er, Yb, Lu) [23,144–147].

When high valent metal centers and amines bearing alkyl chains longer than C_2 are involved, activation of the amine and reduction of the metal may be observed. Thus, during the purification of $Nb(O_2CNEt_2)_5$ from hot heptane, the pale yellow mixture turned blue with evolution of CO_2 and $Nb(O_2CNEt_2)_4$ was isolated in high yield. The analogous thermal treatment of Nb $(O_2CNMe_2)_5$ afforded only small amounts of reduction product after 48 h at circa 100 °C [131]. In agreement with the generally observed higher stability of the higher oxidation states going down a group of transition elements, $Ta(O_2CNEt_2)_5$ does not undergo appreciable reduction to Ta (IV) under the same conditions.

The observed thermal behavior of $M(O_2CNR_2)_5$ parallels that of the Nb(V) and Ta(V) amides, $M(NR_2)_5$: these species are stable at ambient temperature in the case of tantalum [148], but easily reduce to the +4 oxidation state in the case of niobium [149], the reduction extent increasing on increasing the length of the alkyl group. Both steric and electronic effects play an important role [149].

Even bare aquo-complexes can be used as precursors for the preparation of homoleptic complexes by ligand substitution [150]. In this regard, Armelao, Belli Dell'Amico and co-workers reported, in 2014, an innovative method for the preparation of $[Ln(O_2CNBu_2)_3]_n$ (Ln = Nd, Eu, Tb) [151]. In this procedure, the preformed ammonium carbamate in heptane was used to extract the metal ion from an aqueous solution of Ln^{3+} (obtained by dissolving Ln_2O_3 in HCl). The rapid formation of the carbamato complex and the balanced lipophilicity provided by the amine allowed its extraction in the organic layer while retaining the $[R_2NH_2]Cl$ co-product in the aqueous phase. The extraction method was later extended to Ce(III) [152], Tm(III) [153] and Y(III) [154] carbamato complexes and to the hetero-trimetallic derivative $[Tm_{3/4}Tb_{3/4}Eu_{3/4}(O_2CNBu_2)_{12}]$ [153].

In some cases, homoleptic complexes can be prepared directly from the elemental metal and the R_2NH/CO_2 system in coordinating solvents (e.g., THF, acetonitrile) (Scheme 15c). This methodology is effective for alkali, alkali-earth metals [155,156] and zinc [157]. Clearly, these reactions may proceed through the formation of the metal amide in situ. A recent example of this reactivity is represented by $[Zn(O_2CNH^iBu)_2]$, obtained by treating a suspension of Zn powder in 2-methoxyethanol with a stoichiometric amount of $[^iBuNH_3][O_2CNH^iBu]$ [158]. In this context, we also mention the preparation of the non-homoleptic $[Cu(O_2CNMe_2)(Me_2NH)_2]$ from copper metal and $[NMe_2H_2][O_2CNMe_2]$, in the presence of O_2 as external oxidant [157].

Alternative precursors of homoleptic complexes are metal oxides [159], alkoxides [159], metal alkyls, Grignard reagents [160–162] and $MnCp_2$ [163] (Scheme 15d). All these species react with amines and CO_2 under different conditions, by combining an acid/base reaction with the coordination of the in situ generated carbamato ligand.

In this regard, silver carbamates can be prepared from a suspension of Ag_2O, treated with amine under CO_2 atmosphere [159]. This method has not a general applicability, due to unfavorable thermodynamics, but it is not unique to Ag_2O. Both the neutral polymeric $[Zn(O_2CNMe_2)]_n$ and the dimeric anionic carbamate $[Me_2NH_2][Zn_2(O_2CNMe_2)_5]$ were isolated from the reaction of ZnO with $[Me_2NH_2][O_2NMe_2]$ in MeCN [164]. However, the same reactions did not work with other dialkylamines.

Concerning metal alkyls, lithium *N*,*N*-dialkylcarbamates were recently prepared starting from ^nBuLi and CO_2 in the presence of diisopropylamine or pyrrole [165]. A related reaction was reported with NaH, providing a more convenient pathway to $Na(O_2CNEt_2)$ compared to the use of sodium sand [166]. Additionally, in these cases, intermediacy of the in situ formed metal amide is conceivable.

Finally, a preformed carbamato complex can be exploited to obtain homoleptic derivatives (Scheme 15e). This is related to trans-metalation procedures [167] or redox reactions, the latter possibly accompanied by ligand transfer (e.g., reduction of Nb^V, Ta^V or Ti^{IV} to lower-valent derivatives of Nb^{IV}, Ta^{III} and Ti^{III}, respectively) [131,167–170] (Scheme 15e).

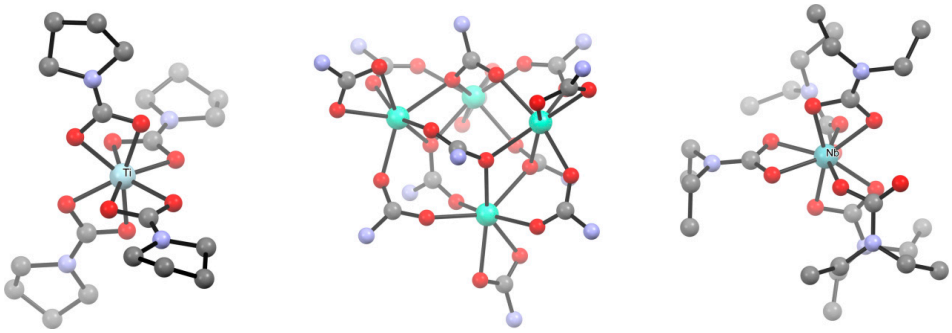

(**a**) (**b**) (**c**)

Scheme 17. View of the X-ray crystal structure of (**a**) [$Ti(O_2CNPyr)_4$] (Pyr = pyrrolidine), (**b**) [$Ln(O_2CN^iPr_2)_3]_4$ (Ln = La, Pr, Nd, Sm, Eu, Gd, Dy, Ho, Er, Yb, Lu) (^{i}Pr groups omitted for clarity), (**c**) [$Nb(O_2CNEt)_5$]. Drawings based on published data [23,144–147,171], H atoms omitted for clarity.

Structural aspects. Homoleptic metal carbamates exhibit a wide range of nuclearities in the solid state, ranging from monometallic complexes to oligomeric and even polymeric structures. The aggregation is realized by bridging coordination of the carbamato moieties, as well as metal-metal bonding in some cases, and can be regulated by the nitrogen substituents, with bulkier groups usually favoring a lower degree of aggregation. For instance, [$Ti(O_2CNR_2)_4$] (R = Me, Et, ^{i}Pr, pyrrolidine; Scheme 17a) and [$Nb(O_2CNR_2)_5$] (R = Me, Et; Scheme 17c) are examples of mononuclear complexes featuring only chelating (***C/1***) or chelating (***C/1***) and monodentate (***M/1***) carbamates, respectively [130,171–174]. On the other hand, homoleptic diethyl or dimethyl carbamato derivatives of W(III), Mo(II) and Sn(II) (Scheme 16c) are dinuclear, featuring bridging ligands (***B/2***) and the first two complexes also M-M bonding [136,175,176]. The structure of [$Bi(O_2CN^iPr_2)_3]_4$ is tetrameric, each Bi being coordinated by one chelating (**C/1**), one bridging (***B/2***) and one bridging-chelating (***C/2***) carbamato groups in a distorted pentagonal bipyramidal environment (Scheme 16b) [135]. Instead, *N*,*N*-diisopropyl carbamates of Ln(III) (Ln = Pr, Nd, Sm, Eu, Gd, Dy, Ho, Er, Yb, Lu) are isostructural and exhibit a tetrameric structure with C_2 symmetry and heptacoordinated metal centers (Scheme 17b) [23,145–147]. In these complexes, the carbamato ligands adopt three different coordination modes, binding one (***C/1***), two (***B/2***) or three (***B/3***) metal centers, respectively. From the collection of all the presented structures, Belli Dell'Amico et al. highlighted a parabolic trend in the decrease of Ln-O bond distances over the lanthanide series [145]. The only exception to this structural motif is represented by the Ce(III) derivative, showing a less symmetrical structure in which it is possible to observe five different coordination modes (***C/1***, ***C/2***, ***B/2***, ***B/3***, ***B/4***) [144]. This particular arrangement leads to a packing in which the metal atoms are not completely surrounded by the ligands, allowing the favorable oxidation to Ce(IV) by means of O_2 (vide infra). Hexanuclear structures are adopted by Mg(II), Mn(II) and Co(II) diethyl carbamates [42].

In some cases, the nuclearity of homoleptic complexes in the solid state has not been determined and a polymeric structure was suggested, based on the insolubility in non-coordinating solvents (e.g., benzene or toluene). This feature is common to several alkali metal carbamates [156,177], including those of bulky 2,2,6,6-tetramethylpiperidine [133]. On the other hand, the lithium diisopropyl derivative [$(LiO_2CN^iPr_2)_{12}(^iPr_2NCOOH)_2$] is a dodecanuclear cluster decorated with a rare carbamic acid ligand [47,84,178], whose formation has been ascribed to adventitious hydrolysis [165].

Unusual coordination environments have been recognized for cerium 3,5-dimetylpyrazole (Me_2pz) carbamates, also due to the chelation of the metal center by the non-carbonatated pyrazole nitrogen [134]. The structure of [$Ce(O_2CMe_2pz)_3]_4$ comprises a 9-coordinate Ce(III) atom displaying three different coordination modes for the ligands (***M/1***, ***C/2***, ***B/3***), while the corresponding Ce(IV) complex (Scheme 16a) and the anionic Ce(III) derivative [Bu_4N][$Ce(O_2CMe_2pz)_4$] are mononuclear based on 8-coordinate cerium center.

3.2. Heteroleptic Carbamato Complexes

Heteroleptic metal carbamato complexes are those including additional ligands in the coordination sphere. Such classification encompasses many derivatives that are closely related to the parent homoleptic compounds, such as mixed chlorido-carbamates or amino/amido-carbamates (vide infra). These can be viewed as intermediate products along the preparative routes that (in principle or in practice) lead to the homoleptic congeners. On the other hand, a large number of complexes presents a single carbamato unit. These include most organometallic derivatives or coordination compounds featuring very sophisticated, multidentate ligands. In such cases, the carbamato ligand is ancillary with respect to the properties and reactivity of the compound itself.

Given the vast and heterogeneous amount of information, the present discussion will provide an overview of the various synthetic methods available for the introduction of a carbamato ligand (Scheme 18), with selected examples taken from the most recent literature. This approach will highlight the applicability and limitations of each method along the periodic table.

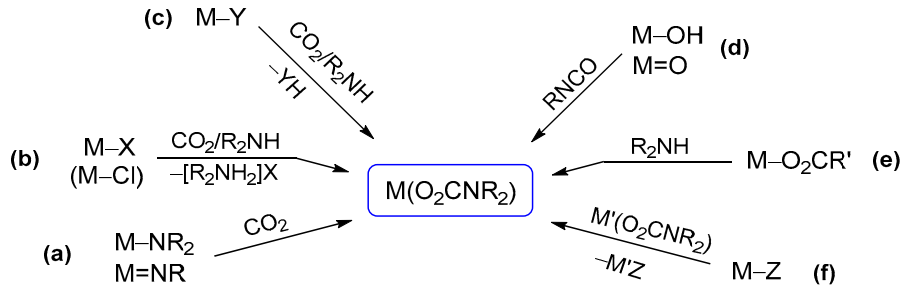

Scheme 18. Main synthetic routes for the assembly of a carbamato ligand on metal complexes: (**a**) carbonation of an M−N bond, (**b**) chloride (or another anionic ligand) substitution, (**c**) coupled ligand substitution/proton transfer reaction, (**d**) coupling of a hydroxido (or oxido) ligand with organic isocyanates, (**e**) reaction of an amine with a metal carboxyl complex and (**f**) ligand transfer route.

Carbon dioxide insertion into M−N bonds (Scheme 18a). The reaction of an alkylamido group with CO_2, leading to the generation of a carbamato ligand, has found widespread use for s-block [42] and early d-transition metals [125,126,128–130,179]. In this regard, new fascinating examples have been recently reported [133,180–186]. The simplest cases are represented by homoleptic metal amido complexes undergoing selective carbonation, leading to mixed amido-carbamato derivatives. For instance, Cotton et al. reported the partial carbonation of Ti(III) amido, resulting in dimeric amido-carbamato compounds, showing diamagnetic behavior due to anti-ferromagnetic coupling [180] (Scheme 19a).

On the other hand, the insertion of CO_2 into M−N bonds was only sparingly applied to lanthanides, actinides and late transition metals [132,187–189] in the beginning. The scenario changed over the last 15 years, as several carbamato complexes obtained by this methodology were reported, and especially organometallic species. These include late d-block metals such as iridium [190,191], nickel [192–197], palladium [198,199], gold [200] and zinc [201–204], f-block metals cerium [134] and uranium [205–209] and p-block metals tin [210] and gallium [211,212]. Furthermore, in situ-formed amide complex of Zn(II) and alkyl-amide of Mg(II) were mixed under carbon dioxide atmosphere to afford a heterobimetallic Zn/Mg alkyl-carbamato derivative [213]. Selected cases are represented in Scheme 19b–d, including a rare type of a primary carbamato ligand in the U(IV) derivative [Cp*(COT^{TIPS2})U(O_2CNH_2)] [206].

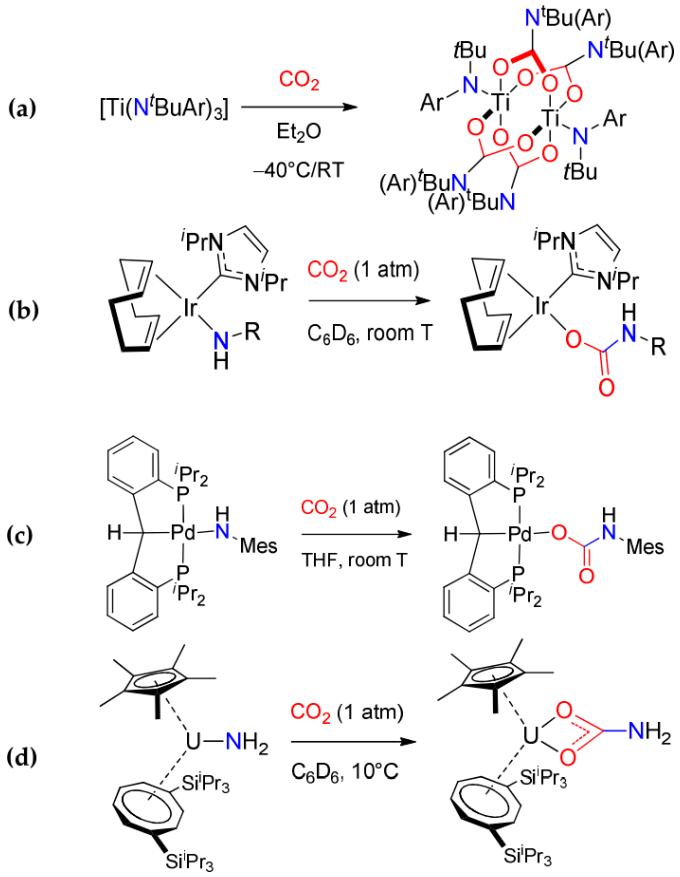

Scheme 19. Syntheses of metal carbamates obtained by carbonation of amido ligands: (**a**) dinuclear Ti(III) amido-carbamates obtained by partial carbonation of the homoleptic amides, (**b**) organometallic Ir(I) carbene, (**c**) Pd(II) PCP-pincer and (**d**) primary U(IV) carbamate complexes.

The generally accepted mechanism [214,215] for low-valent d-transition metals involves a direct nucleophilic attack of the metal-coordinated nitrogen to carbon dioxide, with the generation of an intermediate *N*-bound carbamato/carbamic acid moiety. Subsequent rearrangement provides the typical *O*-coordinated carbamato ligand [187,188,191,192,216]. A further confirmation was recently reported for Mo(0) and W(0) complexes bearing a diphosphino amide pincer ligand (Scheme 20) [185]. In this case, the geometry of the ligand forces the nitrogen atom to remain coordinated after CO_2 addition, thus stabilizing a rare example of monoanionic *N*,*O*-chelating carbamato ligand (***D/1-n***).

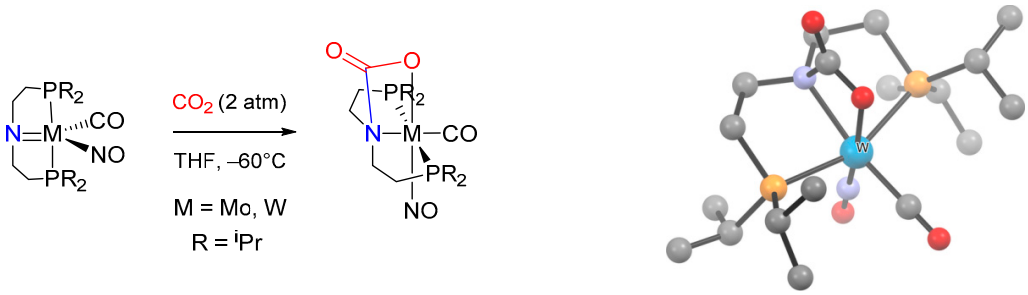

Scheme 20. Carbonation of the diphosphino amide ligands within Mo(0) and W(0) complexes, resulting in the unusual *N*,*O*-bound carbamate ligand, and crystal structure of the tungsten isopropyl derivative (H atoms omitted for clarity). Drawing based on published data [185].

Some of the late transition metal complexes featuring a monodentate carbamate are quite unstable towards decarboxylation, either in solution or in the solid state, especially under vacuum [190–192,198,200]. Among other factors, the relatively strong metal-nitrogen bond may contribute to the reversibility of the CO_2 insertion process.

The insertion of CO_2 into M–N bonds has also been reported for Sc(III) [217], Ti(IV) [218–220], Ni(II) [221], Pd(II) [222] and Ir(III) [223,224] imido complexes. The dianionic carbamyldiide ligand thus generated usually remains coordinated to the metal via N,O (Scheme 21a). Additionally, in this case, a mechanism involving the direct nucleophilic attack of nitrogen to carbon dioxide appears to be favored over a [2 + 2] cycloaddition [185,222]. The cyclic metallacarbamato ligand may undergo further reactions, i.e., a second CO_2 insertion to produce a bis-carbamato (azadicarboxylato) ligand [220,221] or proton abstraction from another ligand, affording an ordinary carbamato ligand [224].

Formation of exotic polyanionic carbamato ligands was observed by addition of CO_2 to a nitrido-bridged diuranium(IV) complex [225,226], and to zirconocene and hafnocene dinitrogen complexes [227,228] (Scheme 21). These systems are prone to double CO_2 insertion, either on the same or on different nitrogen atoms [229].

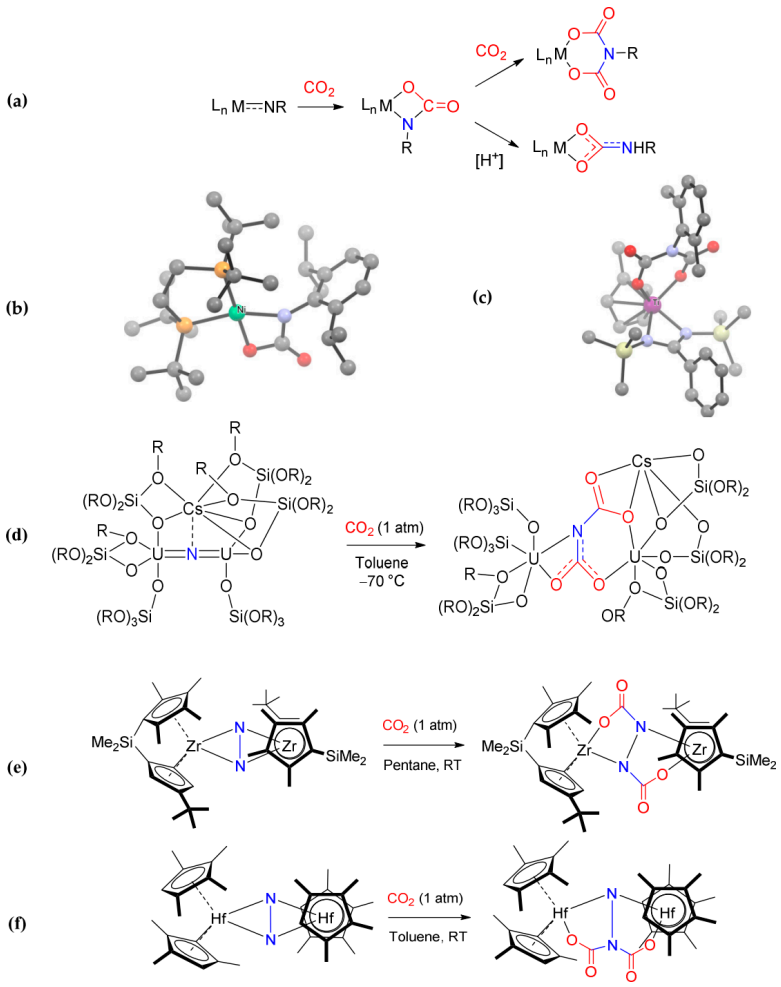

Scheme 21. Insertion of CO_2 into different M–N bonds: (**a**) general reactivity scheme for a metal imido complex with CO_2 and crystal structures of [Ni(ditbpe)(κ^2*N*,*O*-O_2CNXyl)] (**b**) and [Ti(η-C_5H_4Me){$(O_2C)_2$N(-2,6-$C_6H_3Me_2$)}{PhC($SiMe_3$)$_2$}] (**c**); double carbonation of a diuranium bridging nitride ligand (**d**); metal dinitrogen metallocene complexes of zirconium (**e**) and hafnium (**f**). Drawings based on published data [220,221,225,227,228], H atoms omitted for clarity.

Ligand substitution reactions (Scheme 18b). Partial ligand substitution along the $MCl_n/CO_2/R_2NH$ pathway gives access to mixed species such as metal chlorido-carbamates or amino-chlorido-carbamates [42]. For instance, the reaction of $ZnCl_2$ with Et_2NH/CO_2 in THF afforded $[Zn_2(\mu\text{-}O_2CNEt_2)_3Cl(Et_2NH)]$, displaying a paddlewheel structure with bridging (***B/2***) carbamato ligands [230]. A very recent example of partial substitution from a metal chloride is the reaction of $TiCl_4$ with one equivalent of preformed $[TMG][O_2CNEt_2]$ (TMG = tetramethylguanidine), leading to the trinuclear $[TiCl_2(O_2CNEt_2)_2]_3$ [109]. Interestingly, the co-product is not the expected guanidinium chloride but the hexachlorometalate $[TMG]_2[TiCl_6]$ (probably formed via addition of chlorides to unreacted $TiCl_4$), which can be easily removed by filtration.

More in general, metal chlorido complexes can be used as precursors for the installation of carbamato unit(s) [166,171,231–233]. In this setting, treating $TiCp^*_2Cl$, $VOCl_3$ and $NbOCl_3$ with pre-carbonated amines respectively allowed the isolation of $[TiCp^*_2(O_2CNEt_2)]$ [234], $[VO(NMe_2)(O_2CNMe_2)_2]$ [166] and $[NbO(O_2CNEt_2)_3]_2$ [171] (Scheme 22a). Similarly, ruthenium(II) complexes *mer*-$[RuCl(O_2CN^iPr_2)(PPh_3)_3]$ and $[Ru(O_2CN^iPr_2)_2(PPh_3)_2]$ were prepared by chloride/carbamate exchange from $[RuCl_2(PPh_3)_3]$ and the chloro-bridged dimer $[Ru_2Cl_5(PPh_3)_4]^-$, respectively (Scheme 22b) [231].

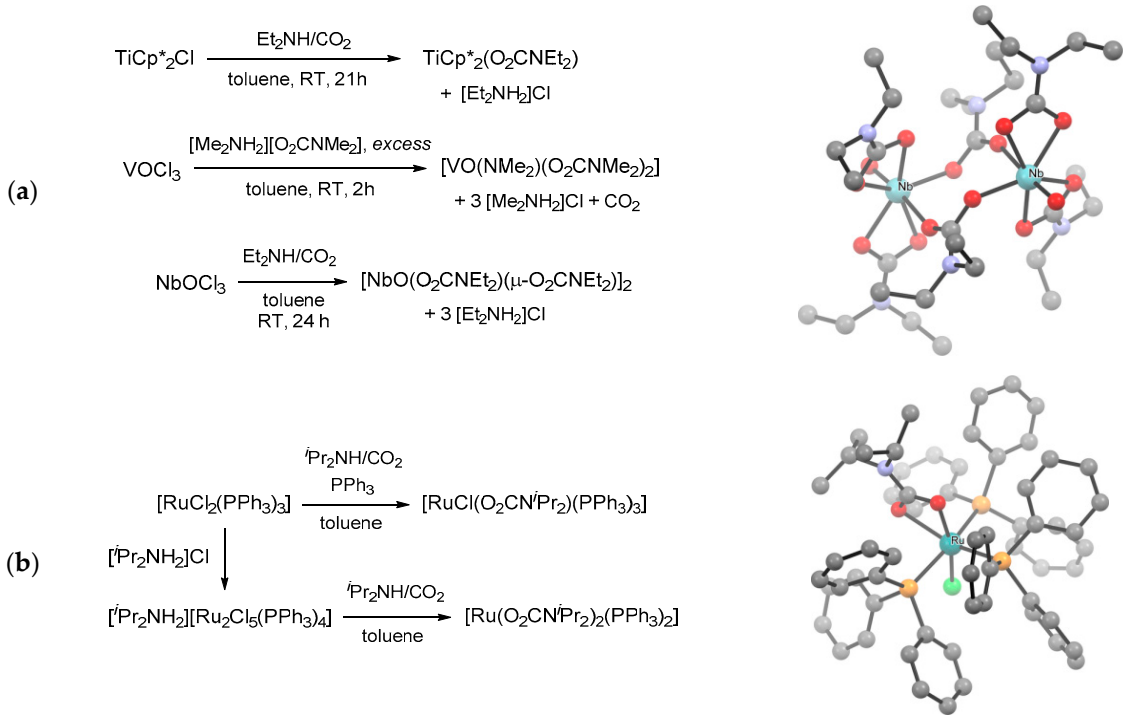

Scheme 22. Metal carbamato complexes obtained by $Cl^-/R_2NCO_2^-$ exchange: reactions of $TiCp^*_2Cl$, V(V) and Nb(V) oxido-chlorides with amines/CO_2 and X-ray structure of $[NbO(O_2CNMe_2)_3]_2$ (**a**); preparation of *mer*-$[RuCl(O_2CN^iPr_2)(PPh_3)_3]$ and $[Ru(O_2CN^iPr_2)_2(PPh_3)_2]$ from Ru(II) chloride precursors and X-ray structure of the former (**b**). Drawings based on published data (H atoms omitted for clarity) [171,231].

Other metal compounds, such as Dy(III) [235], Fe(II) [236], Cu(II) [237–241], Ni(II) [239] and Zn(II) [240–243] perchlorates, nitrates and sulfates, uranyl diacetate [244] or $[Pd(MeCN)_4]^{2+}$ [245] were used as starting materials for the preparation of carbamato derivatives. The reactions are usually carried out in polar organic solvents (MeOH, MeCN) in the presence of amines, polyamines or aza-macrocyclic ligands under CO_2 atmosphere (Scheme 23a). Most importantly, some cases of CO_2 fixation directly from ambient air have been reported [233,235,237–239,241,244,246,247].

The combination of two different salts allowed the preparation of heterobimetallic 3d/4f carbamato compounds, also in a one-pot fashion (Scheme 23b) [246,247]. Such compounds aroused great interest within the scientific community for their magnetic properties.

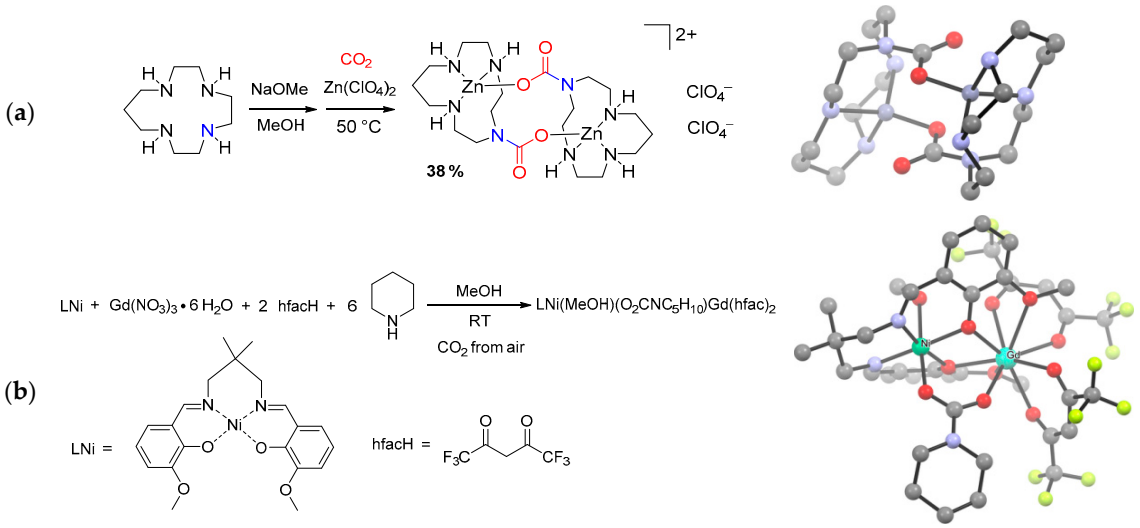

Scheme 23. Synthesis and views of the X-ray crystal structures of: (**a**) a Zn(II) macrocyclic carbamate obtained from [13]aneN4 (1,4,7,10-tetra-azacyclotridecane), $Zn(ClO_4)_2$ and CO_2; (**b**) a heterobimetallic Ni/Gd complex with bridging morpholine carbamato ligands. Drawing based on published data (H atoms omitted for clarity) [242,246].

Coupled ligand substitution/proton transfer reactions (Scheme 18c). In principle, a metal complex bearing a ligand that can be removed upon protonation by amines (or in situ formed carbamic acids/ammonium carbamates) can be a precursor for the installation of a carbamato ligand. Organolithium compounds, Grignard reagents and other d-block and p-block alkyls can be employed to this purpose, hence the generation of the carbamate may proceed through the intermediacy of a metal-amide unit [42]. These reactions are usually conducted in coordinating solvents (e.g., THF, Et_2O), which are often found incorporated in the final complex [165,248]. For instance, the reaction of MeMgBr with *N*-methylaniline and CO_2 in THF leads to the dimer $[Mg(O_2CN(Me)Ph)(THF)_2Br]_2$, where magnesium shows a trigonal bipyramidal coordination geometry [248] (Scheme 24a).

The use of metal oxides or oxido/alkoxido complexes as precursors, although less frequent, may also be included in this category [42]. For instance, octanuclear carbonato-carbamates of general formula $[Me_2NH_2]_n[Mg_8(CO_3)_2(O_2CNMe_2)_{(12+n)}]$ (n = 0–3) were obtained by treating magnesium oxide with $[Me_2NH_2][O_2CNMe_2]$ in toluene, the value of n depending on the reaction conditions. In particular, $[Me_2NH_2]_3[Mg_8(CO_3)_2(O_2CNMe_2)_{15}]$ converted into $[Mg_8(CO_3)_2(O_2CNMe_2)_{12}]$ (n = 0) by heating under vacuum [249]. A basic example of the present synthetic procedure is provided by a Bi(III) complex with an amino-alkoxido ligand [250]: carbonation of the pendant amino group is followed by intramolecular proton transfer and ligand slippage, yielding the carbamato moiety (Scheme 24b).

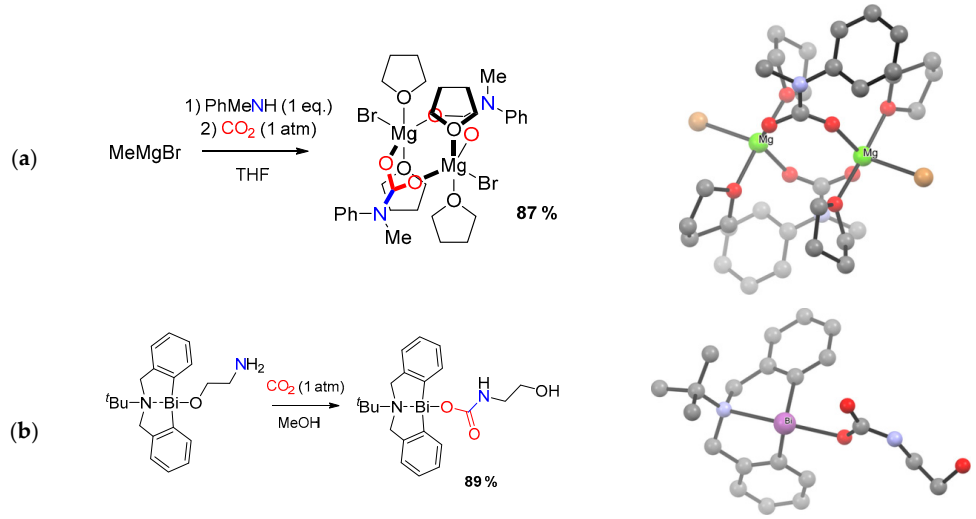

Scheme 24. Synthesis and views of X-ray structures of: (**a**) dinuclear Mg carbamate from Grignard reagent; (**b**) Bi(III) carbamato complex from carbonation of amino-alkoxide ligand. Drawings based on published data (H atoms omitted for clarity) [248,250].

Reaction of hydroxido(oxido) ligands with organic isocyanates (Scheme 18d). The reaction of a M–OH (or M=O) moiety with an organic isocyanate represents a further possibility to build a carbamato ligand. In the past, only a few metal carbamato complexes were obtained by this route, namely Hg(II) [251], Os(II) [252] and Pt(IV) [253] derivatives. Recently, the family of metal carbamates generated in this way have greatly expanded, including lanthanide compounds [254,255], Ti(IV)-oxido [220], Re(I)-carbonyl [256], Co(III)-pentamine [257] and Ni(II) pincer complexes [258,259]. Moreover, this method has gained increasing importance in the preparation of Pt(IV) compounds (Scheme 25). More precisely, coupling of a Pt(IV) (bis)hydroxo species with an alkyl or aryl isocyanate affords the corresponding (bis)carbamate. Following optimization [260], allowing the reaction to be conducted in dimethylformamide and not in neat isocyanate, more than 60 different Pt(IV) species were thus prepared, arousing interest as possible anticancer agents (see Section 5) [261–268].

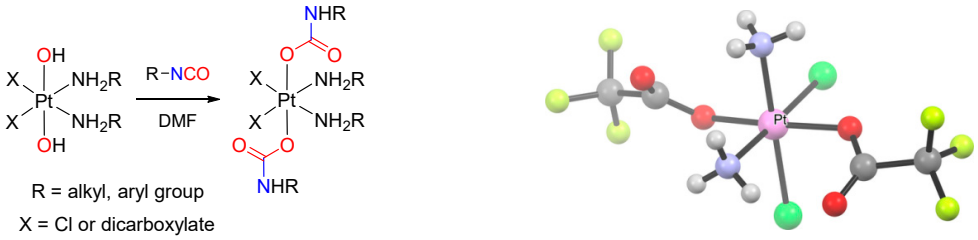

Scheme 25. General reaction of a Pt(IV) (bis)hydroxo species with alkyl/aryl isocyanate affording a Pt(IV) (bis)carbamate and view of the X-ray crystal structure of *cis*,*cis*,*trans*-$[PtCl_2(NH_3)_2(O_2CNCF_3)_2]$. Drawing based on published data [260].

Reaction of an amine with a metal carboxyl complex (Scheme 18e). Another type of synthesis comprises the reactions of amines (or *N*-donors in general) with a metal carboxyl complex, i.e., bicarbonate [269], formate [270,271], carbonate ester [272] or a CO_2 adduct directly [273]. As an example, the intramolecular attack of an amine group belonging to a tetradentate pyridylamine ligand onto a Zn(II)-HCO_3 species resulted in carbamate generation [269] (Scheme 26a). In this regard, a novel synthetic approach consisting in the addition of amines to a Pt(IV)-carbonate ester has been recently proposed (Scheme 26b). This method offers the opportunity for preparing a number of Pt(IV) carbamato derivatives, including some related to secondary amines, thus extending the scope provided by the hydroxide/isocyanate coupling [272].

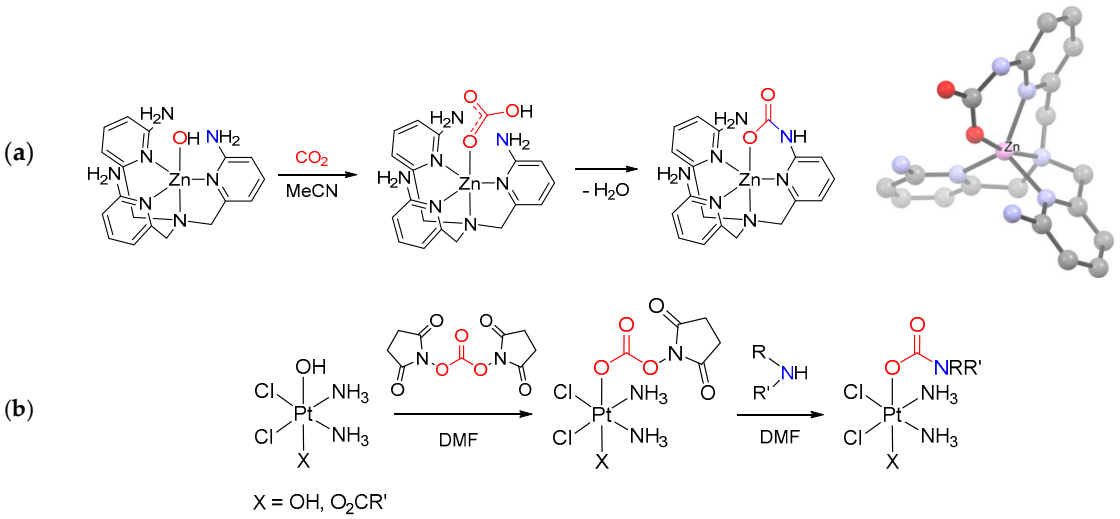

Scheme 26. Metal carboxyl complexes as precursors of metal carbamates. (**a**) Formation and view of the X-ray crystal structure of a Zn(II) carbamate complex containing a *N*,*N*,*N*,*N*-tetradentate ligand, via intramolecular amine/HCO_3 reaction. Drawing based on published data (H atoms omitted for clarity) [269]. (**b**) Reaction of *cis*,*cis*,*trans*-[$PtCl_2(NH_3)_2(OH)X$] with bis(2,5-dioxopyrrolidin-1-yl)carbonate followed by amine addition to the activated ester.

Other methods. Within the plethora of organometallic complexes, another strategy for the installation of a carbamato ligand relies upon the in situ generation of suitable unsaturated fragments [274–276]. For instance, reductive elimination of benzene from a phenyl Ir(III) trispyrazolyl borate compound generated a 16e$^-$ intermediate capable of incorporating CO_2 as a carbamate, with the aid of an ancillary metallapyridine ligand (Scheme 27) [274]. A closely related example is represented by the addition of indole-1-carboxylic acid on a formally 16e$^-$ Cp*Ir(III) amido complex [277].

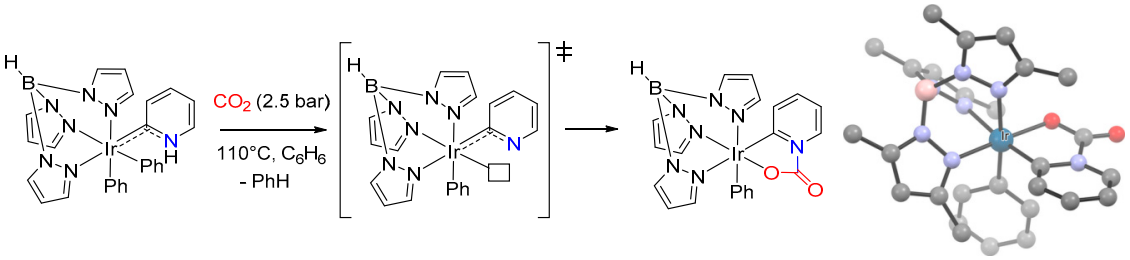

Scheme 27. Synthesis and view of the X-ray crystal structure of Ir(Tp) carbamate. Drawing based on published data (H atoms omitted for clarity) [274].

A peculiar ligand-assisted addition of CO_2 was reported for a Fe(II) compound containing a pyridyl-amine ligand. In this case, carbonation of the amino group belonging to a bidentate ligand resulted in the formation of an eight-membered pyridyl-carbamate. The reaction is readily reversible by heating [278].

The formation of a heterodinuclear Fe/In carbonyl-carbamato complex was reported starting from an iron carbonyl-carbamoyl precursor by reaction with $InMe_3$. The oxygen transfer to the carbamoyl ligand forming the carbamate is possible due to the decomposition of a second carbamoyl unit [279].

Ligand transfer routes (Scheme 18f). Over the years, the trans-metalation reaction has been extensively employed for the targeted synthesis of various metal carbamates, especially organometallics [42]. Typically, this method exploits silver or alkali metal carbamates as transfer reagents, taking advantage of the precipitation of the metal halide side-product (e.g., NaCl, LiCl, AgCl, AgBr) as the driving force of the reaction (Scheme 28a) [109,133,159,166,212,280]. Attempts to realize

trans-metalation based on other combinations of metals may result in carbamato ligand transfer [42] or in the formation of a hetero-bimetallic product [281,282].

Another type of ligand transfer reaction can be performed by mixing equimolar amounts of a metal halide and its corresponding homoleptic carbamate, selectively affording a mixed halido-carbamato complex (Scheme 28b) [109,172].

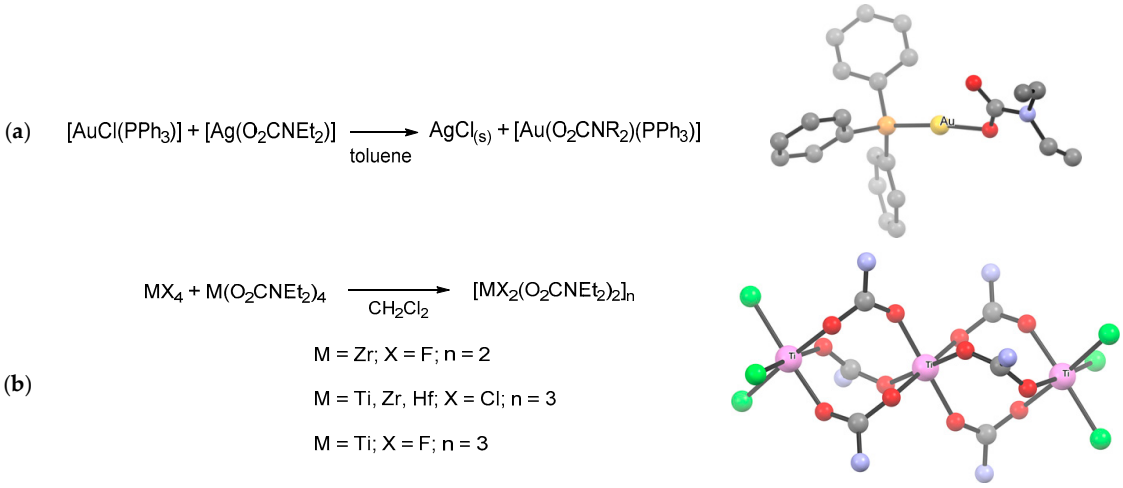

Scheme 28. Synthesis and views of X-ray crystal structures of metal carbamato complexes prepared by ligand transfer reactions: (**a**) $[Au(PPh_3)(O_2CNEt_2)]$ obtained by trans-metalation with silver carbamate; (**b**) combination of Group 4 metal halides and their homoleptic carbamates, affording mixed halido-carbamato complexes and structure of $[Ti_3Cl_6(O_2CNEt_2)_6]$. Drawings based on published data (H atoms and Et groups in the Ti complex omitted for clarity) [109,159].

3.3. Dynamics and Reactivity of Metal Carbamato Complexes

Carbamato ligand dynamics. Metal carbamates may manifest a dynamic behavior, through the occurrence of processes summarized in Scheme 29. Homoleptic metal carbamato complexes have been widely investigated from this perspective.

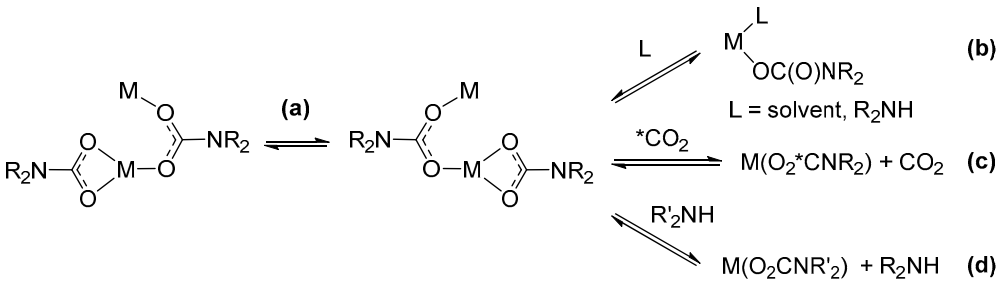

Scheme 29. Dynamics of carbamato ligands in solution: (**a**) intramolecular ligand exchange, (**b**) ligand/solvent (reversible) addition, (**c**) CO_2 exchange with external carbon dioxide, (**d**) transamination reaction.

Carbamato ligands in metal complexes are usually able to exchange their position and their coordination modes in solution, as demonstrated by variable temperature NMR measurements [127,138,248,283–285]. For instance, the two carbamato ligands in $[Mg_2Br_2(\mu\text{-}O_2CNMePh)_2]$ are fluxional, rapidly shifting from bridging (***B*/2**) to bridging-chelating (***C*/2**) mode down to 0 °C, when the exchange turns slow on the NMR time scale [248].

The fluxionality of the carbamato ligand, jointly with the possibility of turning from bidentate to monodentate coordination, permits the entrance of additional ligands in the metal coordination

sphere. The possible subsequent decrease in nuclearity of the metal system may lead to dissolution of the otherwise insoluble metal carbamate. The first observation of such a behavior was reported in 1988 by Calderazzo et al. [286]. Some Cu(II) *N*,*N*-dialkylcarbamates, obtained by the typical $CuCl_2$/amine/CO_2 route in heptane, were no longer soluble in the same solvent following their isolation in the solid state. The authors suggested that the initial solubility could be ascribed to the coordination of one or more amine molecules, present in excess in the reaction mixture. Other examples of metal *N*,*N*-dialkylcarbamates changing their solubility in the presence or absence of amines were later reported [143,287,288]. Analogous equilibria can also explain the solubility of metal carbamates in coordinating solvents [42]. In this regard, THF or TMEDA adducts were recently isolated growing crystals of lithium carbamates [133,165].

Another aspect related to the dynamics of metal carbamato complexes in solution is their ability to interchange the carboxyl unit with external CO_2 while maintaining their structures intact [42,125,127]. This property was confirmed in 2005 by McCowan and Caudle by $^{13}CO_2$ uptake experiments on zinc derivatives [289]. Furthermore, metal carbamates might be susceptible to transamination, exchanging the internal R_2N group with that coming from an external amine. This feature was exploited for the preparation of $[Al(O_2CNEt_2)_3]$ [290], $[Nd(O_2CNEt_2)_3]$ [145], $[Eu(O_2CNBn_2)_3]$ and $[Sm(O_2CNBn_2)_3]$ [151], taking advantage of the volatility of the outgoing amine and/or the lower solubility of the metal carbamato product.

Reactivity with electrophiles. Metal carbamato complexes can be quite reactive towards electrophilic agents. Indeed, carbamato ligands are generally prone to electrophilic attack on the nitrogen or oxygen atom(s). In all cases, the M–O(carbamate) bond(s) is detached, but products vary depending on the type of electrophilic agent, i.e., organic electrophiles or protic species (Scheme 30).

The reactivity with carbon-based electrophiles has been widely studied [42]. The addition of the electrophile to the oxygen atom(s) forms a carbamato ester, while addition to the nitrogen leads to a derivatized amine with release of gaseous CO_2, Scheme 29a.

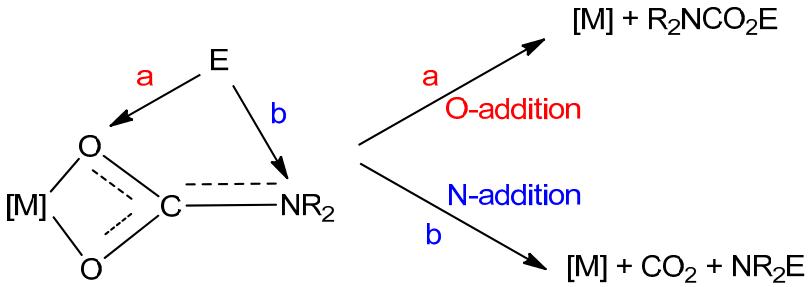

Scheme 30. Possible reactions of an electrophile E with a carbamato ligand.

On these grounds, *O*-addition compounds are kinetic products but they are synthetically relevant since their formation represents a net incorporation of carbon dioxide. For instance, stoichiometric reactions with alkyl halides or acyl halides afford the corresponding urethanes and carbamic-carboxylic anhydrides (Scheme 31) [42]. In general, the regioselectivity of these reactions (*O* vs. *N* addition) is variable depending on the system. Urethanes can undergo a second alkylation giving the ammonium salt, while the carbamic-carboxylic anhydride, in the presence of Cu(II) and Fe(III), decomposes affording the corresponding amide via CO_2 elimination. On the other hand, the use of an *N*-alkylcarbamate in combination with acyl chlorides gives a mixture of isocyanate and carboxylic acid (Scheme 31). A recent example of this reactivity is supplied by the formation of organylsilylurethanes $R_nSi(O_2CNR'_2)_{(4-n)}$ from the reaction of Sn(IV) tetracarbamates with organylchlorosilanes ($R_nSiCl_{(4-n)}$) [291].

In summary, the carbamato ligand in transition metal complexes is a versatile platform to carry out diverse metal-mediated organic transformations, constituting the conceptual basis for the use of metal carbamates in catalysis. The organic chemistry of carbamato ligands will be covered in more detail in Section 4, with a focus on catalytic processes.

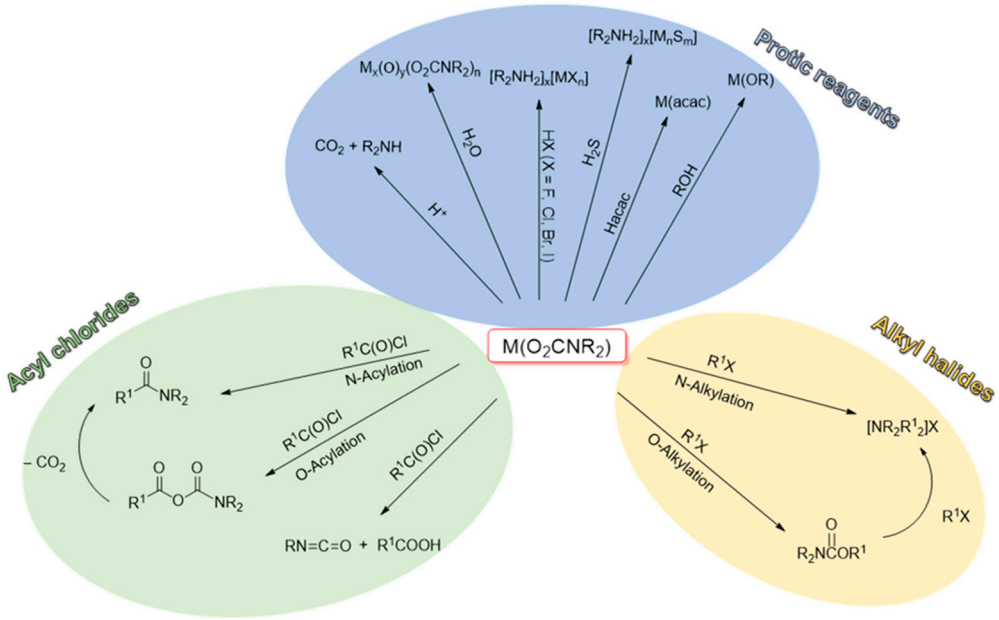

Scheme 31. Reactivity patterns for metal carbamato complexes with electrophilic species.

Conversely, the addition of H^+ from any protic source usually determines the disruption of the carbamato moiety, with the consequent release of the amine and CO_2. On thermodynamic grounds, the formation of gaseous carbon dioxide ($\Delta G°_f = -394.4$ kJ/mol at 25 °C) is the driving force for these degradation reactions.

Water is the simplest protic species and hydrolytic reaction(s) have been observed with reference to almost all the categories of carbamato complexes. Therefore, the presence of water is normally undesired, and moisture sensitivity is the "Achille's heel" of many metal carbamates [42].

Hydrolysis of metal carbamates in the presence of an excess of water generally leads to the metal oxide (or hydroxide) (Scheme 32a). Some of these oxides, or mixed metal oxides, find relevance in the field of material chemistry, a topic that will be discussed in Section 5. Notwithstanding, the reactivity of carbamato complexes with water can be modulated for preparative purposes, avoiding the exhaustive hydrolysis of the metal-carbamato linkages. Thus, the reactions with a carefully controlled amount of water in organic solvents is exploited for the synthesis of well-defined mixed ligand complexes, such as oxido-carbamato species (Scheme 32b).

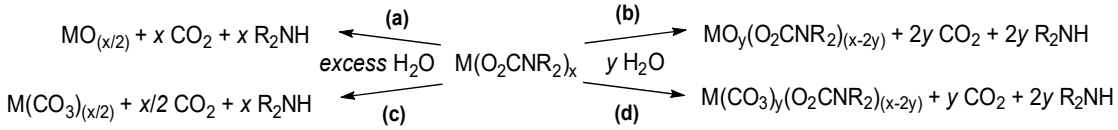

Scheme 32. Hydrolytic processes of metal carbamato complexes: exhaustive hydrolysis to metal oxides (**a**) or carbonates (**c**) or partial hydrolysis to oxido-carbamato (**b**) or carbonato-carbamato (**d**) species.

As a representative example, the octa-titanium complex $[Ti(\mu\text{-}O)(O_2CNEt_2)_2]_8$ $[NH_2Et_2][O_2CNEt_2]$ was generated by hydrolysis of $[Ti(O_2CNEt_2)_4]$ in 1,2-dimethoxyethane using a metal/water ratio of 1 [292]. The structure of the complex shows a chain of almost co-planar titanium atoms encapsulating a diethylammonium cation, while the carbamato anions are located outside the cycle (Scheme 33a). Instead, $[Nb(O_2CNEt_2)_5]$ treated with circa 1 eq. of water in toluene afforded a product of presumable formula $[Nb_2O_3(O_2CNEt_2)_4]$, being reminiscent of the structurally characterized $[Ta_2(\mu\text{-}O)_3(O_2CNEt_2)_4]_4$ based on IR and NMR spectra [171].

Controlled hydrolysis of $[M(O_2CNR_2)_2]_n$ (M/H_2O ratio 4:1) and $[ZnR'(O_2CNR_2)]_4$ in toluene or THF produced the tetranuclear oxido-carbamate $[Zn_4(\mu_4\text{-}O)(O_2CNR_2)_6]$ (R = Me, Et, ^{i}Pr, ^{i}Bu; Scheme 33b) and octanuclear $[M_4(\mu_4\text{-}O)(O_2CN^iPr_2)_6]_2$ (M = Fe, Zn) [143,164,202,203,283]. In the case of $[Zn_4(\mu_4\text{-}O)(O_2CNMe_2)_6]$, the reaction can be reversed by protonating the oxido ligand with $[Me_2NH_2][O_2NMe_2]$, which is rather uncommon [143]. A related tetranuclear cage structure is displayed by $[La_4(\mu_4\text{-}O)(O_2CN^iPr_2)_{10}]$, being the first lanthanide μ-oxido carbamato complex obtained by controlled hydrolysis of the corresponding homoleptic derivative [146]. The bismuth species $[Bi_8O_6(O_2CN^iPr_2)_{12}]$ was serendipitously crystallized from a solution of the homoleptic $[Bi(O_2CN^iPr_2)_3]$ upon prolonged air exposure [135].

In some cases, the interaction of metal carbamates with dioxygen is an equivalent to the hydrolytic treatment, except for the additional oxidation of the metal centers. For instance, the reaction of $[Ce(O_2CN^iPr_2)_3]_4$ with dioxygen proceeded with Ce(III) to Ce(IV) oxidation and moderate structure rearrangement to give the μ-oxido derivative $[Ce_4(\mu_3\text{-}O)_2(O_2CN^iPr_2)_{12}]$. The same reaction was also performed in the solid state [144]. Oxygenation of the homoleptic Fe(II) carbamate or controlled hydrolysis of the homoleptic Fe(III) carbamate led to the μ-oxido Fe(III) carbamate $[Fe_2(\mu\text{-}O)(O_2CNR_2)_4]$ (R = Et, ^{i}Pr) [143]. Conversely, $[Mn(O_2CN^iPr_2)_2]_n$ is air stable in the solid state, although its complete conversion to the Mn(III) derivative $[Mn_4O_3(O_2CN^iPr_2)_6]$ is viable in the presence of water; this result suggests that the preliminary formation of μ-oxido moieties might trigger the subsequent oxidation of the metal center.

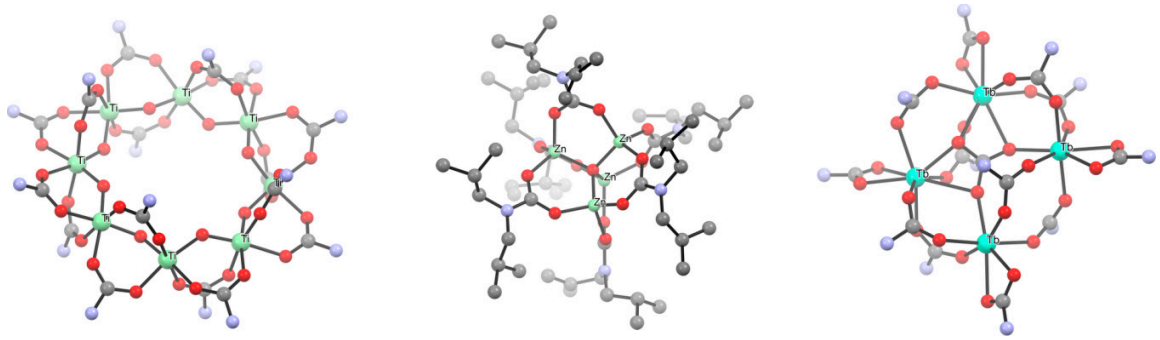

(**a**) (**b**) (**c**)

Scheme 33. Views of X-ray crystal structures of mixed oxido-carbamato complexes obtained by controlled hydrolysis: (**a**) $[Ti_8O_8(O_2CNEt_2)_{16}]\cdot[NH_2Et_2]\cdot[O_2CNEt_2]$ (Et groups, ammonium cation and *N*,*N*-diethylcarbamate anion omitted for clarity); (**b**) $[Zn_4(\mu_4\text{-}O)(O_2CN^iBu_2)_6]$ (H atoms omitted for clarity); (**c**) $[NH_2Bu_2]_2[Tb_4(CO_3)(O_2CNBu_2)_{12}]$ (Bu groups and ammonium cation omitted for clarity). Drawings based on published data [151,283,292].

Hydrolysis of rare earth carbamato complexes often results in the formation of a carbonate (Scheme 32c,d) [293]. Indeed, the extraction method described above related to homoleptic lanthanide complexes (Section 3.1) proceeds to the formation of mixed carbonato-carbamato species, $[NH_2Bu_2]_2[Ln_4(CO_3)(O_2CNBu_2)_{12}]$ (Ln = Tb, Sm, Eu, Tm) (Scheme 33c), in case the separated organic phase is not promptly dried. This is probably ascribable to the quite fast reaction of carbamato ligands with residual traces of water [151,153]. Compounds $[NH_2Bu_2]_2[Ln_4(CO_3)(O_2CNBu_2)_{12}]$ can be further converted into $[Ln_4(CO_3)(O_2CNBu_2)_{10}]$ (Ln = La, Sm) upon evaporation under vacuum [146,151]. Complexes $[Ln_2(CO_3)(O_2CN^iPr_2)_4]$ (Ln = Nd, Eu, Gd) were obtained by controlled hydrolysis (M/H_2O ratio = 2) of the corresponding homoleptic metal carbamates [146]. Accordingly, the exhaustive hydrolysis of some lanthanide carbamates (Ln = Ce, Nd, Eu, Gd, Tb) and $[Y(O_2CNBu_2)_4]$ led to the carbonates $M_2(CO_3)_3$ and not the oxides [146,152,154].

The reactivity of metal carbamato complexes with other protic species (HX) can be used to install different ligands (X^-) on the metal center. These include alcohols, β-diketonates and hydrogen halides, providing access to metal alkoxides, diketonates and halometallates (Scheme 31) [42]. For instance,

reactions of the tin alkylcarbamates $[SnR'_n(O_2CNR_2)_{(4-n)}]$ in neat alcohol (R″OH) at high temperature produces the corresponding alkoxystannanes $[SnR'_n(OR'')_{(4-n)}]$ in moderate to high yields [294]. Homoleptic lanthanide carbamates were recently reported to react with pentafluorophenol in the presence of 1,10-phenanthroline to form $[Ln(OC_6F_5)_3(phen)_3]$ (Ln = Nd, Tb) [295]. A further example is given by the β-diketonato complex $[Tb(dbm)_3]$, which was obtained upon reaction of $[Tb(O_2CNBu_2)_3]$ with dibenzoylmethane (Hdbm) [153]. A new entry into this category is represented by terminal alkynes: $[Sn(O_2CNEt_2)]_4$ reacts with phenylacetylene in refluxing toluene, to afford the homoleptic Sn(IV) alkynyl derivative $[Sn(CCPh)_4]$ [296].

Silanol groups (≡Si−OH) on the surface of silica and other similar oxides also offer a reactive site for metal carbamates, leading to the derivatization of such materials with metal carbamato fragments (see Section 5 for details).

Reactivity with nucleophiles. In contrast to the reactivity of carbon dioxide, the CO_2 moiety within a carbamato ligand is not susceptible to nucleophilic attack and this feature enables specific modifications to the coordinative sphere of metal carbamato complexes. For instance, carbonylation [42], hydrogenation [231] and ligand exchange reactions using methyl lithium or pyridines [278,297] have been performed without affecting the integrity of the carbamato ligand(s).

The reactions of the tetrameric Zn alkylcarbamates $[ZnR'(O_2CNR_2)]_4$ (R = ^{i}Pr, ^{i}Bu; R = Me, Et) with various *N*-donors provide a striking example of the versatility of the coordinated carbamato fragment. In fact, pyridine addition gives the dinuclear $[ZnMe(O_2CNR_2)(py)]_2$ with switching of the carbamato coordination from triply (***B/3***) to doubly bridging (***B/2***) [201]. Differently, addition of diamines or guanidines gives the mononuclear complexes $[Zn(N)(N)(O_2CNR_2)_2]$, featured by chelating (***C/1***) or monodentate (***M/1***) carbamates, according to the electronic properties of the *N*-ligand [298,299].

3.4. Crystallographic and Spectroscopic Features of Carbamato Ligands

A collection of crystallographic data for metal carbamato complexes published from 2004 to 2020 is reported in Table S3 (ESI). We selected C−O and C−N distances, as well as the O−C−O angle (Scheme 34a), as diagnostic structural parameters to be discussed with respect to the different coordination modes (see Scheme 13 for the ***M***/***C***/***B***/***D*** nomenclature adopted). Clearly, this analysis does not include the electronic/geometric effects exerted by different metal centers as well as the nature of substituents on the nitrogen atom.

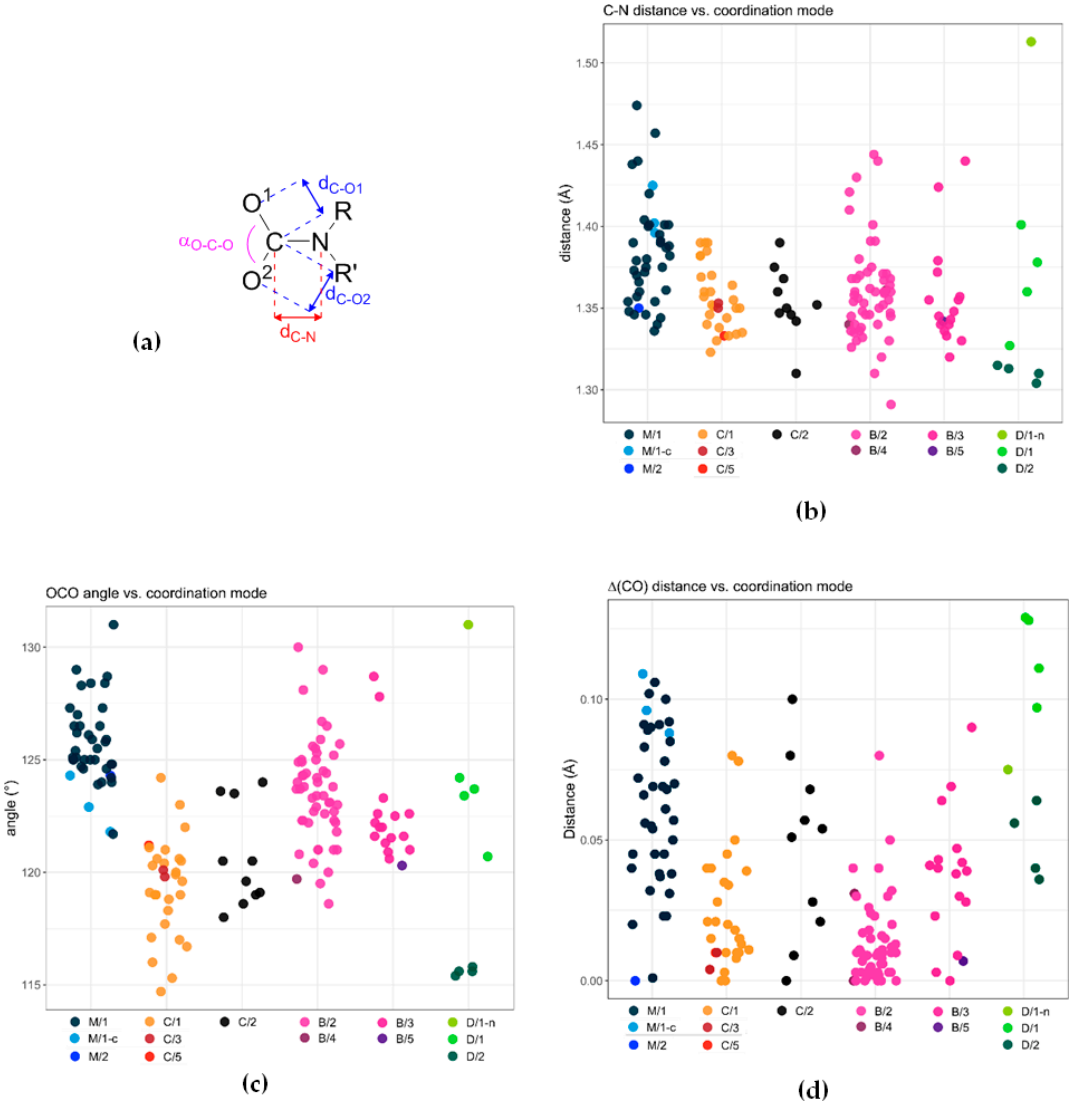

Scheme 34. Selected structural parameters for carbamato ligands (**a**) and their distribution according to the coordination mode (**b**–**d**). Data taken from Table S3 (ESI). See Scheme 13 for the ***M***/***C***/***B***/***D*** nomenclature adopted.

The majority of carbon-nitrogen bond distances within carbamato ligands are distributed within the range 1.33–1.41 Å (Scheme 34b), suggestive of a substantial delocalization of the nitrogen lone pair on the CO_2 moiety. Remarkably, such N → CO_2 interaction is not significantly influenced by the denticity of the carbamato ligand (compare ***B/2***, ***B/3***, ***B/5*** and ***C/1***, ***C/2***, ***C/3***, ***C/5***).

Conversely, the C–O distances and the O–C–O angle are affected by the ligand coordination mode. As expected, the CO_2 angle is smaller in chelating carbamates (‘***C***’ series in Scheme 13; 120 ± 2°), compared to the other bonding situations (123–126 ° range) (Scheme 34c). The two C–O bond lengths are quite different in monodentate carbamato ligands (‘***M***’ series in Scheme 13), averaging 1.29 ± 0.02 Å and 1.23 ± 0.02 Å; this feature reflects a prevailing double bond character of the C–O bond not involved in coordination. The difference between the two types of C–O distances ($\Delta d_{C\text{-}O}$, Scheme 34d) is reduced to a few pm for chelating (***C/1***) and, particularly, bidentate bridging ligands (***B/2***; $\Delta d_{C\text{-}O}$ = 0.01 ± 0.01 Å). Binding to an additional metal center breaks the symmetry of the system and $\Delta d_{C\text{-}O}$ increases (compare ***C/1*** with ***C/2*** and ***B/2*** with ***B/3***).

Dianionic carbamyldiide ligands (***D/1*** and ***D/2*** modes in Scheme 13) possess crystallographic features that are markedly different from those of ordinary carbamato ligands. For instance, in the *N*,*O*-chelating mode (***D/1***), the two C–O bond lengths (1.32–1.37 Å and 1.22–1.24 Å) reveal a net double and single bond character, whereas a rather small O–C–O angle (≈116°) is observed when both oxygen atoms are involved in coordination (***D/2***).

From a spectroscopic point of view, diagnostic features of carbamato ligands are the ^{13}C-NMR resonance and the IR absorptions related to the NCO_2 moiety. A collection of solution NMR and solid-state IR data for metal carbamato complexes, along with the coordination mode(s) of the carbamato ligand in the solid state, can be found in Table S4 (ESI). Trends emerging from the analysis of structurally-characterized compounds, with due caution, can be a guidance for the characterization of further compounds.

The ^{13}C-NMR chemical shift of the carbamyl carbon in metal carbamato complexes is typically around 160 ppm. In cases where a single coordination mode was determined, signals ascribable to monodentate carbamates (***M/1*** mode) were reported in the 156–164 ppm range. Signals belonging to chelating (***C/1***) and bridging (***B/2***) carbamato ligands fall in the upper half of this interval and even beyond (up to 170 ppm) (Scheme 35a). However, it has to be considered that the number and the position of the ^{13}C-NMR resonances in solution systems might not be discriminating where multiple coordination modes are adopted. Indeed, quite often only an average value is observed at ambient temperatures, due the rapid exchange between carbamato ligands in solution [210]. In such cases, ^{13}C-NMR measurements at low temperatures provide distinct chemical shifts for the carbamates in the different coordination fashions [138,284]. The few spectroscopic data available for carbamyldiide ligands, in the chelating *N*,*O* mode (***D/1***), show a downfield-shifted ^{13}C-NMR signal (165–175 ppm).

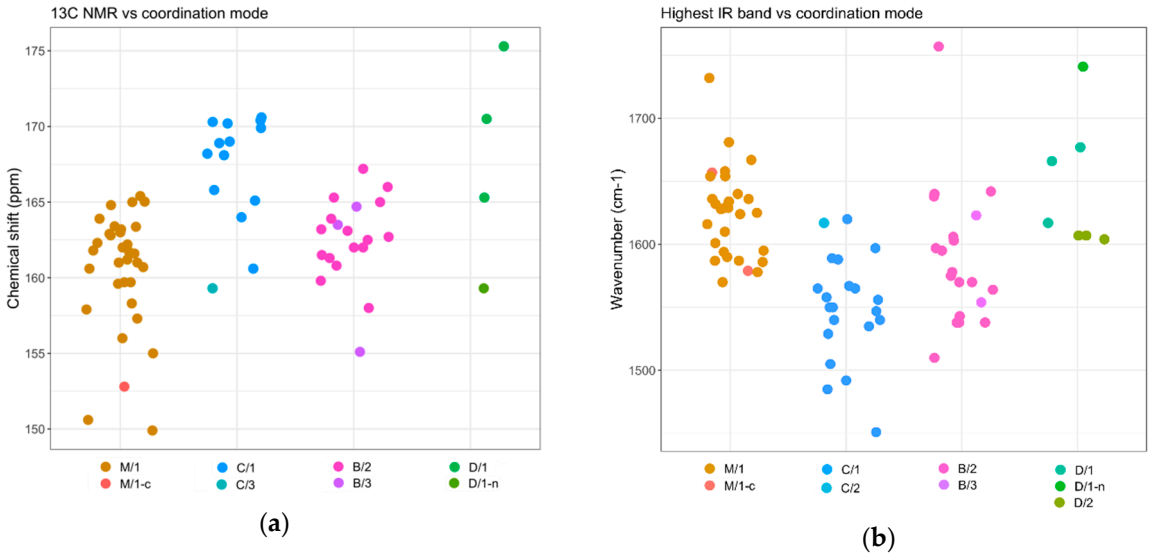

Scheme 35. Selected spectroscopic data for metal carbamato complexes and their distribution according to the coordination mode: ^{13}C-NMR chemical shift of the carbamyl carbon (**a**) and highest IR band ascribable to the NCO_2 moiety (**b**). Data refer to Table S4 (ESI).

Metal carbamato complexes generally show multiple medium/strong IR bands in the region 1300–1700 cm^{-1}, which are ascribable to stretching vibrations of the NCO_2 moiety [42]. The highest-frequency IR band has been typically assigned to the C=O stretching/CO_2 antisymmetric stretching, in analogy to metal-carboxylates [300,301]. However, the involvement of the N atom in the π-system makes the signal assignment far less clear-cut than in metal carboxylates [242]. As previously pointed out [42], the position of the IR bands may give some indications on the coordination mode of the carbamate. In this regard, the wavenumber of the highest IR absorption versus the coordination mode, for compounds having a univocal association between the two, can be visualized in Scheme 35b.

Monodentate ligands (***M/1***) are featured by an intense absorption generally ranging from 1600 to 1660 cm^{-1}, and occasionally higher. Conversely, lack of a band above 1600 cm^{-1} has been interpreted in terms of an absence of terminal ligands, although in some cases hydrogen bonding involving the uncoordinated oxygen atom may reduce the wavenumber below 1600 cm^{-1} [42]. On the other hand, chelating (***C/1***) and bidentate (***B/1***) ligands display their highest-frequency band in the 1535–1600 cm^{-1} range, associated to a second strong band around 1490–1530 cm^{-1}. However, the positions of these absorptions do not allow a clear distinction between the two coordination modes [42].

4. Catalysis with Metal Carbamates

Despite that carbamato complexes have been known for more than 50 years [122] and their reactivity has been widely studied during this time, a systematic investigation on their catalytic behavior began only recently. As a matter of fact, homoleptic carbamates and related systems possess a number of properties that make them attractive candidates for applications in catalysis: in particular, they are easily available from relatively cost effective and nontoxic chemicals all across the periodic table, and exhibit a considerable structural diversity (Section 3). Basically, two aspects mentioned above constitute the key to the interest in the potential use of metal carbamato complexes as catalysts. First, the formation of the carbamato unit is a way to fix CO_2, which is also exploited in nature with reference to some Ni(II) [302] and Zn(II) [303–305] enzymes. Trapped CO_2 can be used as a C1 synthon in organic synthesis, and the stoichiometric reactions of metal carbamates with organic electrophiles can lead to CO_2 incorporating products (Section 3.4). This result can be achieved even using the metal species in a catalytic amount, with the carbamato ligand(s) playing an active role in the process. The second aspect has a broader significance, and is related to the possible generation of a vacant site on the metal center, due to both the flexibility of the carbamato ligand adapting from bi- to monodentate coordination, and to its ability to behave as a leaving group, following the interaction with proton-active substances.

In this section, the relevance of carbamato complexes as catalytic precursors and/or intermediates in organic reactions will be discussed, starting from CO_2 activation reactions. The proposed mechanisms will be outlined, in order to highlight the presumable role of the carbamato ligand in the catalytic cycle.

4.1. CO_2 Activation Routes

The formation of carbamato complexes is considered a key step in metal-mediated reactions such as the CO_2/aziridine coupling [306–308] and the CO_2 cycloaddition to propargyl amines [113,309–312] or aminoalcohols [306]. The production of oxazolidinones (cyclic carbamates) via CO_2/aziridine coupling is one of the most widely investigated carbon dioxide fixation processes, and many species have been evaluated as catalytic precursors, such as Al(III) [313], Cr(III) [314] and Co(III) [315] salen complexes, and Cu(II) [316] and Zn(II) [317] porphyrin complexes. Regarding the cycloadditon of CO_2 to propargylamines, catalysts based on late transition metals are privileged since they offer the possibility to activate the alkyne reactant via η^2-coordination [113,318]. The synthesis of cyclic carbamates starting from amino-alcohols and CO_2 is a less explored route if compared with the other ones, and a limited number of catalysts have been studied in this regard, based on cesium, silicon and tin [319–321].

The generally accepted mechanisms for these reactions are outlined in Scheme 36a–c. In all cases, the intermediate generation of a carbamato ligand is postulated upon interaction of the *N*-donor and CO_2 with the metal center. Afterwards, electrophilic attack on the oxygen atoms (Scheme 36a,b), combined with a nucleophilic attack on the carbon atom (Scheme 36c), generates the product.

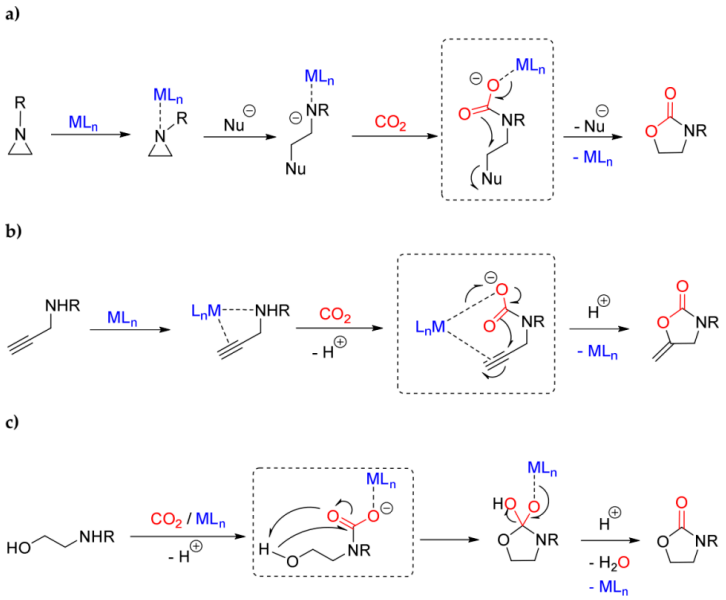

Scheme 36. Generally-accepted mechanisms for metal-mediated aziridine/CO_2 coupling (**a**), CO_2 cycloaddition to propargylamines (**b**) and aminoalcohols (a 2-aminoalcohol is drawn as example) (**c**). The intermediate carbamate in each pathway is circled.

In addition to the above mentioned reactions, Jiang et al. reported the involvement of Cu(II) and Cu(III) carbamates in the oxidative coupling of arylboronic acids [322] and in the cyclization of enynes [323] from amines and CO_2. In order to support the hypothesis of an in situ formed Cu(II) carbamate, the catalytic activity of $[Cu(O_2CNBn)_2(NHBn_2)_2]$ was evaluated, providing moderate to good results in term of product yields.

An interesting case of CO_2 activation was reported in 2016 by Norris et al. The authors described the role of carbon dioxide in the evolution of H_2 from water using a Ru(II) complex. In this particular system, CO_2 works as a co-catalyst in association with the ruthenium complex, generating a carbamate as a reaction intermediate (Scheme 37) [270].

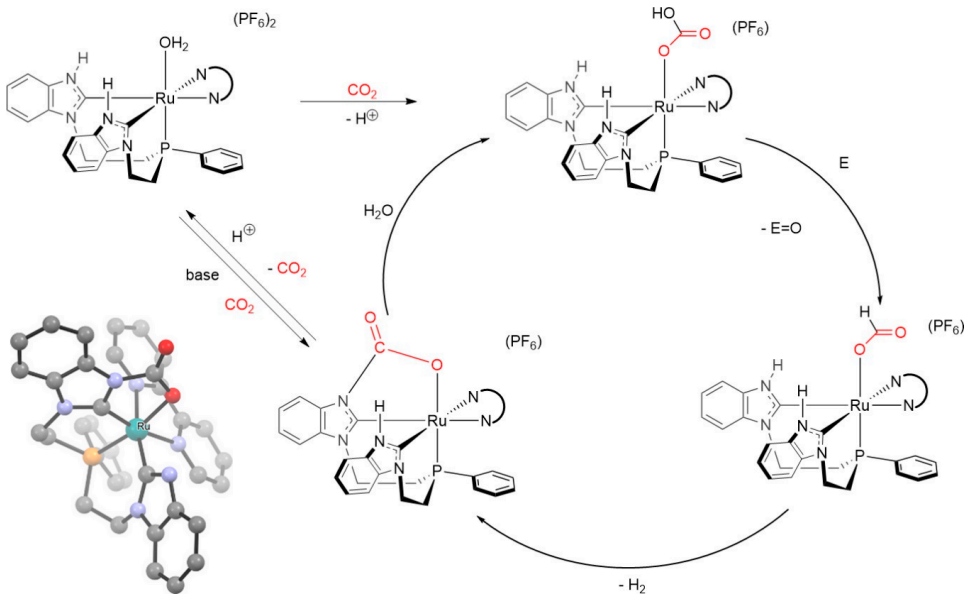

Scheme 37. H_2O to H_2 conversion catalyzed by a Ru(II) complex with the assistance of CO_2 and view of the X-ray crystal structure of the supposed metal carbamato intermediate. Drawings based on published data (H atoms omitted for clarity) [270].

Although the formation of a metal carbamate represents a generally accepted step in many carbon dioxide activation reactions, the direct use of carbamato complexes as catalytic precursors is a recent approach. Thus, a systematic screening of the catalytic activity of homoleptic carbamates of silicon, tin and some d-transition metals for the CO_2/epoxide coupling reaction was performed, in conjunction with tetrabutylammonium bromide as a co-catalyst, under solvent-free and ambient conditions [134,290,324]. Then, Ag(I), Cu(I) and Cu(II) carbamates were tested as catalysts for the carboxylation of terminal alkynes [325] and in the cycloaddition reaction of CO_2 to propargyl alcohols [326] (Scheme 38).

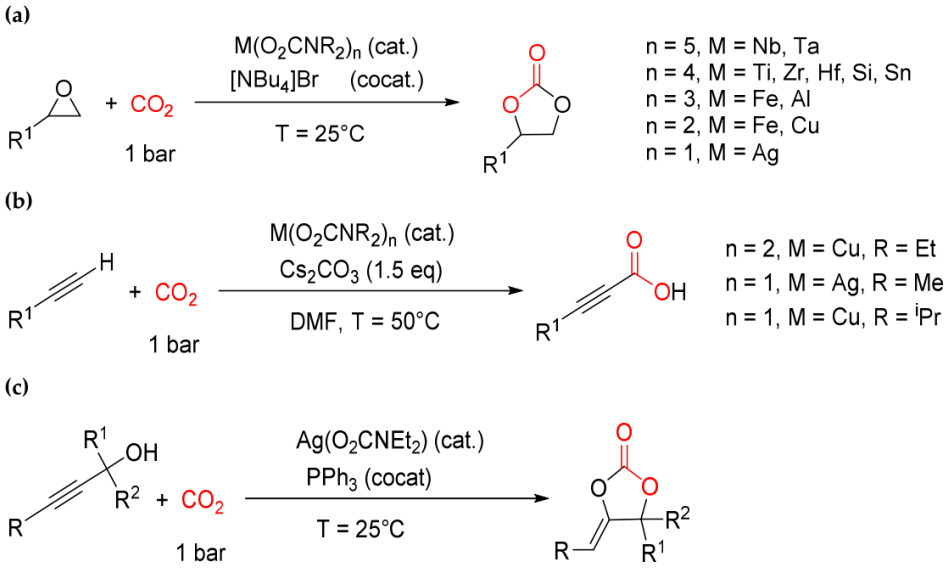

Scheme 38. Cycloaddition of CO_2 to epoxides (**a**), carboxylation of terminal alkynes (**b**) and cycloaddition of CO_2 to propargyl alcohols (**c**) mediated by homoleptic metal carbamates.

Interestingly, $[Fe(O_2CNR_2)_3]$ (R = Et, ^{i}Pr, Bn) revealed a promising catalytic activity for the production of cyclic carbonates from CO_2 and epoxides [324]. It is remarkable that an inexpensive catalyst, based on a nontoxic metal element and working at ambient temperature and CO_2 pressure, is an appealing requisite in terms of sustainability [327]. The catalytic mechanism was elucidated by NMR and DFT analyses, suggesting the occurrence of an unusual dynamic CO_2 pre-activation, possibly responsible for the activity of the complex in mild conditions (Scheme 39). The CO_2 pre-activation occurs through the preliminary incorporation of the CO_2 reactant in a carbamato ligand, followed by transfer to the organic substrate and ready restoring of the carbamato unit guaranteed by external CO_2. A similar pathway was recently proposed by Bayer et al., studying the CO_2/epoxide coupling by means of dimethylpirazolate cerium amides and cerium carbamates [134].

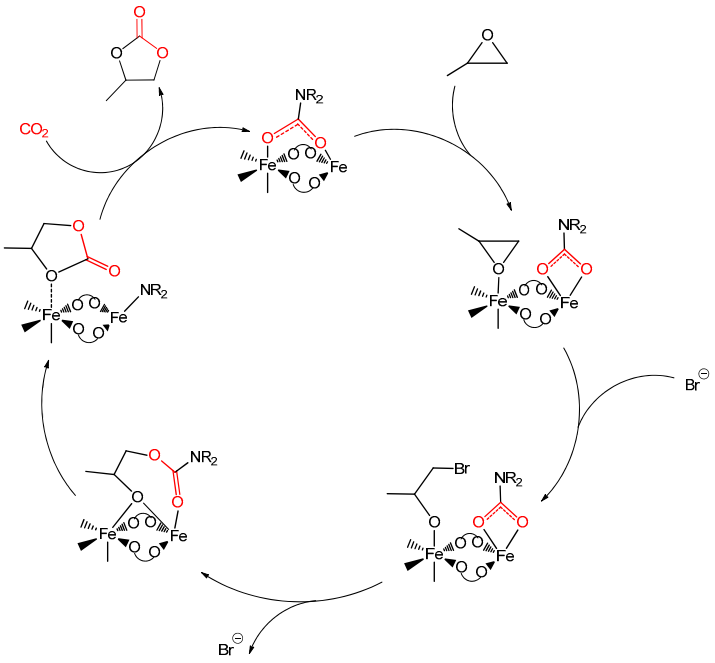

Scheme 39. Proposed mechanism for the epoxide/CO_2 coupling via dynamic trapping of carbon dioxide into an iron(III) carbamate. The remaining carbamato ligands in the structure are omitted for clarity.

In summary, metal carbamates are easy-to-synthesize complexes and their ligands can adapt their coordination mode or can be protonated to form a vacant site on the metal center. Moreover, carbamato ligands themselves represent a pre-activation form of carbon dioxide and can exchange the CO_2 fragment within the ligand with external carbon dioxide (see Section 3.3), suggesting some potential in the dynamic activation of this molecule. All these characteristics, combined with the possibility of employing a nontoxic metal center, delineate metal carbamates as potential catalytic systems useful in CO_2 activation reactions and deserving of further studies and progress.

4.2. Other Catalytic Processes

Polymerization. The first study concerning the catalytic activity of metal carbamates in a polymerization reaction was reported in 2009 [328]. More precisely, $[Nb(O_2CNR_2)_5]$ (R = Me, Et) were employed in the ring opening metathesis polymerization (ROMP) of norbornene in the presence of methylaluminoxane (MAO). Interestingly, such niobium catalysts are very active in chlorobenzene and especially $[Nb(O_2CNEt_2)_5]$ was tagged as the most active niobium catalyst ever reported for norbornene-ROMP. The increased steric hindrance around the metal center in the ethyl derivative is believed to favor α-hydrogen elimination and thus to accelerate the reaction.

Subsequently, $[TiCl_2(O_2CNMe_2)_2]$ [139], $[Ti(O_2CNR_2)_4]$ (R = Me, Et, Pyrr) [139,172,329], $[Nb(O_2CNR_2)_5]$ (R = Me, Et), $[Nb(O_2CNEt_2)_4]$ and $[Nb(O_2CNEt_2)_3]$ [280] were studied in ethylene and propylene (homo)polymerization and ethylene/1-hexene copolymerization. Notably, the catalytic activities of these carbamato complexes were higher compared to those of the respective metal halide precursors. Concerning the ligand framework, the steric hindrance of the alkyl group enhances the catalytic performance in ethylene polymerization (Et > Me), presumably by inhibiting the formation of inactive polymetallic species. On the other hand, in propylene polymerization, an increase of steric hindrance around the metal center results in a drop of catalytic activity, imputable to the easier attack of the incoming monomer when the *N*-alkyl group is small [139].

Group 4 metal tetrakis-carbamato complexes, i.e., $[M(O_2CNR_2)_4]$ (M = Ti, Zr, Hf; R = Et, ^{i}Pr), were also studied as catalysts in the ring opening polymerization (ROP) of *rac*-lactide [330]. As already

observed for other catalytic processes, the titanium compounds showed a lower activity compared to that of zirconium and hafnium and the best results were obtained with the most sterically hindered R group. The polymerization mechanism was enlightened by IR and NMR studies, revealing two different pathways depending on the catalyst type. For zirconium and hafnium derivatives, *rac*-lactide coordination to the metal center occurs following α-hydrogen elimination promoted by the basic character of the carbamato ligand (Scheme 40a). Conversely, in the case of Ti(IV), a radical polymerization mechanism is operative, triggered by an initial electron interchange between the carbamato ligand and the *rac*-lactide molecule (Scheme 40b).

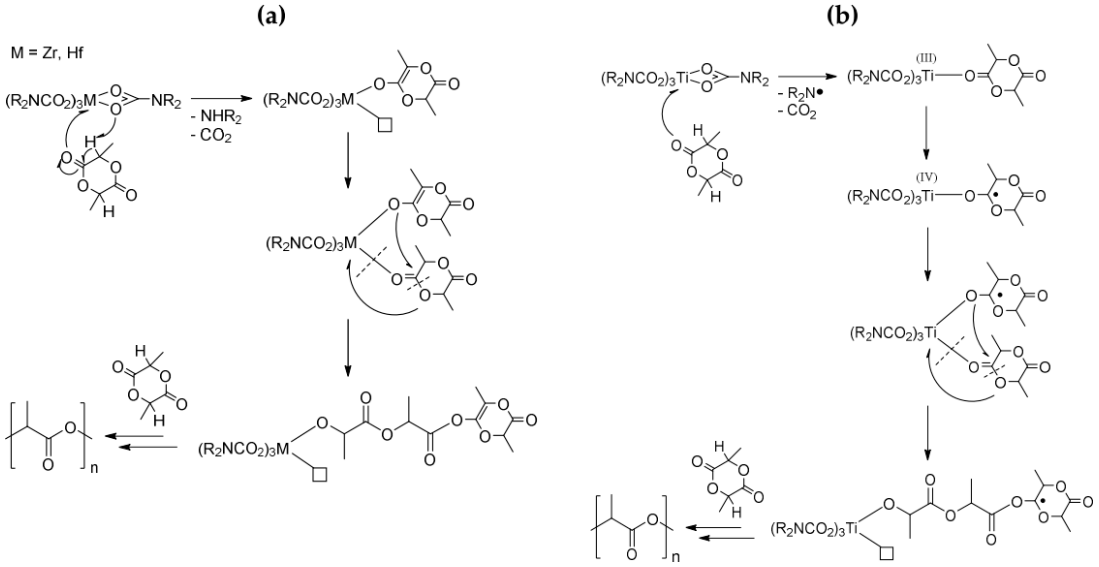

Scheme 40. Proposed mechanisms for the *rac*-lactide polymerization promoted by homoleptic tetracarbamates of Zr, Hf (**a**) or Ti (**b**).

Other catalytic processes. To the best of our knowledge, the first investigation on the catalytic activity of a metal carbamate was reported by Belli Dell'Amico et al. in 2004 [231]. Thus, Ru(II) carbamates of formula $[Ru(O_2CN^iPr_2)_2(PPh_3)_2]$ and $[RuCl(O_2CN^iPr_2)(PPh_3)_3]$ were tested in the 1-octene H_2 hydrogenation at atmospheric pressure, in toluene at ambient temperature. The catalysts were recovered unchanged at the end of the process, suggesting that the required alkene coordination during the catalytic cycle is ensured by a simple coordination switch of the carbamato unit(s) from chelating to monodentate.

In other cases, transition metal catalysts have been reported to work via intermediate formation of carbamato ligands [331,332]. For instance, the conversion of cyclobutanes to Z-enol carbamates catalyzed by $Cp_2Zr(CH_2{=}CH_2)$ was postulated to pass through a Zr(IV) carbamate [331]; additionally, a potassium carbamate was detected as an intermediate in the catalyzed Lossen rearrangement of hydroxamic acids to isocyanate [332].

5. Other Applications

Metal carbamato complexes have been investigated in several research areas beside catalysis, especially during the last decade. In material chemistry, the viable degradation of easily-accessible d/f metal homoleptic carbamato complexes has been exploited to obtain nanostructured metal oxides, whereas silver carbamato complexes have been used as precursors to nanomaterials. In addition, both homoleptic and heteroleptic carbamates have been employed to functionalize the shell of silica and other oxides, taking advantage of the controlled reactivity with surface hydroxyl groups. These and other aspects will be detailed in the following, focusing on the reactivity of the carbamato moiety and the properties of the complexes relevant to each application.

Metal carbamates as precursors to nanostructured metal oxides. Over the last 15 years, carbamato complexes have been widely investigated for the preparation of nanostructured metal oxides, arousing interest for their electric, magnetic, optical and catalytic properties. The formation of a metal oxide from a metal carbamate basically takes place via either thermal degradation or exhaustive hydrolysis. The thermal degradation of homoleptic carbamates or oxido-carbamates under inert atmosphere usually proceeds quantitatively at temperatures below 500 °C with fragmentation of the organic groups, cleanly affording a metal oxide. The fate of the carbamato ligands during the pyrolytic process depends on the system; in general, multiple products have been detected in the gas phase, including CO_2 and the dialkylamine [42,240,333,334] (Scheme 41a). In some cases, the preferential formation of alkyl isocyanates and alkenes has been recognized (Scheme 41b–d) [335,336].

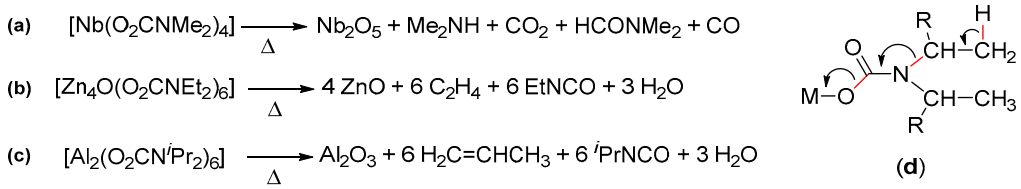

Scheme 41. Products detected by pyrolysis of $[Nb(O_2CNEt_2)_4]$ (**a**); thermal decomposition reactions of $[Zn_4O(O_2CNEt_2)_6]$ (**b**) and $[Al_2(O_2CN^iPr_2)_6]$ (**c**) and proposed fragmentation mechanism (**d**).

Homoleptic *N*,*N*-dialkylcarbamato complexes, or oxido-carbamates, can be easily sublimed under reduced pressure, a fact that can be justified on the basis of their molecular structure and lack of strong intermolecular interactions (e.g., H-bonds) in the solid state [334]. Therefore, such compounds are ideal precursors for the Chemical Vapor Deposition (CVD) technique. Moreover, the use of a single component as oxide precursor ("single source CVD," or SSCVD) is advantageous with respect to classical CVD methods requiring at least two reagents for the gas-phase reaction.

According to the SSCVD methodology, the metal *N*,*N*-dialkylcarbamate is volatilized at 150–200 °C under high vacuum (1–5 × 10^{-6} torr), or under an N_2 flow, and then it is thermally decomposed on a silicon wafer (or another substrate material) around 500 °C. The gap between the two temperatures provides a suitable working window. Hence, thin films of ZnO [336–339], Al_2O_3 [335] and Bi_2O_3 [135] have been prepared from $[Zn_4O(O_2CNEt_2)_6]$, $[Al_6(O_2CN^iPr_2)_{12}]$ or $[Bi(O_2CN^iPr)_3]$. Similarly, heterobimetallic Zn/Mg carbamates of general formula $[Zn_xMg_{4-x}O(O_2CN^iPr_2)_6]$ were useful to prepare $Zn_xMg_{(1-x)}O$ thin films [340,341]. The use of a bimetallic precursor is convenient respect to the co-deposition from two distinct compounds, because the sublimation occurs at a defined temperature, leading to a ratio between the two metals in the mixed oxide that is given by the precursor composition. Metal oxide films obtained through SSCVD can be as low as 200 nm thick and present a smooth surface, low carbon contamination, high density and a single preferred crystallite orientation.

The same principles can be applied to the preparation of metal oxide nanoparticles by thermal decomposition of metal carbamates at 200–300 °C and ordinary pressure. Thus, pyrolysis of $[ZnEt(O_2CNR_2)]_4$ and $[M(O_2CNR_2)_4]$ (M = Zr, Hf, Nb; R = Me, Et, ^{i}Pr) gives ZnO, ZrO_2, HfO_2 and Nb_2O_5 nanoparticles [203,334], whereas Zn/Co and Zn/Mn heterobimetallic carbamates have been employed to obtain $Zn_x(Co, Mn)_{(1-x)}O$ mixed oxide nanoparticles [281,282]. In these cases, the excessive volatilization of the metal carbamate is a possible disadvantage [334].

Operating in the condensed phase, the transformation of a metal carbamate into its oxide can be realized by thermal degradation but also by reaction with protic species (Section 3.3). For instance, thin films of Al_2O_3 were deposited from solvothermal decomposition of $[Al_6(O_2CN^iPr_2)_{12}]$ in dry benzene [342]. Additionally, hybrid procedures are known, involving a thermally-assisted degradation in the presence of protic species such as alcohols, oleic acid or hydrogen peroxide in organic solvents, to afford ZnO or CuO nanoparticles [158,343,344]. Among the reactions with protic species, the hydrolytic route is the privileged one and has been optimized to access various oxide nanoparticles. In order to control the reaction and to obtain a finely dispersed powder, a water/THF mixture is conveniently added

to a solution of the metal carbamate in toluene or heptane under inert atmosphere. For compounds based on Y, Ce and other lanthanides, exhaustive hydrolysis produces the metal carbonate, which can be subsequently calcined to give the oxide (Scheme 42a) [152,154]. When the hydrolysis is carried out in the presence of additional metal precursor(s) (as a carbamate, or a hydrolysable species in general), a mixed carbonate is obtained with a composition regulated by the relative amounts of the reactants. Upon further thermal treatment, mixed metal oxide nanoparticles with a desired composition, such as $Ce_{1.65}Tb_{0.35}O_{3.82}$, $Ce_{1.80}La_{0.20}O_{3.90}$, La_2CuO_4, $Y_3Al_5O_{12}$ and $Y_{2.98}Nd_{0.02}Al_5O_{12}$, are finally produced (Scheme 42b) [146,154,297].

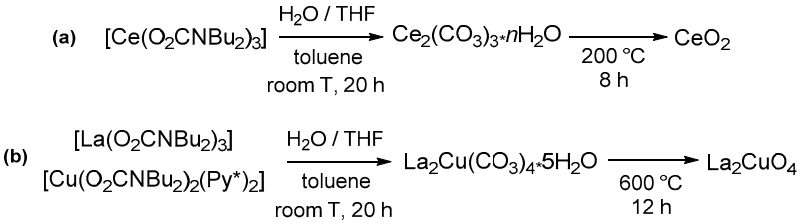

Scheme 42. General protocol for the preparation of oxides from metal carbamates applied to the preparation of CeO_2 (**a**) and mixed La/Cu oxide (**b**) nanoparticles. Py* = substituted pyridine.

Silver carbamates as precursors to silver metal nanoparticles. Silver carbamato complexes possess a peculiar chemistry. In fact, owing to the relatively low stability of Ag_2O ($\Delta G°_f$ = −11.2 kJ/mol at 25 °C), this is essentially the only metal oxide that can be used as precursor to homoleptic carbamates (see Section 3.1) (Scheme 43a). On the other hand, Ag_2O is thermally unstable upon mild heating (Scheme 43b), and therefore, the hydrolytic thermolysis of silver carbamates generates metallic silver (Scheme 43c). Likewise, elemental silver is recovered from the reactions of silver carbamates with mild reducing agents (Scheme 43d) [159]. The deposition of silver is usually fast and quantitative, accompanied by the formation of volatile side products.

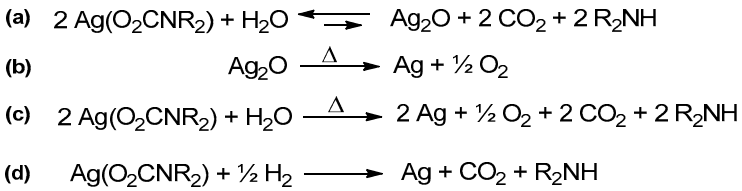

Scheme 43. Hydrolysis (forward reaction) or preparation (backward reaction) of a silver carbamate (**a**); thermal decomposition of silver oxide (**b**); hydrolytic thermolysis (**c**) or reduction (**d**) of a silver carbamate.

On account of these considerations, commercial alcoholic solutions of silver *N*-alkylcarbamates are used to access silver metal nanoparticles (AgNP). The decomposition is most commonly carried out by hydrolytic thermolysis with conventional or microwave heating or, in some cases, by using H_2 or hydrazine as a reducing agent. The generated silver nanoparticles can be adsorbed on various matrices such as polymers (PVA, PMMA, PET), graphene, thiol-modified carbon nanotubes or fabrics (cotton, silk). The resulting silver-coated materials have been investigated for their conductive properties [345–348] and/or antibacterial/antimicrobial activity [349–355]. In addition, if the reduction is performed in the presence of ethyl cellulose, a silver paste is obtained, and this can be deposited on a suitable substrate and sintered to provide a silver conductive film [356–358].

The synthesis of silver nanoparticles (and related nanocomposites) by thermolysis of silver carbamates is preferable respect to more traditional protocols (i.e., reduction of $AgNO_3$ with $NaBH_4$ or sodium citrate), in that it does not require any reducing agent and thus avoids the presence of undesired inorganic species in solution. Moreover, the colloidal AgNP dispersion is stabilized by the

ammonium carbamate co-product acting as surfactant (vide infra), and the spherical particles exhibit a rather narrow size distribution [352,357].

Metal carbamates as precursors for surface functionalization. Metal carbamato complexes are prone to react with a variety of protic species; these reactions are thermodynamically driven by the release of CO_2 (Section 3.3). Alkyl and aryl silanols, although possessing a relatively mild Brönsted acidity, promptly react with metal carbamates affording the corresponding siloxide derivatives (Scheme 44a) [42,359]. This reactivity is replicated on the surface of silica due to the presence of {≡Si–OH} groups. The ensuing "grafting reaction" consists in the protonation of the carbamato moiety, with consequent release of CO_2 and the amine, and binding of the metal atom to the silica as a siloxide unit (Scheme 44b). Despite a possible molar excess of surface silanols (vide infra), a limited number of carbamato ligands per metal complex are involved in the process, and solid-state spectroscopic measurements (IR, NMR, EPR) agree in that the final metal fragment retains its nuclearity and the geometry of the residual ligands [131,234,360,361]. In other words, the grafting reaction allows the chemical implantation of tailored metal fragments over the surface of silica.

Recently, the study of the reactivity of homoleptic *N*,*N*-dialkylcarbamates with silica has been extended to Cu(II), Nb(III), Nb(V), Ta(V), Tb(III) and Eu(III) derivatives [131,153,362,363]. Silica grafting has been also realized with non-homoleptic complexes of group 4 and 5 metals, wherein the carbamato ligands are the most reactive ones [166,234,290]. Even magnetite nanoparticles [364] and silica/zirconia [362] have been decorated with metal carbamates.

The protocol for the chemical implantation is commonly performed by suspending silica in a solution of the selected metal carbamate in toluene or heptane for a prolonged time (from several hours to days) (Scheme 44c). The reaction is conducted under inert atmosphere with anhydrous solvents and pre-dried silica, to limit the useless consumption of carbamato units by traces of water. A preliminary assessment of the silanol content of silica is useful to establish the minimum OH/metal ratio needed for a quantitative reaction, and thus, to avoid the waste of metal complex in solution.

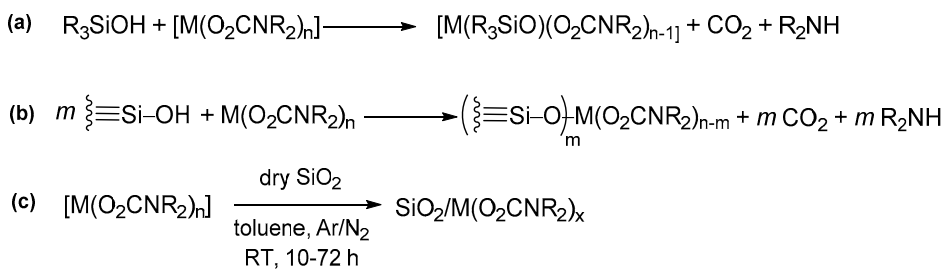

Scheme 44. Reactions of a homoleptic metal carbamates with a model tri-organosilanol (**a**), with surface silanols groups on silica ("grafting reaction") (**b**) and protocol for the chemical implantation on silica (**c**).

The outcome of the grafting process is strongly dependent on the nature of the metal precursor. Indeed, multiple carbamato ligands within the same metal complex or additional basic ligands, i.e., cyclopentadienyls [234], may be involved in the reaction. The process can be featured by a variable selectivity, thus generating different metal fragments on the oxide surface. The average number of reacted carbamato ligands per metal center can be estimated by measuring the volume of CO_2 released during the grafting process. Alternatively, a gas-volumetric titration of the final material provides the number of residual carbamato ligands.

Silica-grafted metal carbamato species have been investigated for their catalytic properties compared to the homogeneous congeners [290]. In addition, the grafted carbamato complex may undergo subsequent chemical modifications. For instance, noble metals such as Cu, Pd and Pt can be chemically or thermally reduced to give the respective silica-supported metal nanoparticles [361,362,365]. Another post-functionalization strategy entails the introduction of additional ligands by replacement of the residual carbamates, and for instance this method has

been adopted to introduce chiral β-diketonates on lanthanide-grafted carbamates for chiroptical luminescence applications [153,363].

Platinum carbamates as anticancer agents. Carbamato complexes of Pt(IV) have been considered as potential anticancer agents (Scheme 45a), and synthetic details have been discussed in Section 3.2. Platinum(IV) carbamato complexes with simple organic substituents on the nitrogen revealed a considerable cytotoxicity against various cancer cell lines, comparable or superior to that of the reference Pt(II) drug cisplatin [260,262,263]. A C_{16} aliphatic chain (fatty acid-like) was introduced through the carbamato ligand to enhance cellular uptake [263,264,266,366–368]. Following a different approach, the incorporation of a maleimide fragment enabled specific interactions with proteins (e.g., addition to thiol residues) for compounds showing a promising anticancer activity in vivo [261,268,369]. The conjugation with suitable targeting groups, to enhance the pharmacological performance, can be achieved via modification of either the axial carboxylato co-ligand [367,370] or the carbamato ligand itself [272,371,372]. Remarkably, all of these Pt(IV) complexes are stable for several hours or even days in physiological aqueous solutions [260,261,263,272]. However, the reduction to Pt(II) by biological reductants triggers the release of the carbamato ligand, which is subsequently hydrolyzed to amine and CO_2 (Scheme 45b) [272]. Thus, the synthetic design of a Pt(IV)-carbamato complex represents a strategy for a controlled and simultaneous release of a cytotoxic Pt(II) compound and (a) biologically active molecule(s) carrying an amino group into cells.

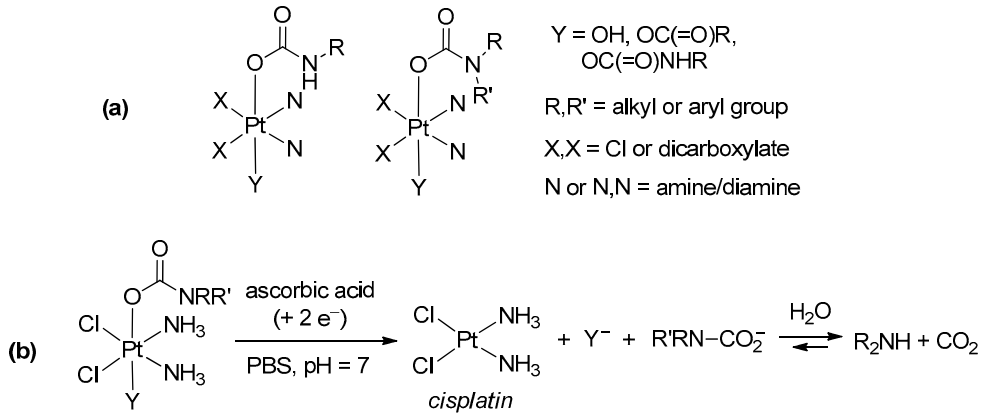

Scheme 45. General structure of Pt(IV) carbamato complexes investigated as potential anticancer agents (**a**) and reduction to Pt(II) derivatives with release of the carbamate ion (**b**).

Metal carbamates for CO_2 capture. The formation of metal carbamates from gaseous CO_2 and a metal amine complex has direct implications in the CO_2 capture and storage (CCS) technology [373–377]. In particular, amine-functionalized metal organic frameworks play an important role in the development of new solid sorbent materials [378].

The most intriguing results are related to recently-synthesized magnesium and manganese MOFs based on hydroxybenzoate ligands, and surface-derivatized with 1,2- and 1,3-diamines (Scheme 46) [376,379]. These systems reveal an extremely high affinity for CO_2 with respect to other gases, even under atmospheric pressure (Pco_2 = 0.39 atm), and are characterized by a peculiar step-shaped isotherm for CO_2 uptake, allowing complete adsorption/desorption cycles in a narrow temperature range.

Contrary to the expected carbonation of the dangling amino group, spectroscopic and X-ray diffraction data agree in indicating the joint formation of a metal carbamato linkage and protonation of the diamine ("ammonium carbamate") [376]. The use of a diamine, instead of a monoamine, provides cooperativity to the system, in that one end of the ligand undergoes reversible CO_2 insertion while the other functions as a proton relay, stabilizing the adjacent unit via H-bonding/ion pairing. Such combination of Lewis/Brønsted acid-base reactivity resembles the one acting in amine/superbase systems (see Section 2.3). The synthesis of diamine-appended MOFs was extended to other transition

metals (Fe, Co, Ni, Zn) and the related CO_2 uptake isotherm varies according to the relative metal-amine/metal-carbamate bond strengths. Further adjustments can be accomplished by changing the *N*-substituents on the diamine [380,381], eventually supplying chirality [382].

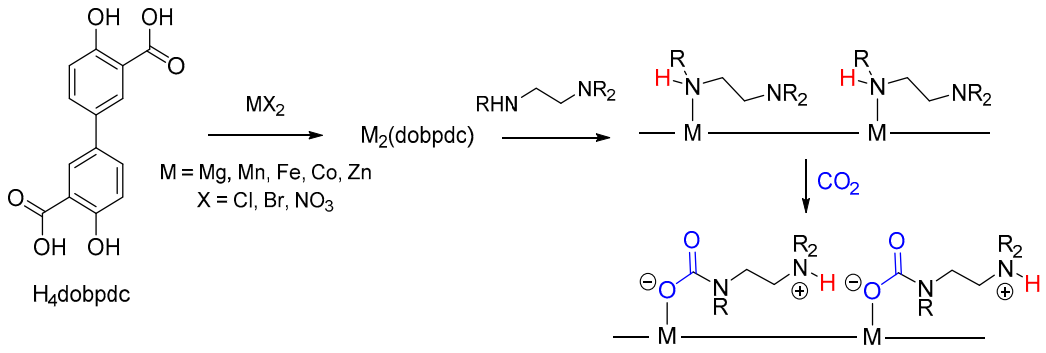

Scheme 46. Preparation of diamine-appended MOFs and insertion of CO_2 affording the ammonium carbamate.

Other applications. Some metal carbamato complexes have been investigated as additives to modify the physico-chemical properties of liquid systems. In this regard, bis-carbamates based on *N*,*N*-di(propylamino)dodecylamine produce under alkaline conditions a stable sodium bis-carbamate that is able to act as a surfactant [383,384]. This system is "switchable," as it can be reversed by heating or bubbling N_2. Moving to non-aqueous systems, homoleptic *N*,*N*-dialkylcarbamates of group 4 and 5 metals have been dissolved in bis(trifluoromethylsulfonyl)imide-based ionic liquids under anhydrous conditions [385]. These complexes showed a surprising solubility in such highly polar media, considering their neutral, nonpolar nature [131]. Spectroscopic measurements and DFT calculations outlined that the coordination sphere of the metal was preserved upon dissolution, paving the way to metal electrodeposition or catalytic processes.

Finally, some heterobimetallic, polynuclear Zn/Dy and Zn/Gd complexes featuring carbamato ligands have been investigated for their low-temperature magnetic properties [247,386].

6. Conclusions

The carbamato unit deriving from the basic combination of a non-tertiary amine with carbon dioxide can be effectively entrapped in molecular complexes of metal (or semimetal) elements across the periodic table. The synthetic procedures are generally straightforward and do not need high pressure equipment, thus allowing the easy access to both homoleptic and hybrid metal species. Several coordination modes are viable for the carbamato ligand, and the interconversion from bi- to monodentate coordination has been often observed, suggesting a versatile character. The reactivity of the metal-coordinated carbamato moiety is reversed respect to that of carbon dioxide; thus, metal carbamates are unreactive towards nucleophilic addition, but they may readily decompose upon treatment with electrophilic (protic) reagents, leading to the liberation of carbon dioxide and the amine. The peculiar and attracting features of this numerous and variegate class of metal compounds render them intriguing candidates in the perspective of various applications, and there has been a significant advance in recent years especially in the fields of catalysis and material chemistry. More specifically, the catalytic potential of metal carbamates appears promising and deserving of further and deeper developments in CO_2-fixation organic routes; indeed, the possible dynamic exchange between the carbamato [CO_2] fragment and external CO_2 may constitute an unusual way for the pre-activation of carbon dioxide, accelerating the overall catalytic process. On the other hand, the facile degradation of the carbamato unit upon contact with acidic groups is a potent tool for the targeted synthesis of metal nanoparticles, films of metal oxides and for the controlled decoration of solid materials with metal units (including lanthanides and heterogeneous systems) providing special properties.

Supplementary Materials: The following are available online at http://www.mdpi.com/1420-3049/25/16/3603/s1, Table S1: Rate (k) and equilibrium (K_{CBM}) constants for the carbamato formation and equilibrium constant (K_{HYD}) for the carbamato hydrolysis at 18 °C in water; Table S2: Selected X-ray bond distances (Å) and angles (°) in amidinium/guanidinium CO_2 adducts; Table S3: Selected bond distances (Å) and angles (°) for carbamato ligands in metal complexes; Table S4: NMR and IR data related to the NCO_2 moiety in structurally characterized metal carbamato complexes.

Author Contributions: G.B., L.B., G.P. and F.M.: bibliography research and writing. All authors have read and agreed to the published version of the manuscript.

Funding: This research received no external funding.

Conflicts of Interest: The authors declare no conflict of interest.

References

1. Smith, P.; Davis, S.J.; Creutzig, F.; Fuss, S.; Minx, J.; Gabrielle, B.; Kato, E.; Jackson, R.B.; Cowie, A.; Kriegler, E.; et al. Biophysical and economic limits to negative CO_2 emissions. *Nat. Clim. Chang.* **2016**, *6*, 42–50. [CrossRef]
2. Aresta, M. *Carbon Dioxide Recovery and Utilization*; Springer: Dordrecht, The Netherlands, 2003; ISBN 978-90-481-6335-9.
3. Wang, W.; Wang, S.; Ma, X.; Gong, J. Recent advances in catalytic hydrogenation of carbon dioxide. *Chem. Soc. Rev.* **2011**, *40*, 3703. [CrossRef] [PubMed]
4. Marques Mota, F.; Kim, D.H. From CO_2 methanation to ambitious long-chain hydrocarbons: Alternative fuels paving the path to sustainability. *Chem. Soc. Rev.* **2019**, *48*, 205–259. [CrossRef] [PubMed]
5. Cherubini-Celli, A.; Mateos, J.; Bonchio, M.; Dell'Amico, L.; Companyó, X. Transition Metal-Free CO_2 Fixation into New Carbon-Carbon Bonds. *Chem. Sus. Chem.* **2018**, *11*, 3056–3070. [CrossRef] [PubMed]
6. Yang, Y.; Lee, J.W. Toward ideal carbon dioxide functionalization. *Chem. Sci.* **2019**, *10*, 3905–3926. [CrossRef]
7. Lu, X.-B. CO_2-Mediated Formation of Chiral Fine Chemicals. In *Carbon Dioxide and Organometallics*; Springer International Publishing: New York, NY, USA, 2015; pp. 171–197, ISBN 9783319220789.
8. Yu, B.; He, L.-N. Upgrading Carbon Dioxide by Incorporation into Heterocycles. *Chem. Sus. Chem.* **2015**, *8*, 52–62. [CrossRef]
9. Aresta, M.; Forti, G. *Carbon Dioxide as a Source of Carbon*; Springer: Dordrecht, The Netherlands, 1987; ISBN 978-94-010-8240-2.
10. Behr, A. Activation of Carbon Dioxide via Coordination to Transition Metal Complexes. In *Catalysis in C1 Chemistry*; Keim, W., Ed.; Catalysis by Metal Complexes; Springer: Dordrecht, The Netherlands, 1983; Volume 3, p. 169, ISBN 978-94-009-7042-7.
11. Braunstein, P.; Matt, D.; Nobel, D. Reactions of carbon dioxide with carbon-carbon bond formation catalyzed by transition-metal complexes. *Chem. Rev.* **1988**, *88*, 747–764. [CrossRef]
12. Sanz-Pérez, E.S.; Murdock, C.R.; Didas, S.A.; Jones, C.W. Direct Capture of CO_2 from Ambient Air. *Chem. Rev.* **2016**, *116*, 11840–11876. [CrossRef]
13. Li, Y.-N.; He, L.-N.; Diao, Z.-F.; Yang, Z.-Z. Carbon Capture with Simultaneous Activation and Its Subsequent Transformation. In *Advances in Inorganic Chemistry*; Academic Press: Cambridge, MA, USA, 2014; pp. 289–345.
14. Tappe, N.A.; Reich, R.M.; D'Elia, V.; Kühn, F.E. Current advances in the catalytic conversion of carbon dioxide by molecular catalysts: An update. *Dalton Trans.* **2018**, *47*, 13281–13313. [CrossRef]
15. Song, Q.-W.; Zhou, Z.-H.; He, L.-N. Efficient, selective and sustainable catalysis of carbon dioxide. *Green Chem.* **2017**, *19*, 3707–3728. [CrossRef]
16. Aresta, M.; Nobile, C.F. (Carbon dioxide)bis(trialkylphosphine)nickel complexes. *J. Chem. Soc. Dalt. Trans.* **1977**, *7*, 708. [CrossRef]
17. Viasus, C.J.; Gabidullin, B.; Gambarotta, S. Linear End—On Coordination Modes of CO_2. *Angew. Chem. Int. Ed.* **2019**, *58*, 14887–14890. [CrossRef] [PubMed]
18. Kim, Y.-E.; Kim, J.; Lee, Y. Formation of a nickel carbon dioxide adduct and its transformation mediated by a Lewis acid. *Chem. Commun.* **2014**, *50*, 11458–11461. [CrossRef] [PubMed]
19. Devillard, M.; Declercq, R.; Nicolas, E.; Ehlers, A.W.; Backs, J.; Saffon-Merceron, N.; Bouhadir, G.; Slootweg, J.C.; Uhl, W.; Bourissou, D. A Significant but Constrained Geometry Pt→Al Interaction: Fixation of CO_2 and CS_2, Activation of H_2 and $PhCONH_2$. *J. Am. Chem. Soc.* **2016**, *138*, 4917–4926. [CrossRef]

20. Aresta, M. Carbon Dioxide Reduction and Uses as a Chemical Feedstock. In *Activation of Small Molecules*; Wiley-VCH Verlag GmbH & Co. KGaA: Weinheim, Germany, 2006; pp. 1–41, ISBN 3527313125.
21. Alvarez, R.; Carmona, E.; Poveda, M.L.; Sanchez-Delgado, R. Carbon dioxide chemistry. The synthesis and properties of trans-bis(carbon dioxide)tetrakis(trimethylphosphine)molybdenum (trans-[$Mo(CO_2)_2(PMe_3)_4$]): The first stable bis(carbon dioxide) adduct of a transition me. *J. Am. Chem. Soc.* **1984**, *106*, 2731–2732. [CrossRef]
22. Janes, T.; Yang, Y.; Song, D. Chemical reduction of CO_2 facilitated by C-nucleophiles. *Chem. Commun.* **2017**, *53*, 11390–11398. [CrossRef]
23. Baisch, U.; Schnick, W. Synthese und Kristallstruktur vonbis-1, 3-Dimethoxyethan-trichloro-samarium(III) undtris-*N*,*N*-Diisopropylcarbamato-samarium(III). *Z. Anorg. Allg. Chem.* **2003**, *629*, 2073–2078. [CrossRef]
24. Murphy, L.J.; Robertson, K.N.; Kemp, R.A.; Tuononen, H.M.; Clyburne, J.A.C. Structurally simple complexes of CO_2. *Chem. Commun.* **2015**, *51*, 3942–3956. [CrossRef]
25. Jiang, Y.; Zhang, X.; Fei, H. *N*-heterocyclic carbene-functionalized metal–organic frameworks for the chemical fixation of CO_2. *Dalton Trans.* **2020**, *49*, 6548–6552. [CrossRef]
26. Wang, Z.; Wang, F.; Xue, X.-S.; Ji, P. Acidity Scale of N-Heterocyclic Carbene Precursors: Can We Predict the Stability of NHC–CO_2 Adducts? *Org. Lett.* **2018**, *20*, 6041–6045. [CrossRef]
27. Hazari, N.; Heimann, J.E. Carbon Dioxide Insertion into Group 9 and 10 Metal–Element σ Bonds. *Inorg. Chem.* **2017**, *56*, 13655–13678. [CrossRef] [PubMed]
28. Zhang, Y.; Hanna, B.S.; Dineen, A.; Williard, P.G.; Bernskoetter, W.H. Functionalization of Carbon Dioxide with Ethylene at Molybdenum Hydride Complexes. *Organometallics* **2013**, *32*, 3969–3979. [CrossRef]
29. Chen, J.-H.; Deng, C.-H.; Fang, S.; Ma, J.-G.; Cheng, P. Binuclear molybdenum alkoxide as the versatile catalyst for the conversion of carbon dioxide. *Green Chem.* **2018**, *20*, 989–996. [CrossRef]
30. Field, L.D.; Jurd, P.M.; Magill, A.M.; Bhadbhade, M.M. Reactions of CO_2 and CS_2 with [$RuH(\eta^2\text{-}CH_2PMe_2)(PMe_3)_3$]. *Organometallics* **2013**, *32*, 636–642. [CrossRef]
31. Braunstein, P.; Matt, D.; Dusausoy, Y.; Fischer, J.; Mitschler, A.; Ricard, L. Complexes of functional phosphines. 4. Coordination properties of (diphenylphosphino)acetonitrile, ethyl (diphenylphosphino)acetate and corresponding carbanions. Characterization of a new facile reversible carbon dioxide insertion into palladium(II) compl. *J. Am. Chem. Soc.* **1981**, *103*, 5115–5125. [CrossRef]
32. Braunstein, P.; Matt, D.; Nobel, D. Carbon dioxide activation and catalytic lactone synthesis by telomerization of butadiene and carbon dioxide. *J. Am. Chem. Soc.* **1988**, *110*, 3207–3212. [CrossRef]
33. Varghese, A.M.; Karanikolos, G.N. CO_2 capture adsorbents functionalized by amine–bearing polymers: A review. *Int. J. Greenh. Gas Control* **2020**, *96*, 103005. [CrossRef]
34. Mazari, S.A.; Ghalib, L.; Sattar, A.; Bozdar, M.M.; Qayoom, A.; Ahmed, I.; Muhammad, A.; Abro, R.; Abdulkareem, A.; Nizamuddin, S.; et al. Review of modelling and simulation strategies for evaluating corrosive behavior of aqueous amine systems for CO_2 capture. *Int. J. Greenh. Gas Control* **2020**, *96*, 103010. [CrossRef]
35. Gelles, T.; Lawson, S.; Rownaghi, A.A.; Rezaei, F. *Recent Advances in Development of Amine Functionalized Adsorbents for CO_2 Capture*; Springer: New York, NY, USA, 2020; Volume 26, ISBN 0123456789.
36. Zhao, T.-X.; Zhai, G.-W.; Liang, J.; Li, P.; Hu, X.-B.; Wu, Y.-T. Catalyst-free N-formylation of amines using BH_3 NH_3 and CO_2 under mild conditions. *Chem. Commun.* **2017**, *53*, 8046–8049. [CrossRef]
37. Hulla, M.; Nussbaum, S.; Bonnin, A.R.; Dyson, P.J. The dilemma between acid and base catalysis in the synthesis of benzimidazole from o-phenylenediamine and carbon dioxide. *Chem. Commun.* **2019**, *55*, 13089–13092. [CrossRef]
38. Hao, L.; Zhang, H.; Luo, X.; Wu, C.; Zhao, Y.; Liu, X.; Gao, X.; Chen, Y.; Liu, Z. Reductive formylation of amines with CO_2 using sodium borohydride: A catalyst-free route. *J. CO_2 Util.* **2017**, *22*, 208–211. [CrossRef]
39. Hulla, M.; Dyson, P.J. Pivotal Role of the Basic Character of Organic and Salt Catalysts in C−N Bond Forming Reactions of Amines with CO_2. *Angew. Chem. Int. Ed.* **2020**, *59*, 1002–1017. [CrossRef] [PubMed]
40. Stec, B. Structural mechanism of RuBisCO activation by carbamylation of the active site lysine. *Proc. Natl. Acad. Sci. USA* **2012**, *109*, 18785–18790. [CrossRef] [PubMed]
41. Cleland, W.W.; Andrews, T.J.; Gutteridge, S.; Hartman, F.C.; Lorimer, G.H. Mechanism of Rubisco: The Carbamate as General Base. *Chem. Rev.* **1998**, *98*, 549–562. [CrossRef]
42. Dell'Amico, D.B.; Calderazzo, F.; Labella, L.; Marchetti, F.; Pampaloni, G. Converting Carbon Dioxide into Carbamato Derivatives. *Chem. Rev.* **2003**, *103*, 3857–3898. [CrossRef]

43. Hampe, E.M.; Rudkevich, D.M. Reversible covalent chemistry of CO_2. *Chem. Commun.* **2002**, *14*, 1450–1451. [CrossRef]
44. Terlouw, J.K.; Schwarz, H. The Generation and Characterization of Molecules by Neutralization-Reionization Mass Spectrometry (NRMS). New Analytical Methods (33). *Angew. Chem. Int. Ed.* **1987**, *26*, 805–815. [CrossRef]
45. Khanna, R.K.; Moore, M.H. Carbamic acid: Molecular structure and IR spectra. *Spectrochim. Acta. Part. A Mol. Biomol. Spectrosc.* **1999**, *55*, 961–967. [CrossRef]
46. Radeglia, R.; Andersch, J.; Schroth, W. Zum dynamischen Strukturverhalten des Dimethylamin—Kohlendioxid-Komplexes (Dimcarb)/On the Dynamic Structure Behaviour of the Dimethylamine—Carbondioxide Complex (Dimcarb). *Zeitschrift für Naturforsch. B* **1989**, *44*, 181–186. [CrossRef]
47. Aresta, M.; Ballivet-Tkatchenko, D.; Belli Dell'Amico, D.; Bonnet, M.C.; Boschi, D.; Calderazzo, F.; Faure, R.; Labella, L.; Marchetti, F. Isolation and structural determination of two derivatives of the elusive carbamic acid. *Chem. Commun.* **2000**, *8*, 1099–1100. [CrossRef]
48. McGhee, W.; Riley, D.; Christ, K.; Pan, Y.; Parnas, B. Carbon Dioxide as a Phosgene Replacement: Synthesis and Mechanistic Studies of Urethanes from Amines, CO_2, and Alkyl Chlorides. *J. Org. Chem.* **1995**, *60*, 2820–2830. [CrossRef]
49. Ishikawa, T. *Superbases for Organic Synthesis*; Ishikawa, T., Ed.; John Wiley & Sons, Ltd.: Chichester, UK, 2009; ISBN 9780470740859.
50. Hu, X.; Yu, Q.; Barzagli, F.; LI, C.; Fan, M.; Gasem, K.A.M.; Zhang, X.; Shiko, E.; Tian, M.; Luo, X.; et al. NMR techniques and prediction models for the analysis of the species formed in CO_2 capture processes with amine-based sorbents: A critical review. *ACS Sustain. Chem. Eng.* **2020**, *8*, 6173–6193. [CrossRef]
51. Bavoh, C.B.; Lal, B.; Osei, H.; Sabil, K.M.; Mukhtar, H. A review on the role of amino acids in gas hydrate inhibition, CO_2 capture and sequestration, and natural gas storage. *J. Nat. Gas Sci. Eng.* **2019**, *64*, 52–71. [CrossRef]
52. Conway, W.; Wang, X.; Fernandes, D.; Burns, R.; Lawrance, G.; Puxty, G.; Maeder, M. Toward the understanding of chemical absorption processes for post-combustion capture of carbon dioxide: Electronic and steric considerations from the kinetics of reactions of $CO_{2\,(aq)}$ with sterically hindered amines. *Environ. Sci. Technol.* **2013**, *47*, 1163–1169. [CrossRef]
53. Ermatchkov, V.; Pérez-Salado Kamps, Á.; Maurer, G. Chemical equilibrium constants for the formation of carbamates in (carbon dioxide + piperazine + water) from 1H-NMR-spectroscopy. *J. Chem. Thermodyn.* **2003**, *35*, 1277–1289. [CrossRef]
54. Fernandes, D.; Conway, W.; Burns, R.; Lawrance, G.; Maeder, M.; Puxty, G. Investigations of primary and secondary amine carbamate stability by 1H NMR spectroscopy for post combustion capture of carbon dioxide. *J. Chem. Thermodyn.* **2012**, *54*, 183–191. [CrossRef]
55. Conway, W.; Wang, X.; Fernandes, D.; Burns, R.; Lawrance, G.; Puxty, G.; Maeder, M. Toward rational design of amine solutions for PCC applications: The kinetics of the reaction of $CO_{2\,(aq)}$ with cyclic and secondary amines in aqueous solution. *Environ. Sci. Technol.* **2012**, *46*, 7422–7429. [CrossRef]
56. Li, L.; Clifford, S.; Puxty, G.; Maeder, M.; Burns, R.; Yu, H.; Conway, W. Kinetic and Equilibrium Reactions of a New Heterocyclic Aqueous 4-Aminomethyltetrahydropyran (4-AMTHP) Absorbent for Post Combustion Carbon Dioxide (CO_2) Capture Processes. *ACS Sustain. Chem. Eng.* **2017**, *5*, 9200–9206. [CrossRef]
57. Kumar, P.S.; Hogendoorn, J.A.; Timmer, S.J.; Feron, P.H.M.; Versteeg, G.F. Equilibrium Solubility of CO_2 in Aqueous Potassium Taurate Solutions: Part 2. Experimental VLE Data and Model. *Ind. Eng. Chem. Res.* **2003**, *42*, 2841–2852. [CrossRef]
58. Coulier, Y.; Lowe, A.R.; Coxam, J.Y.; Ballerat-Busserolles, K. Thermodynamic Modeling and Experimental Study of CO_2 Dissolution in New Absorbents for Post-Combustion CO_2 Capture Processes. *ACS Sustain. Chem. Eng.* **2018**, *6*, 918–926. [CrossRef]
59. Jensen, A.; Jensen, J.B.; Faurholt, C.; Finsnes, E.; Sörensen, J.S.; Sörensen, N.A. Studies on Carbamates. VI. The Carbamate of Glycine. *Acta Chem. Scand.* **1952**, *6*, 395–397. [CrossRef]
60. Xiang, Q.; Fang, M.; Yu, H.; Maeder, M. Kinetics of the reversible reaction of $CO_{2\,(aq)}$ and HCO_{3-} with sarcosine salt in aqueous solution. *J. Phys. Chem. A* **2012**, *116*, 10276–10284. [CrossRef] [PubMed]
61. Jensen, A.; Faurholt, C.; Faurholt, C.; Finsnes, E.; Sörensen, J.S.; Sörensen, N.A. Studies on Carbamates. V. The Carbamates of alpha-Alanine and beta-Alanine. *Acta Chem. Scand.* **1952**, *6*, 385–394. [CrossRef]

62. Majchrowicz, M.E.; Brilman, D.W.F. Solubility of CO_2 in aqueous potassium L-prolinate solutions-absorber conditions. *Chem. Eng. Sci.* **2012**, *72*, 35–44. [CrossRef]
63. Shen, S.; Zhao, Y.; Bian, Y.; Wang, Y.; Guo, H.; Li, H. CO_2 absorption using aqueous potassium lysinate solutions: Vapor–liquid equilibrium data and modelling. *J. Chem. Thermodyn.* **2017**, *115*, 209–220. [CrossRef]
64. Jensen, A.; Jensen, M.B.; Faurholt, C. Studies on Carbamates. VIII. The Carbamates of Benzylamine, Piperidine and Aniline. *Acta Chem. Scand.* **1952**, *6*, 1073–1085. [CrossRef]
65. Jensen, A.; Jensen, M.B.; Faurholt, C.; Sörensen, N.A. Studies on Carbamates. X. The Carbamates of Di-n-Propylamine and Di-iso-Propylamine. *Acta Chem. Scand.* **1954**, *8*, 1129–1136. [CrossRef]
66. Jensen, M.B. Studies on Carbamates. XII. The Carbamates of the Butylamines. *Acta Chem. Scand.* **1957**, *11*, 499–505. [CrossRef]
67. Zhou, W.; Cheng, K.; Kang, J.; Zhou, C.; Subramanian, V.; Zhang, Q.; Wang, Y. New horizon in C1 chemistry: Breaking the selectivity limitation in transformation of syngas and hydrogenation of CO_2 into hydrocarbon chemicals and fuels. *Chem. Soc. Rev.* **2019**, *48*, 3193–3228. [CrossRef]
68. Artz, J.; Müller, T.E.; Thenert, K.; Kleinekorte, J.; Meys, R.; Sternberg, A.; Bardow, A.; Leitner, W. Sustainable Conversion of Carbon Dioxide: An Integrated Review of Catalysis and Life Cycle Assessment. *Chem. Rev.* **2018**, *118*, 434–504. [CrossRef]
69. Martens, J.A.; Bogaerts, A.; De Kimpe, N.; Jacobs, P.A.; Marin, G.B.; Rabaey, K.; Saeys, M.; Verhelst, S. The Chemical Route to a Carbon Dioxide Neutral World. *Chem. Sus. Chem.* **2017**, *10*, 1039–1055. [CrossRef] [PubMed]
70. Aresta, M.; Dibenedetto, A.; Angelini, A. Catalysis for the valorization of exhaust carbon: From CO_2 to chemicals, materials, and fuels. technological use of CO_2. *Chem. Rev.* **2014**, *114*, 1709–1742. [CrossRef] [PubMed]
71. Hu, G.; Smith, K.H.; Wu, Y.; Mumford, K.A.; Kentish, S.E.; Stevens, G.W. Carbon dioxide capture by solvent absorption using amino acids: A review. *Chinese J. Chem. Eng.* **2018**, *26*, 2229–2237. [CrossRef]
72. Fernandes, D.; Conway, W.; Wang, X.; Burns, R.; Lawrance, G.; Maeder, M.; Puxty, G. Protonation constants and thermodynamic properties of amines for post combustion capture of CO_2. *J. Chem. Thermodyn.* **2012**, *51*, 97–102. [CrossRef]
73. Christensen, J.J.; Izatt, R.M.; Wrathall, D.P.; Hansen, L.D. Thermodynamics of proton ionization in dilute aqueous solution. Part XI. pK, ΔH°, and ΔS° values for proton ionization from protonated amines at 25°. *J. Chem. Soc. A* **1969**, 1212–1223. [CrossRef]
74. Dey, A.; Desiraju, G.R.; Mondal, R.; Howard, J.A.K. A 1:1 molecular complex of 4-aminocyclohexanol and (4-hydroxycyclohexyl)carbamic acid. *Acta Crystallogr. Sect. E Struct. Rep. Online* **2004**, *60*, o857–o859. [CrossRef]
75. Mondal, R.; Bhunia, M.K. Crystal Chemistry of 1:1 Molecular Complexes of Carbamate Salts Formed by Slow Aerial Carbonation of Amines. *J. Chem. Crystallogr.* **2008**, *38*, 787–792. [CrossRef]
76. Zhang, W.H.; Li, K.; Li, Q.; Mak, T.C.W. Two inclusion compounds of guanylthiourea and 1,3,5-thiadiazole-5-amido-2-carbamate. *J. Incl. Phenom. Macrocycl. Chem.* **2012**, *74*, 353–359. [CrossRef]
77. Jiang, H.; Novak, I. Piperidine–CO_2–H_2O molecular complex. *J. Mol. Struct.* **2003**, *645*, 177–183. [CrossRef]
78. Madarász, J.; Székely, E.; Halász, J.; Bánsághi, G.; Varga, D.; Simándi, B.; Pokol, G. Ammonium carbamate type self-derivative salts of (R-)- and racemic α-methylbenzylamine: Composition and thermal stability by evolved gas analyses (TG-FTIR and TG/DTA-MS). *J. Therm. Anal. Calorim.* **2013**, *111*, 567–574. [CrossRef]
79. Shi, P.-F.; Xu, T.-T.; Xu, X.-Y.; Niu, S.-R. (3-Ammonio-2-hydroxypropyl)carbamate monohydrate. *Acta. Crystallogr. Sect. E Struct. Rep. Online* **2006**, *62*, o5191–o5193. [CrossRef]
80. Neda, I.; Kaukorat, T.; Fischer, A.K. Unusual Stabilization of 1,2-Diamino Derivatives of Quincorine and Quincoridine by Carbon Dioxide: Persistent Crystallineprim-Ammonium-Carbamate Salts and Their Reactivity towards Isatoic Acid Anhydride. *Eur. J. Org. Chem.* **2003**, *2003*, 3784–3790. [CrossRef]
81. Meijide, F.; Antelo, A.; Alvarez, M.; Soto, V.H.; Trillo, J.V.; Jover, A.; Vázquez Tato, J. Spontaneous Formation in the Solid State of Carbamate Derivatives of Bile Acids. *Cryst. Growth Des.* **2011**, *11*, 356–361. [CrossRef]
82. Jo, E.; Jhon, Y.H.; Choi, S.B.; Shim, J.G.; Kim, J.H.; Lee, J.H.; Lee, I.Y.; Jang, K.R.; Kim, J. Crystal structure and electronic properties of 2-amino-2-methyl-1-propanol (AMP) carbamate. *Chem. Commun.* **2010**, *46*, 9158–9160. [CrossRef] [PubMed]

83. Berkessel, A.; Schröder, M.; Sklorz, C.A.; Tabanella, S.; Vogl, N.; Lex, J.; Neudörfl, J.M. Enantioselective Synthesis of DIANANE, a Novel C_2 -Symmetric Chiral Diamine for Asymmetric Catalysis. *J. Org. Chem.* **2004**, *69*, 3050–3056. [CrossRef]
84. Berkessel, A.; Roland, K.; Schröder, M.; Neudörfl, J.M.; Lex, J. Enantiomerically Pure Isophorone Diamine [3-(Aminomethyl)-3,5,5-trimethylcyclohexylamine]: A Chiral 1,4-Diamine Building Block Made Available on Large Scale. *J. Org. Chem.* **2006**, *71*, 9312–9318. [CrossRef]
85. Fonari, M.S.; Antal, S.; Castañeda, R.; Ordonez, C.; Timofeeva, T.V. Crystalline products of CO_2 capture by piperazine aqueous solutions. *Cryst. Eng. Comm.* **2016**, *18*, 6282–6289. [CrossRef]
86. Garbauskas, M.F.; Goehner, R.P.; Davis, A.M. The structure of two polymorphs of N-(2-ammonioethyl)carbamate, $C_3H_8N_2O_2$. *Acta Crystallogr. Sect. C Cryst. Struct. Commun.* **1983**, *39*, 1684–1686. [CrossRef]
87. Katchalski, E.; Berliner-Klibanski, C.; Berger, A. The Chemical Structure of Some Diamine Carbamates. *J. Am. Chem. Soc.* **1951**, *73*, 1829–1831. [CrossRef]
88. Baidya, M.; Mayr, H. Nucleophilicities and carbon basicities of DBU and DBN. *Chem. Commun.* **2008**, *15*, 1792–1794. [CrossRef]
89. Pereira, F.S.; Lincon Da Silva Agostini, D.; Do Espírito Santo, R.D.; Deazevedo, E.R.; Bonagamba, T.J.; Job, A.E.; González, E.R.P. A comparative solid state 13C NMR and thermal study of CO_2 capture by amidines PMDBD and DBN. *Green Chem.* **2011**, *13*, 2146–2153. [CrossRef]
90. Pereira, F.S.; DeAzevedo, E.R.; da Silva, E.F.; Bonagamba, T.J.; da Silva Agostíni, D.L.; Magalhães, A.; Job, A.E.; Pérez González, E.R. Study of the carbon dioxide chemical fixation—activation by guanidines. *Tetrahedron* **2008**, *64*, 10097–10106. [CrossRef]
91. Villiers, C.; Dognon, J.-P.; Pollet, R.; Thuéry, P.; Ephritikhine, M. An Isolated CO_2 Adduct of a Nitrogen Base: Crystal and Electronic Structures. *Angew. Chem. Int. Ed.* **2010**, *49*, 3465–3468. [CrossRef] [PubMed]
92. Wilm, L.F.B.; Eder, T.; Mück-Lichtenfeld, C.; Mehlmann, P.; Wünsche, M.; Buß, F.; Dielmann, F. Reversible CO_2 fixation by N-heterocyclic imines forming water-stable zwitterionic nitrogen-base-CO_2 adducts. *Green Chem.* **2019**, *21*, 640–648. [CrossRef]
93. Pérez, E.R.; Santos, R.H.A.; Gambardella, M.T.P.; De Macedo, L.G.M.; Rodrigues-Filho, U.P.; Launay, J.C.; Franco, D.W. Activation of carbon dioxide by bicyclic amidines. *J. Org. Chem.* **2004**, *69*, 8005–8011. [CrossRef]
94. Ramkumar, V.; Gardas, R.L. Thermophysical Properties and Carbon Dioxide Absorption Studies of Guanidinium-Based Carboxylate Ionic Liquids. *J. Chem. Eng. Data* **2019**, *64*, 4844–4855. [CrossRef]
95. Nicholls, R.; Kaufhold, S.; Nguyen, B.N. Observation of guanidine-carbon dioxide complexation in solution and its role in the reaction of carbon dioxide and propargylamines. *Catal. Sci. Technol.* **2014**, *4*, 3458–3462. [CrossRef]
96. Heldebrant, D.J.; Jessop, P.G.; Thomas, C.A.; Eckert, C.A.; Liotta, C.L. The reaction of 1,8-diazabicyclo[5.4.0]undec-7-ene (DBU) with carbon dioxide. *J. Org. Chem.* **2005**, *70*, 5335–5338. [CrossRef]
97. Valera Lauridsen, J.M.; Cho, S.Y.; Bae, H.Y.; Lee, J.-W. CO_2 (De)Activation in Carboxylation Reactions: A Case Study Using Grignard Reagents and Nucleophilic Bases. *Organometallics* **2020**, *39*, 1652–1657. [CrossRef]
98. Lv, M.; Wang, P.; Yuan, D.; Yao, Y. Conversion of Carbon Dioxide into Oxazolidinones Mediated by Quaternary Ammonium Salts and DBU. *Chem. Cat. Chem.* **2017**, *9*, 4451–4455. [CrossRef]
99. Yoshida, M.; Mizuguchi, T.; Shishido, K. Synthesis of oxazolidinones by efficient fixation of atmospheric CO_2 with propargylic amines by using a silver/1,8-diazabicyclo[5.4.0] undec-7-ene (DBU) dual-catalyst system. *Chem. Eur. J.* **2012**, *18*, 15578–15581. [CrossRef] [PubMed]
100. Yoshida, M.; Komatsuzaki, Y.; Ihara, M. Synthesis of 5-Vinylideneoxazolidin-2-ones by DBU-Mediated CO_2-Fixation Reaction of 4-(Benzylamino)-2-butynyl Carbonates and Benzoates. *Org. Lett.* **2008**, *10*, 2083–2086. [CrossRef] [PubMed]
101. Kaupmees, K.; Trummal, A.; Leito, I. Basicities of strong bases in water: A computational study. *Croat. Chem. Acta* **2014**, *87*, 385–395. [CrossRef]
102. McGhee, W.D.; Riley, D.P. Palladium-Mediated Synthesis of Urethanes from Amines, Carbon Dioxide, and Cyclic Diolefins. *Organometallics* **1992**, *11*, 900–907. [CrossRef]
103. McGhee, W.D.; Pan, Y.; Riley, D.P. Highly selective generation of urethanes from amines, carbon dioxide and alkyl chlorides. *J. Chem. Soc. Chem. Commun.* **1994**, *25*, 699–700. [CrossRef]
104. Jessop, P.G.; Heldebrant, D.J.; Li, X.; Eckert, C.A.; Liotta, C.L. Reversible nonpolar-to-polar solvent. *Nature* **2005**, *436*, 1102. [CrossRef] [PubMed]

105. Yamada, T.; Lukac, P.J.; George, M.; Weiss, R.G. Reversible, room-temperature ionic liquids. Amidinium carbamates derived from amidines and aliphatic primary amines with carbon dioxide. *Chem. Mater.* **2007**, *19*, 967–969. [CrossRef]
106. Yu, T.; Yamada, T.; Gaviola, G.C.; Weiss, R.G. Carbon dioxide and molecular nitrogen as switches between ionic and uncharged room-temperature liquids comprised of amidines and chiral amino alcohols. *Chem. Mater.* **2008**, *20*, 5337–5344. [CrossRef]
107. Yamada, T.; Lukac, P.J.; Yu, T.; Weiss, R.G. Reversible, room-temperature, chiral ionic liquids. *Amidinium carbamates* derived from amidines and amino-acid esters with carbon dioxide. *Chem. Mater.* **2007**, *19*, 4761–4768. [CrossRef]
108. Biancalana, L.; Bresciani, G.; Chiappe, C.; Marchetti, F.; Pampaloni, G. Synthesis and study of the stability of amidinium/guanidinium carbamates of amines and α-amino acids. *New J. Chem.* **2017**, *41*, 1798–1805. [CrossRef]
109. Bortoluzzi, M.; Bresciani, G.; Marchetti, F.; Pampaloni, G.; Zacchini, S. Synthesis and structural characterization of mixed halide–*N*,*N*-diethylcarbamates of group 4 metals, including a case of unusual tetrahydrofuran activation. *New J. Chem.* **2017**, *41*, 1781–1789. [CrossRef]
110. Carrera, G.V.S.M.; da Ponte, M.N.; Branco, L.C. Synthesis and properties of reversible ionic liquids using CO_2, mono- to multiple functionalization. *Tetrahedron* **2012**, *68*, 7408–7413. [CrossRef]
111. Carrera, G.V.S.M.; Jordão, N.; Santos, M.M.; Da Ponte, M.N.; Branco, L.C. Reversible systems based on CO_2, amino-acids and organic superbases. *RSC Adv.* **2015**, *5*, 35564–35571. [CrossRef]
112. Nicholls, R.L.; McManus, J.A.; Rayner, C.M.; Morales-Serna, J.A.; White, A.J.P.; Nguyen, B.N. Guanidine-Catalyzed reductive amination of carbon dioxide with silanes: Switching between pathways and suppressing catalyst deactivation. *ACS Catal.* **2018**, *8*, 3678–3687. [CrossRef]
113. Liu, X.; Wang, M.-Y.; Wang, S.-Y.; Wang, Q.; He, L.-N. In Situ Generated Zinc(II) Catalyst for Incorporation of CO_2 into 2-Oxazolidinones with Propargylic Amines at Atmospheric Pressure. *Chem. Sus. Chem.* **2017**, *10*, 1210–1216. [CrossRef]
114. Das Neves Gomes, C.; Jacquet, O.; Villiers, C.; Thuéry, P.; Ephritikhine, M.; Cantat, T. A Diagonal Approach to Chemical Recycling of Carbon Dioxide: Organocatalytic Transformation for the Reductive Functionalization of CO_2. *Angew. Chem.* **2012**, *124*, 191–194. [CrossRef]
115. Cerveri, A.; Pace, S.; Monari, M.; Lombardo, M.; Bandini, M. Redox-Neutral Metal-Free Three-Component Carbonylative Dearomatization of Pyridine Derivatives with CO_2. *Chem. -Eur. J.* **2019**, *25*, 15272–15276. [CrossRef]
116. Matulková, I.; Charvátová, H.; Císařová, I.; Štěpnička, P. The crystal structure of the inner salt of 2-[(aminoiminomethyl)amino]ethylcarbamic acid [systematic name: (2-((diaminomethylene)ammonio)ethyl)carbamate], $C_4H_{10}N_4O_2$. *Z. Kristallogr. NCS* **2017**, *232*, 685–687. [CrossRef]
117. Wang, C.; Luo, H.; Jiang, D.E.; Li, H.; Dai, S. Carbon dioxide capture by superbase-derived protic ionic liquids. *Angew. Chem. Int. Ed.* **2010**, *49*, 5978–5981. [CrossRef]
118. Wang, C.; Luo, X.; Luo, H.; Jiang, D.E.; Li, H.; Dai, S. Tuning the basicity of ionic liquids for equimolar CO_2 capture. *Angew. Chem. Int. Ed.* **2011**, *50*, 4918–4922. [CrossRef]
119. Gao, F.; Wang, Z.; Ji, P.; Cheng, J.P. CO_2 absorption by DBU-based protic ionic liquids: Basicity of anion dictates the absorption capacity and mechanism. *Front. Chem.* **2019**, *7*, 1–8. [CrossRef]
120. Zhu, X.; Song, M.; Xu, Y. DBU-Based Protic Ionic Liquids for CO_2 Capture. *ACS Sustain. Chem. Eng.* **2017**, *5*, 8192–8198. [CrossRef]
121. Zhu, X.; Song, M.; Ling, B.; Wang, S.; Luo, X. The Highly Efficient Absorption of CO_2 by a Novel DBU Based Ionic Liquid. *J. Solution Chem.* **2020**, *49*, 257–271. [CrossRef]
122. Chandra, G.; Lappert, M.F. Reactions of amino-derivatives of transition-metals. *Inorg. Nucl. Chem. Lett.* **1965**, *1*, 83–84. [CrossRef]
123. Horley, G.A.; Mahon, M.F.; Molloy, K.C.; Haycock, P.W.; Myers, C.P. Synthesis and Characterization of Novel Homoleptic *N*,*N* -Dialkylcarbamato Complexes of Antimony: Precursors for the Deposition of Antimony Oxides. *Inorg. Chem.* **2002**, *41*, 5052–5058. [CrossRef]

124. Chandra, G.; Jenkins, A.D.; Lappert, M.F.; Srivastava, R.C. Amido-derivatives of metals and metalloids. Part X. Reactions of titanium(IV), zirconium(IV), and hafnium(IV) amides with unsaturated substrates, and some related experiments with amides of boron, silicon, germanium, and tin(IV). *J. Chem. Soc. A Inorg. Phys. Theor.* **1970**, 2550. [CrossRef]
125. Chisholm, M.H.; Extine, M. Tris(dimethylaminato)tris(*N*,*N*-dimethylcarbamato)tungsten(VI). Product of the remarkable reaction between hexakis(dimethylaminato)tungsten and carbon dioxide. *J. Am. Chem. Soc.* **1974**, *96*, 6214–6216. [CrossRef]
126. Chisholm, M.H.; Extine, M.W. Reactions of transition metal-nitrogen. sigma. bonds. 4. Mechanistic studies of carbon dioxide insertion and carbon dioxide exchange reactions involving early transition metal dimethylamido and *N*,*N*-dimethylcarbamato compounds. *J. Am. Chem. Soc.* **1977**, *99*, 792–802. [CrossRef]
127. Chisholm, M.H.; Extine, M.W. Reactions of transition metal-nitrogen. sigma. bonds. 3. Early transition metal *N*,*N*-dimethylcarbamates. Preparation, properties, and carbon dioxide exchange reactions. *J. Am. Chem. Soc.* **1977**, *99*, 782–792. [CrossRef]
128. Chisholm, M.H.; Cotton, F.A.; Extine, M.W.; Rideout, D.C. Reactions of transition-metal-nitrogen.sigma.-bonds. 5. Carbonation of tetrakis(diethylamido)chromium(IV) to yield binuclear chromium(III) and -(II) carbamato complexes. *Inorg. Chem.* **1978**, *17*, 3536–3540. [CrossRef]
129. Chisholm, M.H.; Haitko, D.A.; Murillo, C.A. New. sigma.-ethyl compounds of dimolybdenum (M.tplbond.M) and evidence for dinuclear reductive elimination with a concomitant metal-metal triple to quadruple bond transformation: Et-M. tplbond. M-Et. fwdarw. M::M + C_2H_4 + C_2. *J. Am. Chem. Soc.* **1978**, *100*, 6262–6263. [CrossRef]
130. Chisholm, M.H.; Extine, M. Reactions of transition metal-nitrogen. sigma.-bonds. II. Pentakis(*N*,*N*-dimethylcarbamato)niobium(V) and its facile exchange reaction with carbon dioxide. *J. Am. Chem. Soc.* **1975**, *97*, 1623–1625. [CrossRef]
131. Forte, C.; Pampaloni, G.; Pinzino, C.; Renili, F. *N*,*N*-Dialkylcarbamato derivatives of niobium and tantalum as precursors to metal-functionalized silica surfaces. *Inorg. Chim. Acta* **2011**, *365*, 251–255. [CrossRef]
132. Bagnall, K.W.; Yanir, E. Thorium(IV) and uranium(IV) carbamates. *J. Inorg. Nucl. Chem.* **1974**, *36*, 777–779. [CrossRef]
133. Kennedy, A.R.; Mulvey, R.E.; Oliver, D.E.; Robertson, S.D. Lithium and aluminium carbamato derivatives of the utility amide 2,2,6,6-tetramethylpiperidide. *Dalton Trans.* **2010**, *39*, 6190–6197. [CrossRef]
134. Bayer, U.; Werner, D.; Maichle-Mössmer, C.; Anwander, R. Effective and Reversible Carbon Dioxide Insertion into Cerium Pyrazolates. *Angew. Chem. Int. Ed.* **2020**, *59*, 5830–5836. [CrossRef]
135. Cosham, S.D.; Hill, M.S.; Horley, G.A.; Johnson, A.L.; Jordan, L.; Molloy, K.C.; Stanton, D.C. Synthesis and materials chemistry of bismuth Tris-(di-i-propylcarbamate): Deposition of photoactive Bi_2O_3 thin films. *Inorg. Chem.* **2014**, *53*, 503–511. [CrossRef]
136. Stewart, C.A.; Dickie, D.A.; Tang, Y.; Kemp, R.A. Insertion reactions of CO_2, OCS, and CS_2 into the Sn-N bonds of $(Me_2N)_2Sn$: NMR and X-ray structural characterization of the products. *Inorg. Chim. Acta.* **2011**, *376*, 73–79. [CrossRef]
137. Calderazzo, F.; Dell'Amico, G.; Netti, R.; Pasquali, M. Dialkylcarbamato Complexes of Transition Elements. 1. A New Method for the Synthesis of *N*,*N*-Dialkylcarbamato and *N*,*N*-Dialkyldithiocarbamato Complexes of Uranium(IV). *Inorg. Chem.* **1978**, *17*, 471–473. [CrossRef]
138. Belli Dell'Amico, D.; Calderazzo, F.; Dell'Innocenti, M.; Guldenpfennig, B.; Ianelli, S.; Pelizzi, G.; Robino, P. *N*,*N*-Dialkylcarbamates of Silicon and Aluminium. *Gazz. Chim. Ital.* **1993**, *123*, 283–288.
139. Hayatifar, M.; Forte, C.; Pampaloni, G.; Kissin, Y.V.; Maria Raspolli Galletti, A.; Zacchini, S. Titanium complexes bearing carbamato ligands as catalytic precursors for propylene polymerization reactions. *J. Polym. Sci. Part A Polym. Chem.* **2013**, *51*, 4095–4102. [CrossRef]
140. Albinati, A.; Carraro, M.L.; Gross, S.; Rancan, M.; Rizzato, S.; Tondello, E.; Venzo, A. Synthesis and Characterisation of a New $Cu(O_2CNAllyl_2)_2$ Carbamato Complex and an Unusual Polymeric Cu^I Complex $[Cu^I_2Cl_4(NHAllyl_2)_4]_n$: New Insigh. *Eur. J. Inorg. Chem.* **2009**, *35*, 5346–5351. [CrossRef]
141. Dell'Amico, D.B.; Calderazzo, F.; Labella, L.; Marchetti, F. *N*,*N*-Di-iso-propylcarbamato Complexes of Boron. *Inorg. Chem.* **2008**, *47*, 5372–5376. [CrossRef] [PubMed]
142. Levashov, A.S.; Buryi, D.S.; Latypova, A.R. Indium *tris*(*N*,*N*-diethylcarbamate), Method of Its Production and Obtaining of Films of Indium Oxide on Its Basis. 2018. RU 2649147 C1 20180330. Available online: https://www.elibrary.ru/item.asp?id=38150566 (accessed on 3 July 2020).

143. Belli Dell'Amico, D.; Labella, L.; Marchetti, F.; Mastrorilli, P.; Samaritani, S.; Todisco, S. Oxidation by dioxygen of manganese(II) and iron(II) complexes. *Polyhedron* **2013**, *65*, 275–281. [CrossRef]
144. Baisch, U.; Dell' Amico, D.B.; Calderazzo, F.; Labella, L.; Marchetti, F.; Vitali, D. Reaction of a tetranuclear *N*,*N*-di-iso-propylcarbamato complex of cerium(III) with dioxygen: Synthesis and X-ray characterization of both the oxidation product and its precursor. *J. Mol. Catal. A Chem.* **2003**, *204–205*, 259–265. [CrossRef]
145. Baisch, U.; Dell'Amico, D.B.; Calderazzo, F.; Labella, L.; Marchetti, F.; Merigo, A. *N*,*N*-dialkylcarbamato lanthanide complexes, a series of isotypical coordination compounds. *Eur. J. Inorg. Chem.* **2004**, *6*, 1219–1224. [CrossRef]
146. Belli Dell'Amico, D.; Biagini, P.; Chiaberge, S.; Falchi, L.; Labella, L.; Lezzerini, M.; Marchetti, F.; Samaritani, S. Partial and exhaustive hydrolysis of lanthanide *N*,*N*-dialkylcarbamato complexes. A viable access to lanthanide mixed oxides. *Polyhedron* **2015**, *102*, 452–461. [CrossRef]
147. Pineda, E.M.; Lan, Y.; Fuhr, O.; Wernsdorfer, W.; Ruben, M. Exchange-bias quantum tunnelling in a CO_2-based Dy_4-single molecule magnet. *Chem. Sci.* **2017**, *8*, 1178–1185. [CrossRef]
148. Bradley, D.C.; Thomas, I.M. Metallo-Organic compounds containing metal-nitrogen bonds: Part III. Dialkylamino compounds of tantalum. *Can. J. Chem.* **1962**, *40*, 1355–1360. [CrossRef]
149. Bradley, D.C.; Thomas, I.M. Metallo-Organic compounds containing metal-nitrogen bonds: Part II. Some dialkylamino derivatives of Nb(V) and Nb(IV). *Can. J. Chem.* **1962**, *40*, 449–454. [CrossRef]
150. Dell'Amico, D.B.; Calderazzo, F.; Farnocchi, S.; Labella, L.; Marchetti, F. The NHR_2/CO_2 system as a metal ion extraction reagent from aqueous solution into hydrocarbons: Copper(II) and zinc(II). *Inorg. Chem. Commun.* **2002**, *5*, 848–852. [CrossRef]
151. Armelao, L.; Belli Dellamico, D.; Biagini, P.; Bottaro, G.; Chiaberge, S.; Falvo, P.; Labella, L.; Marchetti, F.; Samaritani, S. Preparation of *N*,*N* -dialkylcarbamato lanthanide complexes by extraction of lanthanide ions from aqueous solution into hydrocarbons. *Inorg. Chem.* **2014**, *53*, 4861–4871. [CrossRef] [PubMed]
152. Belli Dell'Amico, D.; De Sanctis, M.; Ishak, R.; Dolci, S.; Labella, L.; Lezzerini, M.; Marchetti, F. Cerium(III) *N*,*N*-dibutylcarbamate as precursor to nanocrystalline cerium dioxide. *Polyhedron* **2015**, *99*, 170–176. [CrossRef]
153. Armelao, L.; Belli Dellamico, D.; Bellucci, L.; Bottaro, G.; Labella, L.; Marchetti, F.; Samaritani, S. Smart Grafting of Lanthanides onto Silica via *N*,*N*-Dialkylcarbamato Complexes. *Inorg. Chem.* **2016**, *55*, 939–947. [CrossRef]
154. Belli Dell'Amico, D.; Biagini, P.; Bongiovanni, G.; Chiaberge, S.; Di Giacomo, A.; Labella, L.; Marchetti, F.; Marra, G.; Mura, A.; Quochi, F.; et al. A convenient preparation of nano-powders of Y_2O_3, $Y_3Al_5O_{12}$ and Nd:$Y_3Al_5O_{12}$ and study of the photoluminescent emission properties of the neodymium doped oxide. *Inorg. Chim. Acta.* **2018**, *470*, 149–157. [CrossRef]
155. Belforte, A.; Calderazzo, F. Formation of alkylurethanes from carbon dioxide by regioselective O-alkylation of alkali-metal *N*,*N*-diethylcarbamates in the presence of complexing agents. *J. Chem. Soc. Dalt. Trans.* **1989**, *5*, 1007–1009. [CrossRef]
156. Belforte, A.; Dell'Amico, D.B.; Calderazzo, F. Incorporation and deoxygenation of carbon dioxide: A metal-assisted facile conversion of carbon dioxide and primary amines to isocyanates. *Chem. Ber.* **1988**, *121*, 1891–1897. [CrossRef]
157. Klunker, J.; Biedermann, M.; Schäfer, W.; Hartung, H. *N*,*N*-Dimethylcarbamato-Komplexe von Kupfer und Zink. *Z. Anorg. Allg. Chem.* **1998**, *624*, 1503–1508.
158. Kim, K.A.; Cha, J.R.; Yun, S.W.; Gong, M.S. Preparation of zinc oxide nanoparticles at low temperature using new organometallic zinc carbamate precursor. *Bull. Korean Chem. Soc.* **2015**, *36*, 1426–1432. [CrossRef]
159. Alessio, R.; Dell'Amico, D.B.; Calderazzo, F.; Englert, U.; Guarini, A.; Labella, L.; Strasser, P. *N*,*N*-Dialkylcarbamato Complexes of the d10 cations of copper, silver, and gold. *Helv. Chim. Acta.* **1998**, *81*, 219–230. [CrossRef]
160. Tyler Caudle, M. Carboxylate-shift-like dynamic equilibrium in bromomagnesium diethylcarbamate. *Inorg. Chem.* **1999**. [CrossRef]
161. Srivastava, R.S.; Singh, G.; Nakano, M.; Osakada, K.; Ozawa, F.; Yamamoto, A. Synthesis, characterization, and carbonylation reactions of methylpalladium amide, carbamate, and alkyl carbonate complexes. *J. Organomet. Chem.* **1993**, *451*, 221–229. [CrossRef]
162. Ozawa, F.; Ito, T.; Yamamoto, A. Reactions of Carbon Dioxide with Palladium Ccomplexes. Synthesis and Characterization of Carbamato Complexes of Palladium(II). *Chem. Lett.* **1979**, *8*, 735–738. [CrossRef]

163. Belforte, A.; Calderazzo, F.; Zanazzi, P.F. Synthesis and reactivity of *N*,*N*-dialkylcarbamato complexes of manganese(II). Crystal and molecular structure of $[Mn_6(O_2CNEt_2)_{12}]$, a hexamer with four five-co-ordinated manganese(II) atoms. *J. Chem. Soc. Dalt. Trans.* **1988**, 2921–2926. [CrossRef]
164. Dell'Amico, D.B.; Calderazzo, F.; Labella, L.; Marchetti, F.; Mazzoncini, I. *N*,*N*-dimethylcarbamato complexes of zinc. *Inorg. Chim. Acta* **2006**, *359*, 3371–3374. [CrossRef]
165. Gauld, R.M.; Kennedy, A.R.; McLellan, R.; Barker, J.; Reid, J.; Mulvey, R.E. Diverse outcomes of CO_2 fixation using alkali metal amides including formation of a heterobimetallic lithium-sodium carbamato-anhydride via lithium-sodium bis-hexamethyldisilazide. *Chem. Commun.* **2019**, *55*, 1478–1481. [CrossRef] [PubMed]
166. Bresciani, G.; Bortoluzzi, M.; Zacchini, S.; Gabbani, A.; Pineider, F.; Marchetti, F.; Pampaloni, G. Synthesis and Structural Characterization of Non-Homoleptic Carbamato Complexes of V^{V} and W^{VI} and Their Facile Implantation onto Silica Surfaces. *Eur. J. Inorg. Chem.* **2018**, *10*, 1176–1184. [CrossRef]
167. Calderazzo, F.; Pampaloni, G.; Sperrlea, M.; Englert, U. Electron-and Ligand-Transfer Reactions Involving *N*,*N*-Dialkylcarbamates. Synthesis and Molecular Structure of $V_2[\eta^5\text{-}(C_5H_5)]_2[O_2CN(C_2H_5)_2]_4$. *Zeitschrift für Naturforsch. B* **1992**, *47*, 389–394. [CrossRef]
168. Arimondo, P.B.; Calderazzo, F.; Englert, U.; Maichle-Moessmer, C.; Pampaloni, G.; Straehle, J. Preparation and characterization of dialkylcarbamato derivatives of niobium and tantalum. *J. Chem. Soc. Dalt. Trans.* **1996**, *3*, 311–319. [CrossRef]
169. Belli Dell'Amico, D.; Calderazzo, F.; Gingl, F.; Labella, L.; Straehle, J. *N*,*N*-dialkylcarbamato complexes of chromium(III). Crystal and molecular structure of two non-homoleptic products of chromium(III), $Cr_3(\mu_3\text{-}O)(O_2CNEt_2)_6Cl(NHEt_2)$ and $Cr_2(O_2CN^iPr_2)_5Cl$. *Gazz. Chim. Ital.* **1994**, *124*, 375–380.
170. Arimondo, P.B.; Calderazzo, F.; Hiemeyer, R.; Maichle-Mössmer, C.; Marchetti, F.; Pampaloni, G.; Strähle, J. Synthesis and Crystal Structure of a Self-Assembled, Octanuclear Oxo-Tantalum(V) Derivative Containing the First Example of a Transition Metal $M_8(\mu\text{-}O)_{12}$ Cage. *Inorg. Chem.* **1998**, *37*, 5507–5511. [CrossRef] [PubMed]
171. Bortoluzzi, M.; Ghini, F.; Hayatifar, M.; Marchetti, F.; Pampaloni, G.; Zacchini, S. Oxido- and sulfidoniobium(V) *N*,*N*-diethylcarbamates: Synthesis, characterization and DFT study. *Eur. J. Inorg. Chem.* **2013**, 3112–3118. [CrossRef]
172. Forte, C.; Hayatifar, M.; Pampaloni, G.; Galletti, A.M.R.; Renili, F.; Zacchini, S. Ethylene polymerization using novel titanium catalytic precursors bearing *N*,*N*-dialkylcarbamato ligands. *J. Polym. Sci. Part A Polym. Chem.* **2011**, *49*, 3338–3345. [CrossRef]
173. Straessler, N.A.; Caudle, M.T.; Groy, T.L. Tetrakis (*N*,*N*-diethylcarbamato)titanium(IV). *Acta. Crystallogr. Sect. E Struct. Rep. Online* **2008**, *64*, m48. [CrossRef] [PubMed]
174. Dell'Amico, D.B.; Calderazzo, F.; Ianelli, S.; Labella, L.; Marchetti, F.; Pelizzi, G. Stepwise substitution of *N*,*N*-di-isopropylcarbamato groups of $Ti(O_2CNiPr_2)_4$ by triphenylsilanol leading from eight- to six- and four-co-ordinated titanium(IV). *J. Chem. Soc. Dalt. Trans.* **2000**, 4339–4342. [CrossRef]
175. Chisholm, M.H.; Cotton, F.A.; Extine, M.W.; Stults, B.R. The tungsten-tungsten triple bond. 6. Hexakis(*N*,*N*-dimethylcarbamato)ditungsten and dimethyltetrakis(*N*,*N*-diethylcarbamato)ditungsten. Structures and dynamical solution behavior. *Inorg. Chem.* **1977**, *16*, 603–611. [CrossRef]
176. Belforte, A.; Belli Dell'Amico, D.; Calderazzo, F.; Devillers, M.; Englert, U. Chromium(II) and molybdenum(II) *N*,*N*-diethylcarbamato complexes from metal halides/carbon dioxide/diethylamine: Crystal and molecular structure of the quadruply metal-metal-bonded $Mo_2(O_2CNEt_2)_4$. *Inorg. Chem.* **1993**, *32*, 2282–2286. [CrossRef]
177. Aresta, M.; Dibenedetto, A.; Quaranta, E. Reaction of alkali-metal tetraphenylborates with amines in the presence of CO_2: A new easy way to aliphatic and aromatic alkali-metal carbamates. *J. Chem. Soc. Dalt. Trans.* **1995**, *20*, 3359. [CrossRef]
178. Esparza-Ruiz, A.; Herrmann, C.; Chen, J.; Patrick, B.O.; Polishchuk, E.; Orvig, C. Synthesis and in vitro anticancer activity of ferrocenyl-aminoquinoline-carboxamide conjugates. *Inorg. Chim. Acta.* **2012**, *393*, 276–283. [CrossRef]
179. Chisholm, M.H.; Reichert, W.W. Bis(dimethylamido)tetrakis(*N*,*N*-dimethylcarbamato)dimolybdenum. *Inorg. Chem.* **1978**, *17*, 767–769. [CrossRef]
180. Mendiratta, A.; Cummins, C.C.; Cotton, F.A.; Ibragimov, S.A.; Murillo, C.A.; Villagrán, D. A Diamagnetic Dititanium(III) Paddlewheel Complex with No Direct Metal−Metal Bond. *Inorg. Chem.* **2006**, *45*, 4328–4330. [CrossRef] [PubMed]

181. Bresciani, G.; Bortoluzzi, M.; Zacchini, S.; Marchetti, F.; Pampaloni, G. Structural Characterization of a Fluorido-Amide of Niobium, and Facile CO_2 Incorporation Affording a Fluorido-Carbamate. *Eur. J. Inorg. Chem.* **2018**, *8*, 999–1006. [CrossRef]
182. Habereder, T.; Nöth, H.; Paine, R.T. Synthesis and Reactivity of New Bis(tetramethylpiperidino)(phosphanyl)alumanes. *Eur. J. Inorg. Chem.* **2007**, *27*, 4298–4305. [CrossRef]
183. Normand, A.T.; Daniliuc, C.G.; Wibbeling, B.; Kehr, G.; Le Gendre, P.; Erker, G. Phosphido- and Amidozirconocene Cation-Based Frustrated Lewis Pair Chemistry. *J. Am. Chem. Soc.* **2015**, *137*, 10796–10808. [CrossRef] [PubMed]
184. McNevin, M.J.; Hagadorn, J.R. Dititanium Complexes of Preorganized Binucleating Bis(amidinates). *Inorg. Chem.* **2004**, *43*, 8547–8554. [CrossRef]
185. Chakraborty, S.; Blacque, O.; Berke, H. Ligand assisted carbon dioxide activation and hydrogenation using molybdenum and tungsten amides. *Dalton Trans.* **2015**, *44*, 6560–6570. [CrossRef]
186. Dickie, D.A.; Parkes, M.V.; Kemp, R.A. Insertion of Carbon Dioxide into Main-Group Complexes: Formation of the $[N(CO_2)_3]_3^-$ Ligand. *Angew. Chem. Int. Ed.* **2008**, *47*, 9955–9957. [CrossRef]
187. Hartwig, J.F.; Bergman, R.G.; Andersen, R.A. Insertion reactions of carbon monoxide and carbon dioxide with ruthenium benzyl, arylamido, and aryloxide complexes: A comparison of the reactivity of ruthenium-carbon, ruthenium-nitrogen, and ruthenium-oxygen bonds. *J. Am. Chem. Soc.* **1991**, *113*, 6499–6508. [CrossRef]
188. Park, S.; Rheingold, A.L.; Roundhill, D.M. Synthesis and reaction chemistry of monomeric and dimeric amide complexes of platinum(II). *Organometallics* **1991**, *10*, 615–623. [CrossRef]
189. Rahim, M.; White, C.; Rheingold, A.L.; Ahmed, K.J. Mononuclear arylamido complexes of iridium(I). *Organometallics* **1993**, *12*, 2401–2403. [CrossRef]
190. Dobereiner, G.E.; Wu, J.; Manas, M.G.; Schley, N.D.; Takase, M.K.; Crabtree, R.H.; Hazari, N.; Maseras, F.; Nova, A. Mild, Reversible Reaction of Iridium(III) Amido Complexes with Carbon Dioxide. *Inorg. Chem.* **2012**, *51*, 9683–9693. [CrossRef] [PubMed]
191. Truscott, B.J.; Nelson, D.J.; Slawin, A.M.Z.; Nolan, S.P. CO_2 fixation employing an iridium(I)-hydroxide complex. *Chem. Commun.* **2014**, *50*, 286–288. [CrossRef]
192. Schmeier, T.J.; Nova, A.; Hazari, N.; Maseras, F. Synthesis of PCP-Supported Nickel Complexes and their Reactivity with Carbon Dioxide. *Chem. Eur. J.* **2012**, *18*, 6915–6927. [CrossRef]
193. Mousa, A.H.; Bendix, J.; Wendt, O.F. Synthesis, Characterization, and Reactivity of PCN Pincer Nickel Complexes. *Organometallics* **2018**, *37*, 2581–2593. [CrossRef]
194. Cámpora, J.; Matas, I.; Palma, P.; Álvarez, E.; Graiff, C.; Tiripicchio, A. Monomeric Alkoxo and Amido Methylnickel(II) Complexes. Synthesis and Heterocumulene Insertion Chemistry. *Organometallics* **2007**, *26*, 3840–3849. [CrossRef]
195. Hao, J.; Vabre, B.; Mougang-Soumé, B.; Zargarian, D. Small Molecule Activation by $POC_{sp}{}^3OP$-Nickel Complexes. *Chem. -Eur. J.* **2014**, *20*, 12544–12552. [CrossRef] [PubMed]
196. Kim, J.; Park, K.; Lee, Y. Synthesis and characterization of a four-coordinate nickel carbamato species $(MeSiP^iPr_2)Ni(OC(O)NHMes)$ generated from the reaction of $(MeSiP^iPr_2)Ni(NHMes)$ with CO_2. *Inorg. Chim. Acta* **2017**, *460*, 55–62. [CrossRef]
197. Kim, J.; Kim, Y.-E.; Park, K.; Lee, Y. A Silyl-Nickel Moiety as a Metal–Ligand Cooperative Site. *Inorg. Chem.* **2019**, *58*, 11534–11545. [CrossRef]
198. Seul, J.-M.; Park, S. Palladium(II) p-Tolylamide and Reaction with CO_2 to Generate a Carbamato Derivative. *Bull. Korean Chem. Soc.* **2010**, *31*, 3745–3748. [CrossRef]
199. Comanescu, C.C.; Iluc, V.M. E-H (E = N, O) bond activation by a nucleophilic palladium carbene. *Polyhedron* **2018**, *143*, 176–183. [CrossRef]
200. Johnson, M.W.; Shevick, S.L.; Toste, F.D.; Bergman, R.G. Preparation and reactivity of terminal gold(I) amides and phosphides. *Chem. Sci.* **2013**, *4*, 1023–1027. [CrossRef]
201. Tang, Y.; Kassel, W.S.; Zakharov, L.N.; Rheingold, A.L.; Kemp, R.A. Insertion reactions of carbon dioxide into Zn-N bonds: Syntheses and structures of tetrameric and dimeric alkylzinc carbamato complexes. *Inorg. Chem.* **2005**, *44*, 359–364. [CrossRef] [PubMed]
202. Malik, M.A.; O'Brien, P.; Motevalli, M.; Abrahams, I. The adoption of the beryllium acetate structural motif in zinc oxycarbamates, oxythiocarbamates and oxythiophosphinates. *Polyhedron* **2006**, *25*, 241–250. [CrossRef]

203. Domide, D.; Kaifer, E.; Mautz, J.; Walter, O.; Behrens, S.; Himmel, H. Synthesis and Characterisation of Some New Zinc Carbamate Complexes Formed by CO_2 Fixation and Their Use as Precursors for ZnO Particles under Mild Conditions. *Eur. J. Inorg. Chem.* **2008**, *20*, 3177–3185. [CrossRef]
204. Kahnes, M.; Görls, H.; Westerhausen, M. Synthesis of Dimeric Methylzinc *N*,*N*-Bis(2-pyridylmethyl)carbamate via Addition of CO_2 to a Methylzinc Amide. *Z. Anorg. Allg. Chem.* **2011**, *637*, 397–400. [CrossRef]
205. Webster, C.L.; Langeslay, R.R.; Ziller, J.W.; Evans, W.J. Synthetic Utility of Tetrabutylammonium Salts in Uranium Metallocene Chemistry. *Organometallics* **2016**, *35*, 520–527. [CrossRef]
206. Higgins Frey, J.A.; Cloke, F.G.N.; Roe, S.M. Synthesis and Reactivity of a Mixed-Sandwich Uranium(IV) Primary Amido Complex. *Organometallics* **2015**, *34*, 2102–2105. [CrossRef]
207. Schmidt, A.-C.; Heinemann, F.W.; Maron, L.; Meyer, K. A Series of Uranium (IV, V, VI) Tritylimido Complexes, Their Molecular and Electronic Structures and Reactivity with CO_2. *Inorg. Chem.* **2014**, *53*, 13142–13153. [CrossRef]
208. Matson, E.M.; Fanwick, P.E.; Bart, S.C. Formation of Trivalent U–C, U–N, and U–S Bonds and Their Reactivity toward Carbon Dioxide and Acetone. *Organometallics* **2011**, *30*, 5753–5762. [CrossRef]
209. Bart, S.C.; Anthon, C.; Heinemann, F.W.; Bill, E.; Edelstein, N.M.; Meyer, K. Carbon Dioxide Activation with Sterically Pressured Mid- and High-Valent Uranium Complexes. *J. Am. Chem. Soc.* **2008**, *130*, 12536–12546. [CrossRef]
210. Harris, L.A.M.; Coles, M.P.; Fulton, J.R. Synthesis and reactivity of tin amide complexes. *Inorg. Chim. Acta* **2011**, *369*, 97–102. [CrossRef]
211. Feier-Iova, O.; Linti, G. Synthesis and Structure of a Carbamato-bridgded Digallyl-ferrocenophane—Fixation of Carbon Dioxide with Aminogallanes. *Z. Anorg. Allg. Chem.* **2008**, *634*, 559–564. [CrossRef]
212. Uhl, W.; Willeke, M.; Hepp, A.; Pleschka, D.; Layh, M. A Dimeric Gallium Hydrazide as an Active Lewis Pair—Complexation and Activation of Me_2GaH and Various Heterocumulenes. *Z. Anorg. Allg. Chem.* **2017**, *643*, 387–397. [CrossRef]
213. Hill, M.R.; Jensen, P.; Russell, J.J.; Lamb, R.N. Synthesis and properties of Zn-Mg heterobimetallic carbamates. Crystal structures of the first reported single source precursors for $Zn_xMg_{1-x}O$ thin films. *J. Chem. Soc. Dalt. Trans.* **2008**, 2751–2758. [CrossRef] [PubMed]
214. Vummaleti, S.V.C.; Talarico, G.; Nolan, S.P.; Cavallo, L.; Poater, A. Mechanism of CO_2 Fixation by Ir I-X Bonds (X = OH, OR, N, C). *Eur. J. Inorg. Chem.* **2015**, *2015*, 4653–4657. [CrossRef]
215. Truscott, B.J.; Kruger, H.; Webb, P.B.; Bühl, M.; Nolan, S.P. The Mechanism of CO_2 Insertion into Iridium(I) Hydroxide and Alkoxide Bonds: A Kinetics and Computational Study. *Chem. -Eur. J.* **2015**, *21*, 6930–6935. [CrossRef]
216. Vadivelu, P.; Suresh, C.H. Metal- and Ligand-Assisted CO_2 Insertion into Ru–C, Ru–N, and Ru–O Bonds of Ruthenium(II) Phosphine Complexes: A Density Functional Theory Study. *Inorg. Chem.* **2015**, *54*, 502–512. [CrossRef]
217. Chu, J.; Lu, E.; Liu, Z.; Chen, Y.; Leng, X.; Song, H. Reactivity of a Scandium Terminal Imido Complex Towards Unsaturated Substrates. *Angew. Chem. Int. Ed.* **2011**, *50*, 7677–7680. [CrossRef]
218. Boyd, C.L.; Clot, E.; Guiducci, A.E.; Mountford, P. Pendant Arm Functionalized Benzamidinate Titanium Imido Compounds: Experimental and Computational Studies of Their Reactions with CO_2. *Organometallics* **2005**, *24*, 2347–2367. [CrossRef]
219. Dubberley, S.R.; Friedrich, A.; Willman, D.A.; Mountford, P.; Radius, U. Synthesis and Reactivity of Calix[4]arene-Supported Group 4 Imido Complexes. *Chem. -Eur. J.* **2003**, *9*, 3634–3654. [CrossRef]
220. Guiducci, A.E.; Boyd, C.L.; Clot, E.; Mountford, P. Reactions of cyclopentadienyl-amidinate titanium imido compounds with CO_2: Cycloaddition-extrusion vs. cycloaddition-insertion. *Dalton Trans.* **2009**, *30*, 5960. [CrossRef] [PubMed]
221. Mindiola, D.J.; Waterman, R.; Iluc, V.M.; Cundari, T.R.; Hillhouse, G.L. Carbon–Hydrogen Bond Activation, C–N Bond Coupling, and Cycloaddition Reactivity of a Three-Coordinate Nickel Complex Featuring a Terminal Imido Ligand. *Inorg. Chem.* **2014**, *53*, 13227–13238. [CrossRef] [PubMed]
222. Goodner, S.J.; Grünwald, A.; Heinemann, F.W.; Munz, D. Carbon Dioxide Activation by a Palladium Terminal Imido Complex. *Aust. J. Chem.* **2019**, *72*, 900. [CrossRef]
223. Glueck, D.S.; Wu, J.; Hollander, F.J.; Bergman, R.G. Monomeric (pentamethylcyclopentadienyl)iridium imido compounds: Synthesis, structure, and reactivity. *J. Am. Chem. Soc.* **1991**, *113*, 2041–2054. [CrossRef]

224. Kinauer, M.; Diefenbach, M.; Bamberger, H.; Demeshko, S.; Reijerse, E.J.; Volkmann, C.; Würtele, C.; Van Slageren, J.; De Bruin, B.; Holthausen, M.C.; et al. An iridium(III/IV/V) redox series featuring a terminal imido complex with triplet ground state. *Chem. Sci.* **2018**, *9*, 4325–4332. [CrossRef]
225. Falcone, M.; Chatelain, L.; Mazzanti, M. Nucleophilic Reactivity of a Nitride-Bridged Diuranium(IV) Complex: CO_2 and CS_2 Functionalization. *Angew. Chem. Int. Ed.* **2016**, *55*, 4074–4078. [CrossRef]
226. Falcone, M.; Poon, L.N.; Fadaei Tirani, F.; Mazzanti, M. Reversible Dihydrogen Activation and Hydride Transfer by a Uranium Nitride Complex. *Angew. Chem. Int. Ed.* **2018**, *57*, 3697–3700. [CrossRef]
227. Bernskoetter, W.H.; Lobkovsky, E.; Chirik, P.J. Nitrogen–Carbon Bond Formation from N_2 and CO_2 Promoted by a Hafnocene Dinitrogen Complex Yields a Substituted Hydrazine. *Angew. Chem. Int. Ed.* **2007**, *46*, 2858–2861. [CrossRef]
228. Knobloch, D.J.; Toomey, H.E.; Chirik, P.J. Carboxylation of an ansa -Zirconocene Dinitrogen Complex: Regiospecific Hydrazine Synthesis from N_2 and CO_2. *J. Am. Chem. Soc.* **2008**, *130*, 4248–4249. [CrossRef]
229. Ma, X.; Tang, Y.; Lei, M. Mechanistic Studies on the Carboxylation of Hafnocene and ansa -Zirconocene Dinitrogen Complexes with CO_2. *Organometallics* **2013**, *32*, 7077–7082. [CrossRef]
230. McCowan, C.S.; Buss, C.E.; Young, V.G.; McDonnell, R.L.; Caudle, M.T. Chloro(diethylamino)*tris*(μ-diethylcarbamato)dizinc(II): An example of the generality of the threefold paddlewheel structure in carbamatozinc chemistry. *Acta. Crystallogr. Sect. E Struct. Rep. Online* **2004**, *60*, 285–287. [CrossRef]
231. Dell'Amico, D.B.; Calderazzo, F.; Englert, U.; Labella, L.; Marchetti, F.; Specos, M. New *N*,*N*-diisopropylcarbamato complexes of ruthenium(II) as catalytic precursors for olefin hydrogenation. *Eur. J. Inorg. Chem.* **2004**, *19*, 3938–3945. [CrossRef]
232. Mochizuki, K.; Kondou, H.; Ando, K.; Kawasumi, T.; Takahashi, J. Degradation of urea mediated by dinickel(II) complexes with the binucleating ligand *N*,*N*′-bis[2-(*N*,*N*-dimethyl)aminoethyl]-*N*,*N*′-dimethyl-1,3-diamino-2-hydroxypropane (HL). *Inorg. Chim. Acta* **2016**, *441*, 50–56. [CrossRef]
233. Lozan, V.; Holldorf, J.; Kersting, B. Preparation and characterization of macrocyclic dinickel complexes coligated by monoalkyl- and dialkylcarbamates. *Inorg. Chim. Acta* **2009**, *362*, 793–798. [CrossRef]
234. Calucci, L.; Forte, C.; Pampaloni, G.; Pinzino, C.; Renili, F. Chemical implantation of Group 4 cations on silica via cyclopentadienyl- and *N*,*N*-dialkylcarbamato derivatives. *Inorg. Chim. Acta* **2010**, *363*, 33–40. [CrossRef]
235. Zhang, K.; Guo, F.-S.; Wang, Y.-Y. Two {Dy_2} single-molecule magnets formed via an in situ reaction by capturing CO_2 from atmosphere under ambient conditions. *Dalton Trans.* **2017**, *46*, 1753–1756. [CrossRef]
236. Neis, C.; Weyhermüller, T.; Bill, E.; Stucky, S.; Hegetschweiler, K. Carbamates of Polyamines–Versatile Building Blocks for the Construction of Polynuclear Metal Complexes. *Eur. J. Inorg. Chem.* **2008**, *7*, 1019–1021. [CrossRef]
237. Bramsen, F.; Bond, A.D.; McKenzie, C.J.; Hazell, R.G.; Moubaraki, B.; Murray, K.S. Self-Assembly of the Octanuclear Cluster $[Cu_8(OH)_{10}(NH_2(CH_2)_2CH_3)_{12}]^{6+}$ and the One-Dimensional N-Propylcarbamate-Linked Coordination Polymer $\{[Cu(O_2CNH(CH_2)_2CH_3(NH_2(CH_2)_2CH_3)_3](ClO_4)\}_n$. *Chem. Eur. J.* **2005**, *11*, 825–831. [CrossRef]
238. García-España, E.; Gaviña, P.; Latorre, J.; Soriano, C.; Verdejo, B. CO_2 Fixation by Copper(II) Complexes of a Terpyridinophane Aza Receptor. *J. Am. Chem. Soc.* **2004**, *126*, 5082–5083. [CrossRef]
239. Vo, T.T.; Parrish, D.A.; Shreeve, J.M. 1,1-Diamino-2,2-dintroethene (FOX-7) in Copper and Nickel Diamine Complexes and Copper FOX-7. *Inorg. Chem.* **2012**, *51*, 1963–1968. [CrossRef]
240. Kalia, S.B.; Kumar, R.; Bharti, M.; Christopher, J. Experimental investigations of thermal stability of some morpholinecarbamic acid complexes of copper(II) and zinc(II). *J. Therm. Anal. Calorim.* **2017**, *127*, 1291–1306. [CrossRef]
241. Bedeković, N.; Stilinović, V. Morpholine-*N*-carboxylate as a ligand in coordination chemistry–Syntheses and structures of three heteroleptic copper(ii) and zinc complexes. *J. Mol. Struct.* **2020**, *1205*, 127627. [CrossRef]
242. Notni, J.; Schenk, S.; Görls, H.; Breitzke, H.; Anders, E. Formation of a Unique Zinc Carbamate by CO_2 Fixation: Implications for the Reactivity of Tetra-Azamacrocycle Ligated Zn(II) Complexes. *Inorg. Chem.* **2008**, *47*, 1382–1390. [CrossRef] [PubMed]
243. Rodriguez, M.A.; Sava, D.F.; Nenoff, T.M. catena -Poly[zinc-*tris*(μ-dimethylcarbamato-κ^2O:O′)-zinc-μ-(2-phenylbenzimidazolido-κ^2 *N*:*N*′]. *Acta. Crystallogr. Sect. E Struct. Rep. Online* **2012**, *68*, m59–m60. [CrossRef]

244. Masci, B.; Thuéry, P. A Tetrahomodioxacalix[6]arene as a Ditopic Ligand for Uranyl Ions with Carbonate or Carbamate Bridges. *Supramol. Chem.* **2003**, *15*, 101–108. [CrossRef]
245. Anillo, A.; Dell'Amico, D.B.; Calderazzo, F.; Nardelli, M.; Pelizzi, G.; Rocchi, L. Dialkylcarbamato complexes of palladium(II). Crystal structure of trans-$[Pd(O_2CNEt_2)_2(NHEt_2)_2]$. *J. Chem. Soc. Dalt. Trans.* **1991**, *11*, 2845. [CrossRef]
246. El Rez, B.; Costes, J.-P.P.; Duhayon, C.; Vendier, L.; Sutter, J.-P.P. Structural determinations of carbamato-bridging ligands derived from atmospheric CO_2 in 3d-4f complexes. *Polyhedron* **2015**, *89*, 213–218. [CrossRef]
247. Yin, C.-L.; Hu, Z.-B.; Long, Q.-Q.; Wang, H.-S.; Li, J.; Song, Y.; Zhang, Z.-C.; Zhang, Y.-Q.; Pan, Z.-Q. Single molecule magnet behaviors of Zn_4Ln_2 (Ln = Dy III, Tb III) complexes with multidentate organic ligands formed by absorption of CO_2 in air through in situ reactions. *Dalton Trans.* **2019**, *48*, 512–522. [CrossRef]
248. Caudle, M.T.; Brennessel, W.W.; Young, V.G. Structural variability and dynamics in carboxylato- and carbamatomagnesium bromides. Relationship to the carboxylate shift. *Inorg. Chem.* **2005**, *44*, 3233–3240. [CrossRef]
249. Dell' Amico, D.B.; Calderazzo, F.; Labella, L.; Marchetti, F.; Martini, M.; Mazzoncini, I. *N*,*N*-Dimethylcarbamato derivatives of magnesium starting from the metal oxide. *C. R. Chim.* **2004**, *7*, 877–884. [CrossRef]
250. Yin, S.-F.; Maruyama, J.; Yamashita, T.; Shimada, S. Efficient Fixation of Carbon Dioxide by Hypervalent Organobismuth Oxide, Hydroxide, and Alkoxide. *Angew. Chem. Int. Ed.* **2008**, *47*, 6590–6593. [CrossRef] [PubMed]
251. Bloodworth, A.J.; Serlin, J. Organometallic oxides, alkoxides, and peroxides. Part IV. Reaction of phenylmercury(II) alkoxides, oxide, and hydroxide with organic isocyanates. *J. Chem. Soc. Perkin Trans. 1* **1973**, *7*, 261–267. [CrossRef]
252. Edwards, A.J.; Elipe, S.; Esteruelas, M.A.; Lahoz, F.J.; Oro, L.A.; Valero, C. Synthesis and Reactivity of the Unusual Five-Coordinate Hydrido−Hydroxo Complex $OsH(OH)(CO)(P^iPr_3)_2$. *Organometallics* **1997**, *16*, 3828–3836. [CrossRef]
253. Giandomenico, C.M.; Abrams, M.J.; Murrer, B.A.; Vollano, J.F.; Rheinheimer, M.I.; Wyer, S.B.; Bossard, G.E.; Higgins, J.D. Carboxylation of Kinetically Inert Platinum(IV) Hydroxy Complexes. An Entr.acte.ee into Orally Active Platinum(IV) Antitumor Agents. *Inorg. Chem.* **1995**, *34*, 1015–1021. [CrossRef] [PubMed]
254. Zhang, C.; Liu, R.; Zhang, J.; Chen, Z.; Zhou, X. Reactivity of lanthanocene hydroxides toward ketene, isocyanate, lanthanocene alkyl, and triscyclopentadienyllanthanide complexes. *Inorg. Chem.* **2006**, *45*, 5867–5877. [CrossRef]
255. Xu, X.P.; Qi, R.P.; Xu, B.; Yao, Y.M.; Nie, K.; Zhang, Y.; Shen, Q. Synthesis, reactivity and structural characterization of lanthanide hydroxides stabilized by a carbon-bridged bis(phenolate) ligand. *Polyhedron* **2009**, *28*, 574–578. [CrossRef]
256. Cuesta, L.; Gerbino, D.C.; Hevia, E.; Morales, D.; Navarro Clemente, M.E.; Pérez, J.; Riera, L.; Riera, V.; Miguel, D.; Del Río, I.; et al. Reactivity of Molybdenum and Rhenium Hydroxo-Carbonyl Complexes toward Organic Electrophiles. *Chem. Eur. J.* **2004**, *10*, 1765–1777. [CrossRef]
257. Jackson, W.G.; McKeon, J.A.; Balahura, R.J. N -Methylmonothiocarbamatopentamminecobalt(III): Restricted C–N Bond Rotation and the Acid-Catalyzed O- to S-Bonded Rearrangement. *Inorg. Chem.* **2004**, *43*, 4889–4896. [CrossRef]
258. Yao, C.; Chakraborty, P.; Aresu, E.; Li, H.; Guan, C.; Zhou, C.; Liang, L.-C.; Huang, K.-W. Monomeric nickel hydroxide stabilized by a sterically demanding phosphorus–nitrogen PN 3 P-pincer ligand: Synthesis, reactivity and catalysis. *Dalton Trans.* **2018**, *47*, 16057–16065. [CrossRef]
259. Martínez-Prieto, L.M.; Palma, P.; Cámpora, J. Monomeric alkoxide and alkylcarbonate complexes of nickel and palladium stabilized with the iPr PCP pincer ligand: A model for the catalytic carboxylation of alcohols to alkyl carbonates. *Dalton Trans.* **2019**, *48*, 1351–1366. [CrossRef]
260. Wilson, J.J.; Lippard, S.J. Synthesis, Characterization, and Cytotoxicity of Platinum(IV) Carbamate Complexes. *Inorg. Chem.* **2011**, *50*, 3103–3115. [CrossRef] [PubMed]
261. Pichler, V.; Mayr, J.; Heffeter, P.; Dömötör, O.; Enyedy, É.A.; Hermann, G.; Groza, D.; Köllensperger, G.; Galanksi, M.; Berger, W.; et al. Maleimide-functionalised platinum(IV) complexes as a synthetic platform for targeted drug delivery. *Chem. Commun.* **2013**, *49*, 2249. [CrossRef] [PubMed]

262. Pichler, V.; Göschl, S.; Meier, S.M.; Roller, A.; Jakupec, M.A.; Galanski, M.; Keppler, B.K. Bulky *N*,*N*-((Di)alkylethane-1,2-diamineplatinum(II) Compounds as Precursors for Generating Unsymmetrically Substituted Platinum(IV) Complexes. *Inorg. Chem.* **2013**, *52*, 8151–8162. [CrossRef]
263. Zheng, Y.-R.R.; Suntharalingam, K.; Johnstone, T.C.; Yoo, H.; Lin, W.; Brooks, J.G.; Lippard, S.J. Pt(IV) prodrugs designed to bind non-covalently to human serum albumin for drug delivery. *J. Am. Chem. Soc.* **2014**, *136*, 8790–8798. [CrossRef] [PubMed]
264. Qi, L.; Lu, Z.; Lang, W.H.; Guo, L.; Ma, C.G.; Sun, G.H. Binding of a potential anti-hepatoma drug cis,cis,trans-[$Pt(NH_3)_2Cl_2(O_2CCH_2CH_2COOH)$-$(OCONHC_{16}H_{33})$] with serum albumin—Thermodynamic and conformational investigations. *New J. Chem.* **2015**, *39*, 9234–9241. [CrossRef]
265. Xu, Z.; Wang, Z.; Yiu, S.-M.; Zhu, G. Mono- and di-bromo platinum(IV) prodrugs via oxidative bromination: Synthesis, characterization, and cytotoxicity. *Dalton Trans.* **2015**, *44*, 19918–19926. [CrossRef]
266. Li, W.; Jiang, M.; Cao, Y.; Yan, L.; Qi, R.; Li, Y.; Jing, X. Turning Ineffective Transplatin into a Highly Potent Anticancer Drug via a Prodrug Strategy for Drug Delivery and Inhibiting Cisplatin Drug Resistance. *Bioconjug. Chem.* **2016**, *27*, 1802–1806. [CrossRef]
267. Feng, B.; Zhou, F.; Xu, Z.; Wang, T.; Wang, D.; Liu, J.; Fu, Y.; Yin, Q.; Zhang, Z.; Yu, H.; et al. Versatile Prodrug Nanoparticles for Acid-Triggered Precise Imaging and Organelle-Specific Combination Cancer Therapy. *Adv. Funct. Mater.* **2016**, *26*, 7431–7442. [CrossRef]
268. Mayr, J.; Heffeter, P.; Groza, D.; Galvez, L.; Koellensperger, G.; Roller, A.; Alte, B.; Haider, M.; Berger, W.; Kowol, C.R.; et al. An albumin-based tumor-targeted oxaliplatin prodrug with distinctly improved anticancer activity in vivo. *Chem. Sci.* **2017**, *8*, 2241–2250. [CrossRef]
269. Yamaguchi, S.; Takahashi, T.; Wada, A.; Funahashi, Y.; Ozawa, T.; Jitsukawa, K.; Masuda, H. Fixation of CO_2 by Hydroxozinc(II) Complex with Pyridylamino Type Ligand. *Chem. Lett.* **2007**, *36*, 842–843. [CrossRef]
270. Norris, M.R.; Flowers, S.E.; Mathews, A.M.; Cossairt, B.M. H_2 Production Mediated by CO_2 via Initial Reduction to Formate. *Organometallics* **2016**, *35*, 2778–2781. [CrossRef]
271. Jayarathne, U.; Hazari, N.; Bernskoetter, W.H. Selective Iron-Catalyzed N -Formylation of Amines using Dihydrogen and Carbon Dioxide. *ACS Catal.* **2018**, *8*, 1338–1345. [CrossRef]
272. Babu, T.; Sarkar, A.; Karmakar, S.; Schmidt, C.; Gibson, D. Multiaction Pt(IV) Carbamate Complexes Can Codeliver Pt(II) Drugs and Amine Containing Bioactive Molecules. *Inorg. Chem.* **2020**, *59*, 5182–5193. [CrossRef] [PubMed]
273. Chen, B.; Neumann, R. Coordination of Carbon Dioxide to the Lewis Acid Site of a Zinc-Substituted Polyoxometalate and Formation of an Adduct Using a Polyoxometalate-2,4,6-Trimethylpyridine Frustrated Lewis Pair. *Eur. J. Inorg. Chem.* **2018**, *6*, 791–794. [CrossRef]
274. Cristóbal, C.; Hernández, Y.A.; López-Serrano, J.; Paneque, M.; Petronilho, A.; Poveda, M.L.; Salazar, V.; Vattier, F.; Álvarez, E.; Maya, C.; et al. Reactivity Studies of Iridium Pyridylidenes [$TpMe_2Ir(C_6H_5)_2(C(CH)_2C(R)NH]$ (R=H, Me, Ph). *Chem. Eur. J.* **2013**, *19*, 4003–4020. [CrossRef]
275. Zhu, Y.; Smith, D.A.; Herbert, D.E.; Gatard, S.; Ozerov, O.V. C–H and C–O oxidative addition in reactions of aryl carboxylates with a PNP pincer-ligated Rh(I) fragment. *Chem. Commun.* **2012**, *48*, 218–220. [CrossRef] [PubMed]
276. Mathis, C.L.; Geary, J.; Ardon, Y.; Reese, M.S.; Philliber, M.A.; VanderLinden, R.T.; Saouma, C.T. Thermodynamic Analysis of Metal–Ligand Cooperativity of PNP Ru Complexes: Implications for CO_2 Hydrogenation to Methanol and Catalyst Inhibition. *J. Am. Chem. Soc.* **2019**, *141*, 14317–14328. [CrossRef]
277. Ueno, A.; Kayaki, Y.; Ikariya, T. Heterolysis of NH-indoles by bifunctional amido complexes and applications to carboxylation with carbon dioxide. *Organometallics* **2014**, *33*, 4479–4485. [CrossRef]
278. Roth, C.E.; Dibenedetto, A.; Aresta, M. Synthesis and Characterization of Chloro- and Alkyliron Complexes with N-Donor Ligands and Their Reactivity towards CO_2. *Eur. J. Inorg. Chem.* **2015**, *30*, 5066–5073. [CrossRef]
279. Neumüller, B.; Esser, M.; Petz, W. Formation of Unusual Complexes from the Reaction of [$C(NMe_2)_3$][$(CO)_4Fe\{C(O)NMe_2\}$] with $InMe_3$; Crystal Structures of [$C(NMe_2)_3]_3[Fe_2(CO)_6(\mu$-$CO)\{\mu$-$InFe(CO)_4(\mu$-$O_2CNMe_2)InFe(CO)_4\}$] and [$C(NMe_2)_3]_2[\{(CO)_4Fe\}_2In(O_2CNMe_2)]$·THF. *Z. Anorg. Allg. Chem.* **2007**, *633*, 314–319. [CrossRef]
280. Marchetti, F.; Pampaloni, G.; Patil, Y.; Galletti, A.M.R.; Renili, F.; Zacchini, S. Ethylene Polymerization by Niobium(V) *N*,*N*-Dialkylcarbamates Activated with Aluminum Co-catalysts. *Organometallics* **2011**, *30*, 1682–1688. [CrossRef]

281. Domide, D.; Hübner, O.; Behrens, S.; Walter, O.; Wadepohl, H.; Kaifer, E.; Himmel, H.J. Synthesis and reactivity of a new oxidation-labile heterobimetallic Mn_6Zn_2 carbamate cluster and precursor to nanosized magnetic oxide particles. *Eur. J. Inorg. Chem.* **2011**, *3*, 1387–1394. [CrossRef]
282. Domide, D.; Walter, O.; Behrens, S.; Kaifer, E.; Himmel, H.-J. Synthesis of Heterobimetallic Zn/Co Carbamates: Single-Source Precursors of Nanosized Magnetic Oxides Under Mild Conditions. *Eur. J. Inorg. Chem.* **2011**, *2011*, 860–867. [CrossRef]
283. Haywood, P.F.; Hill, M.R.; Roberts, N.K.; Craig, D.C.; Russell, J.J.; Lamb, R.N. Synthesis and Isomerisation Reactions of Tetranuclear and Octanuclear (Carbamato)zinc Complexes. *Eur. J. Inorg. Chem.* **2008**, *12*, 2024–2032. [CrossRef]
284. Buhro, W.E.; Chisholm, M.H.; Martin, J.D.; Huffman, J.C.; Folting, K.; Streib, W.E. Reactions involving carbon dioxide and mixed amido-phosphido dinuclear compounds. $M_2(NMe_2)_4(PR_2)_2$(M.tplbond.M), where M = Mo and W. Comparative study of the insertion of carbon dioxide into metal-nitr. *J. Am. Chem. Soc.* **1989**, *111*, 8149–8156. [CrossRef]
285. Ito, H.; Ito, T. Dialkylcarbamato Complexes of Ni(II), Zn(II), and Cd(II)–Tetraazacycloalkanes Obtained from CO_2-Uptake, and X-Ray Structure of (Diethylcarbamato)((7*RS*,14*RS*)5,5,7,12,12,14-hexamethyl-1,4,8,11-tetraaza-cyclotetradecane)nickel(II) Perchlorate. *Bull. Chem. Soc. Jpn.* **1985**, *58*, 1755–1760. [CrossRef]
286. Agostinelli, E.; Belli Dell'Amico, D.; Calderazzo, F.; Fiorani, D.; Pelizzi, G. Synthesis, properties and crystal and molecular strucrture of $Cu_2(O_2CNEt_2)_4$ $2NHEt_2$. *Gazz. Chim. Ital.* **1988**, *188*, 729–740.
287. Belli, D.; Amico, D.; Boschi, D.; Calderazzo, F.; Ianelli, S.; Labella, L.; Marchetti, F.; Pelizzi, G.; Guy, E.; Quadrelli, F. *N*,*N*-Dialkylcarbamato m-oxo derivatives of iron (III). *Inorg. Chim. Acta.* **2000**, *302*, 882–891. [CrossRef]
288. Belli, D.; Amico, D.; Calderazzo, F.; Giurlani, U.; Pelizzi, G. Synthesis and Reactivity of *N*,*N*-Dialkylcarbamato Complexes of Titanium (III) and Vanadium (III). Crystal and Molecular Structure of an Anionic Dimeric Titanium (III) Derivative. *Chem. Ber.* **1987**, *6*, 955–964.
289. Shawn McCowan, C.; Tyler Caudle, M. Evidence for unimolecular CO_2 elimination in C–N bond metathesis reactions of basic carbamatozinc complexes $Zn_4O(O_2CAm)_6$ (Am = N-diethylamino, N-piperidyl, N-pyrrolidyl). *Dalton Trans.* **2005**, *6*, 238–246. [CrossRef]
290. Bresciani, G.; Marchetti, F.; Rizzi, G.; Gabbani, A.; Pineider, F.; Pampaloni, G. Metal *N*,*N*-dialkylcarbamates as easily available catalytic precursors for the carbon dioxide/propylene oxide coupling under ambient conditions. *J. CO_2 Util.* **2018**, *28*, 168–173. [CrossRef]
291. Buryi, D.S.; Levashov, A.S. The Reaction of Tin Tetracarbamates with Organyl Chlorosilanes: A Novel Synthetic Route Towards O-Silylurethanes. *Russ. J. Gen. Chem.* **2019**, *89*, 924–928. [CrossRef]
292. Belli Dell'Amico, D.; Calderazzo, F.; Costa, L.; Franchi, E.; Gini, L.; Labella, L.; Marchetti, F. Octanuclear μ-oxo *N*,*N*-diethylcarbamato derivatives of titanium(IV) obtained by a high-yielding hydrolytic process. *J. Mol. Struct.* **2008**, *890*, 295–297. [CrossRef]
293. Dell'Amico, D.B.; Calderazzo, F.; Labella, L.; Marchetti, F. Triphenylphosphine-substituted *N*,*N*-di-iso-propylcarbamate of ruthenium(II) and its reactions with carbon monoxide. *J. Organomet. Chem.* **2000**, *596*, 144–151. [CrossRef]
294. Komarov, N.V.; Ryzhkova, N.A.; Andreev, A.A. Synthesis of alkoxystannanes by reactions of O-(organylstannyl) carbamates with alcohols. *Russ. Chem. Bull.* **2004**, *53*, 936–938. [CrossRef]
295. Armelao, L.; Belli Dell'Amico, D.; Bottaro, G.; Falvo, P.; Labella, L.; Marchetti, F.; Parisi, D.; Samaritani, S. From lanthanide chlorides to lanthanide pentafluorophenolates via lanthanide *N*,*N*-dialkylcarbamates. *Polyhedron* **2015**, *85*, 770–776. [CrossRef]
296. Levashov, A.S.; Andreev, A.A.; Buryi, D.S.; Konshin, V.V. A reaction of tin tetra(*N*,*N*-diethylcarbamate) with phenylacetylene as a new route to tetra(phenylethynyl)tin. *Russ. Chem. Bull.* **2014**, *63*, 775–776. [CrossRef]
297. Belli Dell'Amico, D.; Di Giacomo, A.; Falchi, L.; Labella, L.; Marelli, M.; Evangelisti, C.; Lezzerini, M.; Marchetti, F.; Samaritani, S. A convenient preparation of La_2CuO_4 from molecular precursors. *Polyhedron* **2017**, *123*, 33–38. [CrossRef]
298. Domide, D.; Neuhäuser, C.; Kaifer, E.; Wadepohl, H.; Himmel, H.J. Synthesis of trinuclear, dinuclear and mononuclear carbamato-zinc complexes from tetranuclear precursors: A top-down synthetic approach to new carbamates. *Eur. J. Inorg. Chem.* **2009**, *14*, 2170-0178. [CrossRef]

299. Neuhäuser, C.; Domide, D.; Mautz, J.; Kaifer, E.; Himmel, H.J. Electron density controlled carbamate ligand binding mode: Towards a better understanding of metalloenzyme activity. *Dalton Trans.* **2008**, *4*, 1821–1824. [CrossRef]
300. Deacon, G. Relationships between the carbon-oxygen stretching frequencies of carboxylato complexes and the type of carboxylate coordination. *Coord. Chem. Rev.* **1980**, *33*, 227–250. [CrossRef]
301. Nakamoto, K. *Infrared and Raman Spectra of Inorganic and Coordination Compounds*; John Wiley & Sons, Inc.: Hoboken, NJ, USA, 2008; ISBN 9780470405840.
302. Jabri, E.; Carr, M.; Hausinger, R.; Karplus, P. The crystal structure of urease from Klebsiella aerogenes. *Science* **1995**, *268*, 998–1004. [CrossRef]
303. Benning, M.M.; Hong, S.-B.; Raushel, F.M.; Holden, H.M. The Binding of Substrate Analogs to Phosphotriesterase. *J. Biol. Chem.* **2000**, *275*, 30556–30560. [CrossRef]
304. Thoden, J.B.; Phillips, G.N.; Neal, T.M.; Raushel, F.M.; Holden, H.M. Molecular Structure of Dihydroorotase: A Paradigm for Catalysis through the Use of a Binuclear Metal Center. *Biochemistry* **2001**, *40*, 6989–6997. [CrossRef]
305. Abendroth, J.; Niefind, K.; May, O.; Siemann, M.; Syldatk, C.; Schomburg, D. The Structure of L-Hydantoinase from Arthobacter aurescens Leads to an Understanding of Dihydropyrimidinase Substrate and Enantio Specificity. *Biochemistry* **2002**, *41*, 8589–8597. [CrossRef] [PubMed]
306. Niemi, T.; Repo, T. Antibiotics from Carbon Dioxide: Sustainable Pathways to Pharmaceutically Relevant Cyclic Carbamates. *Eur. J. Org. Chem.* **2019**, *6*, 1180–1188. [CrossRef]
307. Lamb, K.J.; Ingram, I.D.V.; North, M.; Sengoden, M. Valorization of Carbon Dioxide into Oxazolidinones by Reaction with Aziridines. *Curr. Green Chem.* **2019**, *6*, 32–43. [CrossRef]
308. Carminati, D.; Gallo, E.; Damiano, C.; Caselli, A.; Intrieri, D. Ruthenium Porphyrin Catalyzed Synthesis of Oxazolidin-2-ones by Cycloaddition of CO_2 to Aziridines. *Eur. J. Inorg. Chem.* **2018**, *48*, 5258–5262. [CrossRef]
309. Arshadi, S.; Banaei, A.; Ebrahimiasl, S.; Monfared, A.; Vessally, E. Solvent-free incorporation of CO_2 into 2-oxazolidinones: A review. *RSC Adv.* **2019**, *9*, 19465–19482. [CrossRef]
310. Ghosh, S.; Khan, T.S.; Ghosh, A.; Chowdhury, A.H.; Haider, M.A.; Khan, A.; Islam, S.M. Utility of Silver Nanoparticles Embedded Covalent Organic Frameworks as Recyclable Catalysts for the Sustainable Synthesis of Cyclic Carbamates and 2-Oxazolidinones via Atmospheric Cyclizative CO_2 Capture. *ACS Sustain. Chem. Eng.* **2020**, *8*, 5495–5513. [CrossRef]
311. Li, J.-Y.; Song, Q.-W.; Zhang, K.; Liu, P. Catalytic Conversion of Carbon Dioxide through C-N Bond Formation. *Molecules* **2019**, *24*, 182. [CrossRef] [PubMed]
312. Cao, C.; Xia, S.; Song, Z.; Xu, H.; Shi, Y.; He, L.; Cheng, P.; Zhao, B. Highly Efficient Conversion of Propargylic Amines and CO_2 Catalyzed by Noble-Metal-Free [Zn_{116}] Nanocages. *Angew. Chem. Int. Ed.* **2020**, *59*, 8586–8593. [CrossRef]
313. Sengoden, M.; North, M.; Whitwood, A. Synthesis of Oxazolidinones using Carbon Dioxide as a C-1 Building Block and an Aluminium-based Catalyst. *Chem. Sus. Chem.* **2019**, *12*, 3296–3303. [CrossRef]
314. Adhikari, D.; Miller, A.W.; Baik, M.H.; Nguyen, S.T. Intramolecular ring-opening from a CO_2-derived nucleophile as the origin of selectivity for 5-substituted oxazolidinone from the (salen)Cr-catalyzed [aziridine + CO_2] coupling. *Chem. Sci.* **2015**, *6*, 1293–1300. [CrossRef] [PubMed]
315. Zhou, F.; Xie, S.L.; Gao, X.T.; Zhang, R.; Wang, C.H.; Yin, G.Q.; Zhou, J. Activation of (salen)CoI complex by phosphorane for carbon dioxide transformation at ambient temperature and pressure. *Green Chem.* **2017**, *19*, 3908–3915. [CrossRef]
316. Wang, X.; Gao, W.Y.; Niu, Z.; Wojtas, L.; Perman, J.A.; Chen, Y.S.; Li, Z.; Aguila, B.; Ma, S. A metal-metalloporphyrin framework based on an octatopic porphyrin ligand for chemical fixation of CO_2 with aziridines. *Chem. Commun.* **2018**, *54*, 1170–1173. [CrossRef] [PubMed]
317. Chen, Y.; Luo, R.; Yang, Z.; Zhou, X.; Ji, H. Imidazolium-based ionic liquid decorated zinc porphyrin catalyst for converting CO_2 into five-membered heterocyclic molecules. *Sustain. Energy Fuels* **2018**, *2*, 125–132. [CrossRef]
318. Kayaki, Y.; Mori, N.; Ikariya, T. Palladium-catalyzed carboxylative cyclization of a-allenyl amines in dense carbon dioxide. *Tetrahedron Lett.* **2009**, *47*, 6491–6493. [CrossRef]
319. Foo, S.W.; Takada, Y.; Yamazaki, Y.; Saito, S. Dehydrative synthesis of chiral oxazolidinones catalyzed by alkali metal carbonates under low pressure of CO_2. *Tetrahedron Lett.* **2013**, *54*, 4717–4720. [CrossRef]

320. Takada, Y.; Foo, S.W.; Yamazaki, Y.; Saito, S. Catalytic fluoride triggers dehydrative oxazolidinone synthesis from CO_2. *RSC Adv.* **2014**, *4*, 50851–50857. [CrossRef]
321. Tominaga, K.; Sasaki, Y. Synthesis of 2-Oxazolidinones from CO_2 and 1,2-Aminoalcohols Catalyzed by n-Bu_2SnO. *Synlett* **2002**, *02*, 0307–0309. [CrossRef]
322. Xiong, W.; Qi, C.; Guo, T.; Zhang, M.; Chen, K.; Jiang, H. A copper-catalyzed oxidative coupling reaction of arylboronic acids, amines and carbon dioxide using molecular oxygen as the oxidant. *Green Chem.* **2017**, *19*, 1642–1645. [CrossRef]
323. Wang, L.; Qi, C.; Cheng, R.; Liu, H.; Xiong, W.; Jiang, H. Direct Access to Trifluoromethyl-Substituted Carbamates from Carbon Dioxide via Copper-Catalyzed Cascade Cyclization of Enynes. *Org. Lett.* **2019**, *21*, 7386–7389. [CrossRef] [PubMed]
324. Bresciani, G.; Bortoluzzi, M.; Marchetti, F.; Pampaloni, G. Iron(III) *N*,*N*-Dialkylcarbamate-Catalyzed Formation of Cyclic Carbonates from CO_2 and Epoxides under Ambient Conditions by Dynamic CO_2 Trapping as Carbamato Ligands. *Chem. Sus. Chem.* **2018**, *11*, 2737–2743. [CrossRef]
325. Bresciani, G.; Marchetti, F.; Pampaloni, G. Carboxylation of terminal alkynes promoted by silver carbamate at ambient pressure. *New J. Chem.* **2019**, *43*, 10821–10825. [CrossRef]
326. Bresciani, G.; Bortoluzzi, M.; Ghelarducci, C.; Marchetti, F.; Pampaloni, G. Synthesis of α-Alkylidene Cyclic Carbonates via CO_2 Fixation Promoted by Easily Available Silver Compounds Under Ambient Conditions. (submitted).
327. Anastas, P.; Eghbali, N. Green chemistry: Principles and practice. *Chem. Soc. Rev.* **2010**, *39*, 301–312. [CrossRef]
328. Galletti, A.M.R.; Pampaloni, G.; D'Alessio, A.; Patil, Y.; Renili, F.; Giaiacopi, S. Novel highly active niobium catalysts for ring opening metathesis polymerization of norbornene. *Macromol. Rapid Commun.* **2009**, *30*, 1762–1768. [CrossRef]
329. Hayatifar, M.; Pampaloni, G.; Bernazzani, L.; Capacchione, C.; Kissin, Y.V.; Raspolli Galletti, A.M. A new post-metallocene catalyst for alkene polymerization: Copolymerization of ethylene and 1-hexene with titanium complexes bearing *N*,*N*-dialkylcarbamato ligands. *Polym. Int.* **2014**, *63*, 560–567. [CrossRef]
330. Marchetti, F.; Pampaloni, G.; Pinzino, C.; Renili, F.; Repo, T.; Vuorinen, S. Ring opening polymerization of rac-lactide by group 4 tetracarbamato complexes: Activation, propagation and role of the metal. *Dalton Trans.* **2013**, *42*, 2792–2802. [CrossRef]
331. Tsoglin, E.; Chechik, H.; Karseboom, G.; Chinkov, N.; Stanger, A.; Marek, I. Stereoselective synthesis of metalated cyclobutyl derivatives. *Adv. Synth. Catal.* **2009**, *351*, 1005–1008. [CrossRef]
332. Jašíková, L.; Hanikýřová, E.; Škríba, A.; Jašík, J.; Roithová, J. Metal-assisted lossen rearrangement. *J. Org. Chem.* **2012**, *77*, 2829–2836. [CrossRef] [PubMed]
333. Hill, M.R.; Jones, A.W.; Russell, J.J.; Roberts, N.K.; Lamb, R.N. Dialkylcarbamato magnesium cluster complexes: Precursors to the single-source chemical vapour deposition of high quality MgO thin films. *J. Mater. Chem.* **2004**, *14*, 3198–3202. [CrossRef]
334. Duce, C.; Spepi, A.; Pampaloni, G.; Piccinelli, F.; Tiné, M.R. Thermal decomposition of metal *N*,*N*-dialkylcarbamates. *J. Therm. Anal. Calorim.* **2016**, *123*, 1563–1569. [CrossRef]
335. Duan, X.; Tran, N.H.; Roberts, N.K.; Lamb, R.N. Single-source chemical vapor deposition of clean oriented Al_2O_3 thin films. *Thin Solid Films* **2009**, *517*, 6726–6730. [CrossRef]
336. Deng, H.; Gong, B.; Petrella, A.J.; Russell, J.J.; Lamb, R.N. Characterization of the ZnO thin film prepared by single source chemical vapor deposition under low vacuum condition. *Sci. China, Ser. E Technol. Sci.* **2003**, *46*, 6–11. [CrossRef]
337. Petrella, A.J.; Deng, H.; Roberts, N.K.; Lamb, R.N. Single-Source Chemical Vapor Deposition Growth of ZnO Thin Films Using $Zn_4O(CO_2NEt_2)_6$. *Chem. Mater.* **2002**, *14*, 4339–4342. [CrossRef]
338. Deng, H.; Clausi, D.A. Unsupervised segmentation of synthetic aperture radar sea ice imagery using MRF models. In Proceedings of the First Canadian Conference on Computer and Robot Vision, London, ON, Canada, 17–19 May 2004; Volume 458, pp. 43–50. [CrossRef]
339. Lee, E.; Russell, J.J.; Lamb, R.N. Nanostructural properties of zinc oxide thin films grown on non-planar substrates. *Surf. Interface Anal.* **2006**, *38*, 51–55. [CrossRef]
340. Hill, M.R.; Russell, J.J.; Lamb, R.N. High-quality $Zn_xMg_{1-x}O$ thin films deposited from a single molecular source. Intimate mixing as a means to improved film properties. *Chem. Mater.* **2008**, *20*, 2461–2467. [CrossRef]

341. Trott, G.; Garden, J.A.; Williams, C.K. Heterodinuclear zinc and magnesium catalysts for epoxide/CO_2 ring opening copolymerizations. *Chem. Sci.* **2019**, *10*, 4618–4627. [CrossRef]
342. Duan, X.F.; Tran, N.H.; Roberts, N.K.; Lamb, R.N. Solvothermal approach for low temperature deposition of aluminium oxide thin films. *Thin Solid Films* **2010**, *518*, 4290–4293. [CrossRef]
343. Sgrolli, N.; Imlyhen, N.; Volkman, J.; Raspolli-Galletti, A.M.; Serp, P. Copper-based magnetic catalysts for alkyne oxidative homocoupling reactions. *Mol. Catal.* **2017**, *438*, 143–151. [CrossRef]
344. Kim, K.A.; Cha, J.R.; Gong, M.S.; Kim, J.G. Preparation of ZnO_2 nanoparticles using organometallic zinc(II) isobutylcarbamate in organic solvent. *Bull. Korean Chem. Soc.* **2014**, *35*, 431–435. [CrossRef]
345. Kwak, W.G.; Cha, J.R.; Gong, M.S. Surface modification of polyester fibers by thermal reduction with silver carbamate complexes. *Fibers Polym.* **2016**, *17*, 1146–1153. [CrossRef]
346. Park, M.S.; Lim, T.H.; Jeon, Y.M.; Kim, J.G.; Gong, M.S.; Joo, S.W. Preparation of new polyelectrolyte/silver nanocomposites and their humidity-sensitive properties. *Macromol. Res.* **2008**, *16*, 308–313. [CrossRef]
347. Park, M.S.; Lim, T.H.; Jeon, Y.M.; Kim, J.G.; Joo, S.W.; Gong, M.S. Humidity sensitive properties of copoly(TEAMPS/VP)/silver nanocomposite films. *Sensors Actuators B Chem.* **2008**, *133*, 166–173. [CrossRef]
348. Park, H.S.; Gong, M.S. Facile preparation of nanosilver-decorated MWNTs using silver carbamate complex and their polymer composites. *Bull. Korean Chem. Soc.* **2012**, *33*, 483–488. [CrossRef]
349. Park, H.S.; Park, H.S.; Gong, M.S. Preparation of silver nanocolloids using silver alkylcarbamate complex in organic medium with PVP stabilizer. *Bull. Korean Chem. Soc.* **2010**, *31*, 2575–2580. [CrossRef]
350. Jeon, Y.-M.; Gong, M.-S.; Cho, H.-N. Preparation of silver/PMMA beads via the in sito reduction of a silver alkylcarbamate complex. *Macromol. Res.* **2009**, *17*, 2–4. [CrossRef]
351. Kim, K.A.; Cha, J.R.; Gong, M.S. Facile preparation of silver nanoparticles and application to silver coating using latent reductant from a silver carbamate complex. *Bull. Korean Chem. Soc.* **2013**, *34*, 505–509. [CrossRef]
352. Yun, S.W.; Cha, J.R.; Gong, M.S. Easy preparation of nanosilver-decorated graphene using silver carbamate by microwave irradiation and their properties. *Bull. Korean Chem. Soc.* **2014**, *35*, 2251–2256. [CrossRef]
353. Kwak, W.G.; Oh, M.H.; Gong, M.S. Preparation of silver-coated cotton fabrics using silver carbamate via thermal reduction and their properties. *Carbohydr. Polym.* **2015**, *115*, 317–324. [CrossRef]
354. Kwak, W.G.; Oh, M.H.; Son, S.Y.; Gong, M.S. Silver loading on poly(ethylene terephthalate) fabrics using silver carbamate via thermal reduction. *Macromol. Res.* **2015**, *23*, 509–517. [CrossRef]
355. Ahn, H.Y.; Cha, J.R.; Gong, M.S. Preparation of sintered silver nanosheets by coating technique using silver carbamate complex. *Mater. Chem. Phys.* **2015**, *153*, 390–395. [CrossRef]
356. Liu, J.; Li, X.; Wang, X.; Zeng, X. Electrically conductive thick film made from silver alkylcarbamates. *J. Electron. Mater.* **2010**, *39*, 2267–2273. [CrossRef]
357. Kim, K.Y.; Gong, M.S.; Park, C.K. Preparation of highly stabilized silver nanopowders by the thermal reduction and their properties. *Bull. Korean Chem. Soc.* **2012**, *33*, 3987–3992. [CrossRef]
358. Liu, J.; Jiang, M.; Zeng, X. Electrical conductivity of thick films made from silver methylcarbamate paste. *J. Electron. Mater.* **2013**, *42*, 2990–2997. [CrossRef]
359. Abis, L.; Armelao, L.; Belli Dell'Amico, D.; Calderazzo, F.; Garbassi, F.; Merigo, A.; Quadrelli, E.A. Gold molecular precursors and gold–silica interactions. *J. Chem. Soc. Dalt. Trans.* **2001**, *18*, 2704–2709. [CrossRef]
360. Abis, L.; Calderazzo, F.; Maichle-Mössmer, C.; Pampaloni, G.; Strähle, J.; Tripepi, G. Cyclopentadienyl–diethylcarbamato derivatives of zirconium(IV) and hafnium(IV), $[M(C_5H_5)(O_2CNEt_2)_3]$: Synthesis and use as precursors for chemical implantation on a silica surface. *J. Chem. Soc. Dalt. Trans.* **1998**, *5*, 841–846. [CrossRef]
361. Abis, L.; Dell'amico, D.B.; Busetto, C.; Calderazzo, F.; Caminiti, R.; Ciofi, C.; Garbassi, F.; Masciarelli, G. *N*,*N*-Dialkylcarbamato complexes as precursors for the chemical implantation of metal cations on a silica support. *J. Mater. Chem.* **1998**, *8*, 751–759. [CrossRef]
362. Dell'Amico, D.B.; Bertagnolli, H.; Calderazzo, F.; D'Arienzo, M.; Gross, S.; Labella, L.; Rancan, M.; Scotti, R.; Smarsly, B.M.; Supplit, R.; et al. Nanostructured Copper Oxide on Silica-Zirconia Mixed Oxides by Chemical Implantation. *Chem. -Eur. J.* **2009**, *15*, 4931–4943. [CrossRef]
363. Armelao, L.; Dell'Amico, D.B.; Bellucci, L.; Bottaro, G.; Di Bari, L.; Labella, L.; Marchetti, F.; Samaritani, S.; Zinna, F. Circularly Polarized Luminescence of Silica-Grafted Europium Chiral Derivatives Prepared through a Sequential Functionalization. *Inorg. Chem.* **2017**, *56*, 7010–7018. [CrossRef] [PubMed]

364. Dolci, S.; Domenici, V.; Duce, C.; Tiné, M.R.; Ierardi, V.; Valbusa, U.; Jaglicic, Z.; Boni, A.; Gemmi, M.; Pampaloni, G. Ultrasmall superparamagnetic iron oxide nanoparticles with titanium-*N*,*N*-dialkylcarbamato coating. *Mater. Res. Express* **2014**, *1*, 035401. [CrossRef]
365. Abis, L.; Dell' Amico, D.B.; Busetto, C.; Calderazzo, F.; Garbassi, F.; Tomei, A. *N*,*N*-Dialkylcarbamato complexes as precursors for the chemical implantation of metal cations on a silica support. Part 3 Palladium. *J. Mater. Chem.* **1998**, *8*, 2855–2861. [CrossRef]
366. Awuah, S.G.; Zheng, Y.R.; Bruno, P.M.; Hemann, M.T.; Lippard, S.J. A Pt(IV) Pro-drug Preferentially Targets Indoleamine-2,3-dioxygenase, Providing Enhanced Ovarian Cancer Immuno-Chemotherapy. *J. Am. Chem. Soc.* **2015**, *137*, 14854–14857. [CrossRef]
367. Zhang, G.; Zhu, Y.; Wang, Y.; Wei, D.; Wu, Y.; Zheng, L.; Bai, H.; Xiao, H.; Zhang, Z. PH/redox sensitive nanoparticles with platinum(iv) prodrugs and doxorubicin enhance chemotherapy in ovarian cancer. *RSC Adv.* **2019**, *9*, 20513–20517. [CrossRef]
368. Chen, Q.; Yang, Y.; Lin, X.; Ma, W.; Chen, G.; Li, W.; Wang, X.; Yu, Z. Platinum(iv) prodrugs with long lipid chains for drug delivery and overcoming cisplatin resistance. *Chem. Commun.* **2018**, *54*, 5369–5372. [CrossRef]
369. Sommerfeld, N.S.; Strohhofer, D.; Cseh, K.; Theiner, S.; Jakupec, M.A.; Koellensperger, G.; Galanski, M.; Keppler, B.K. Platinum(IV) Complexes Featuring Axial Michael Acceptor Ligands—Synthesis, Characterization, and Cytotoxicity. *Eur. J. Inorg. Chem.* **2017**, *34*, 4049–4054. [CrossRef]
370. Stilgenbauer, M.; Jayawardhana, A.M.D.S.; Datta, P.; Yue, Z.; Gray, M.; Nielsen, F.; Bowers, D.J.; Xiao, H.; Zheng, Y.-R. A spermine-conjugated lipophilic Pt(IV) prodrug designed to eliminate cancer stem cells in ovarian cancer. *Chem. Commun.* **2019**, *55*, 6106–6109. [CrossRef]
371. Mayr, J.; Hager, S.; Koblmüller, B.; Klose, M.H.M.; Holste, K.; Fischer, B.; Pelivan, K.; Berger, W.; Heffeter, P.; Kowol, C.R.; et al. EGFR-targeting peptide-coupled platinum(IV) complexes. *JBIC J. Biol. Inorg. Chem.* **2017**, *22*, 591–603. [CrossRef]
372. Conibear, A.C.; Hager, S.; Mayr, J.; Klose, M.H.M.; Keppler, B.K.; Kowol, C.R.; Heffeter, P.; Becker, C.F.W. Multifunctional α v β 6 Integrin-Specific Peptide–Pt(IV) Conjugates for Cancer Cell Targeting. *Bioconjug. Chem.* **2017**, *28*, 2429–2439. [CrossRef]
373. Zhang, S.; Li, Y.N.; Zhang, Y.W.; He, L.N.; Yu, B.; Song, Q.W.; Lang, X.D. Equimolar carbon absorption by potassium phthalimide and in situ catalytic conversion under mild conditions. *Chem. Sus. Chem.* **2014**, *7*, 1484–1489. [CrossRef] [PubMed]
374. Tian, M.; Buchard, A.; Wells, S.A.; Fang, Y.; Torrente-Murciano, L.; Nearchou, A.; Dong, Z.; White, T.J.; Sartbaeva, A.; Ting, V.P. Mechanism of CO_2 capture in nanostructured sodium amide encapsulated in porous silica. *Surf. Coatings Technol.* **2018**, *350*, 227–233. [CrossRef]
375. Assaf, K.I.; Qaroush, A.K.; Mustafa, F.M.; Alsoubani, F.; Pehl, T.M.; Troll, C.; Rieger, B.; Eftaiha, A.F. Biomaterials for CO_2 harvesting: From regulatory functions to wet scrubbing applications. *ACS Omega* **2019**, *4*, 11532–11539. [CrossRef] [PubMed]
376. McDonald, T.M.; Mason, J.A.; Kong, X.; Bloch, E.D.; Gygi, D.; Dani, A.; Crocellà, V.; Giordanino, F.; Odoh, S.O.; Drisdell, W.S.; et al. Cooperative insertion of CO_2 in diamine-appended metal-organic frameworks. *Nature* **2015**, *519*, 303–308. [CrossRef]
377. Kim, E.J.; Siegelman, R.L.; Jiang, H.Z.H.; Forse, A.C.; Lee, J.-H.; Martell, J.D.; Milner, P.J.; Falkowski, J.M.; Neaton, J.B.; Reimer, J.A.; et al. Cooperative carbon capture and steam regeneration with tetraamine-appended metal-organic frameworks. *Science* **2020**, *369*, 392–396. [CrossRef]
378. An, J.P.; Fiorella, R.J.; Geib, S.L.; Rosi, N. Synthesis, Structure, Assembly, and Modulation of the CO_2 Adsorption Properties of a Zinc-Adeninate Macrocycle. *J. Am. Chem. Soc.* **2009**, *131*, 8401–8403. [CrossRef]
379. McDonald, T.M.; Lee, W.R.; Mason, J.A.; Wiers, B.M.; Hong, C.S.; Long, J.R. Capture of Carbon Dioxide from Air and Flue Gas in the Alkylamine-Appended Metal–Organic Framework mmen-Mg2(dobpdc). *J. Am. Chem. Soc.* **2012**, *134*, 7056–7065. [CrossRef]
380. Siegelman, R.L.; McDonald, T.M.; Gonzalez, M.I.; Martell, J.D.; Milner, P.J.; Mason, J.A.; Berger, A.H.; Bhown, A.S.; Long, J.R. Controlling Cooperative CO_2 Adsorption in Diamine-Appended Mg_2(dobpdc) Metal–Organic Frameworks. *J. Am. Chem. Soc.* **2017**, *139*, 10526–10538. [CrossRef]
381. Milner, P.J.; Siegelman, R.L.; Forse, A.C.; Gonzalez, M.I.; Runčevski, T.; Martell, J.D.; Reimer, J.A.; Long, J.R. A Diaminopropane-Appended Metal–Organic Framework Enabling Efficient CO_2 Capture from Coal Flue Gas via a Mixed Adsorption Mechanism. *J. Am. Chem. Soc.* **2017**, *139*, 13541–13553. [CrossRef]

382. Martell, J.D.; Porter-Zasada, L.B.; Forse, A.C.; Siegelman, R.L.; Gonzalez, M.I.; Oktawiec, J.; Runčevski, T.; Xu, J.; Srebro-Hooper, M.; Milner, P.J.; et al. Enantioselective Recognition of Ammonium Carbamates in a Chiral Metal–Organic Framework. *J. Am. Chem. Soc.* **2017**, *139*, 16000–16012. [CrossRef]
383. Hellström, A.K.; Oskarsson, H.; Bordes, R. Formation, physicochemical and interfacial study of carbamate surfactants. *J. Colloid Interface Sci.* **2018**, *511*, 84–91. [CrossRef]
384. Hellström, A.-K.; Bordes, R. Reversible flocculation of nanoparticles by a carbamate surfactant. *J. Colloid Interface Sci.* **2019**, *536*, 722–727. [CrossRef] [PubMed]
385. Biancalana, L.; Bresciani, G.; Chiappe, C.; Marchetti, F.; Pampaloni, G.; Pomelli, C.S. Modifying bis(triflimide) ionic liquids by dissolving early transition metal carbamates. *Phys. Chem. Chem. Phys.* **2018**, *20*, 5057–5066. [CrossRef] [PubMed]
386. Zhang, L.; Yang, P.-P.; Li, L.-F.; Hu, Y.-Y.; Mei, X.-L. A tridecanuclear $\{ZnGd_{12}\}$ nanoscopic cluster exhibiting large magnetocaloric effect. *Inorg. Chim. Acta.* **2020**, *499*, 119170. [CrossRef]

Sample Availability: Samples of several compounds cited in this work are available from the authors.